LBL-20850

Lawrence Berkeley Laboratory
UNIVERSITY OF CALIFORNIA

Materials & Molecular
Research Division

AN NMR INVESTIGATION OF DYNAMIC PROCESSES IN COMPLEXES OF NICKEL(II) AND ZINC(II) WITH IMINODIACETATE, N-METHYLIMINODIACETATE AND N-ETHYLIMINODIACETATE

M.R. Wagner
(Ph.D. Thesis)

November 1985

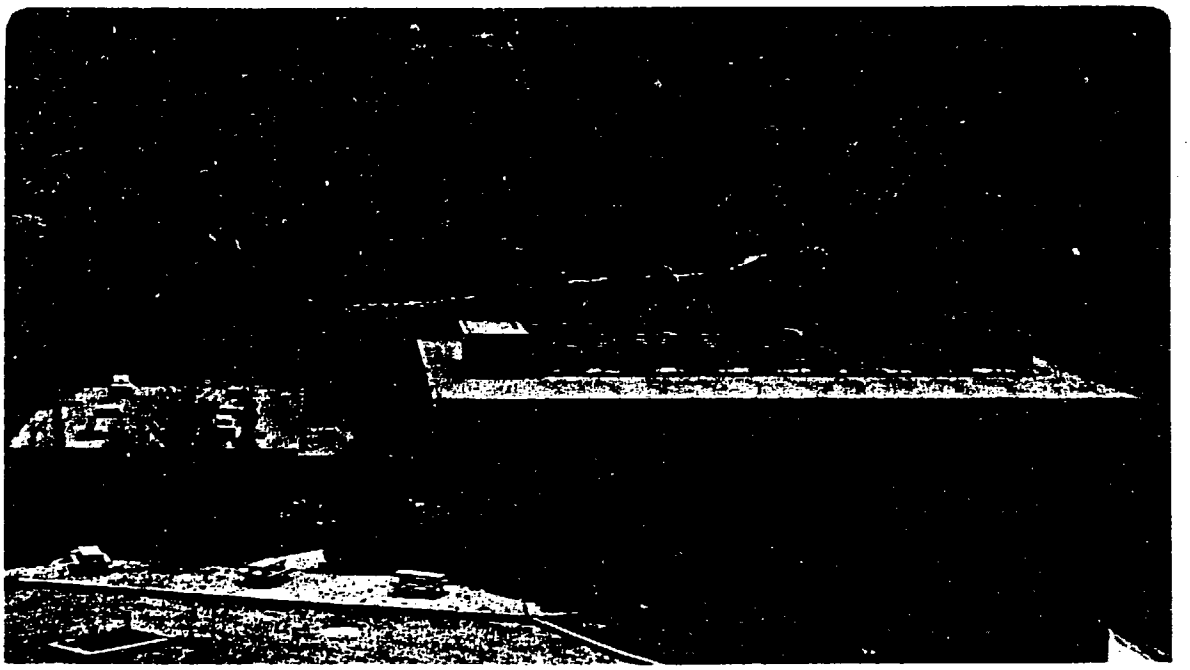

Prepared for the U.S. Department of Energy under Contract DE-AC03-76SF00098

LBL--20850

DE86 007493

AN NMR INVESTIGATION OF DYNAMIC PROCESSES IN COMPLEXES OF NICKEL(II) and ZINC(II) WITH IMINODIACETATE, N-METHYLIMINODIACETATE AND N-ETHYLIMINODIACETATE

Michael Richard Wagner

Ph.D. Thesis

Lawrence Berkeley Laboratory
University of California
Berkeley, California 94720

November, 1985

This research was supported by the Director, Office of Energy Research, Office of Basic Energy Science, Chemical Sciences Division of the United States Department of Energy under Contract No. DE-AC03-76SF00098.

An NMR Investigation of Dynamic Processes in Complexes of Nickel(II) and Zinc(II) with Iminodiacetate, N-Methyliminodiacetate and N-Ethyliminodiacetate

by Michael Richard Wagner

ABSTRACT

Dynamic processes involving diamagnetic zinc(II) complexes and paramagnetic nickel(II) complexes with iminodiacetate (ida), N-methyliminiodiacetate (mida) and N-ethyliminodiacetate (eida) are investigated by nuclear magnetic resonance techniques.

Analysis of oxygen-17 bulk water relaxation rates with an aqueous solution of 1:1 Ni(II):ida reveals that two rate-limiting processes are involved with solvent exchange (Chapter 1). Only one rate-limiting process is seen with the corresponding complexes with mida and eida. The data can be fitted to a model which includes both exchange and an intramolecular rearrangement of coordinated solvent molecules via a Bailar twist-type mechanism.

Analysis of carbon-13 longitudinal relaxation rates of the bis-ligand complexes with zinc(II) are used to determine molecular tumbling rates and methyl rotation rates (Chapter 2). Rotation is rapid about the nitrogen-carbon bond to the methyl group in the

bis-mida complex and about the carbon-carbon bond in the ethyl group with the bis-eida complex. No evidence is seen of rotation about the adjacent carbon-nitrogen bond in the latter complex.

The carbon-13 transverse relaxation rates for the carbons in the bis-ligand complex with Ni(II) are adequately fitted to the Solomon-Bloembergen equation using internuclear carbon-metal distances from crystallographic data and scalar coupling constants from the analysis of the isotropic shift data (Chapter 3).

Three carboxylate carbon peaks are seen with the ^{13}C spectrum of the 1:2 Ni(II):ida complex, which coalesce into a single peak above about 360 K. The peaks are due to the presence of both the cis and trans isomers. The temperature dependence of the shifts can be fitted using a Bailar twist-type model which interconverts the different isomers (Chapter 4).

The mechanism and rate of ligand exchange are determined for the complexes $Zn(II)L_2^{-2}$ (L = mida, eida) in aqueous solution by total lineshape analysis of the proton spectrum at 500 MHz (Chapter 5). In both cases, exchange occurs via a dissociative mechanism. With the bis-mida complex, no evidence is seen of an intramolecular rearrangement process similar to a process previously reported with the corresponding ida complex.

Robert F. Connick

TABLE OF CONTENTS

ACKNOWLEDGEMENT

I am extremely grateful to Professor Robert E. Connick for his efforts. Over the last four years Dr. Connick has worked closely with me in reviewing chemical principles, analyzing data and investigating models for nuclear spin and chemical behavior, primarily for the benefit of my own understanding. All this he has done with tremendous patience, interest and encouragement. Among scholars and educators, Dr. Connick truely is a giant. I am fortunate that he has shared so much of himself with me.

CHAPTER 1

^{17}O LINEWIDTH AND SHIFT ANALYSIS OF BULK-WATER EXCHANGE WITH THE 1:1 NICKEL(II) COMPLEXES WITH IDA, MIDA AND EIDA

CONTENTS

INTRODUCTION

The effect of a non-labile ligand in a metal complex is often studied by observing the substitution of labile ligands at the remaining sites. The reaction is characterized by a forward and reverse rate, when possible. The rates are related to the effect of the non-labile ligand and discussed in terms of steric and electronic effects.

Very often the presence of a non-labile ligand in a complex makes the remaining metal ion sites dissimilar. Coordination of a non-labile monodentate ligand (L) in a hexacoordinated metal ion, for example, creates one trans site (S_a) and four cis sites (S_b) for coordination by additional ligands.

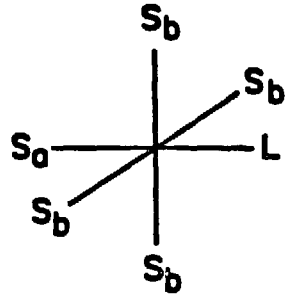

Assuming the additional ligands are labile and undergoing substitution, at least two rate processes are involved in the reaction

mechanism corresponding to the number of different ligand sites. The following discussion pertains to solvent exchange in which a coordinated solvent molecule is replaced by a solvent molecule from the bulk solution.

With more than a single rate process, the number of possible mechanisms for exchange increases. In the simplest case, labile solvent molecules can exchange with free solvent from their respective sites without involving solvent molecules elsewhere in the complex. Other possible mechanisms may involve internal shuffling of coordinated solvent molecules with or without a change in metal coordination number and overall configuration of the complex.

The use of NMR phenomena is well known for the study of ligand exchange with fast reacting metal ions.[1] (For recent examples see References 2,3,4,5.) The possibility of studying two simultaneous rate processes involving a single metal ion complex was demonstrated by Kustin and Vriesenga while observing water exchange in an aqueous solutions of 1:1 Ni(II):NTA (NTA = nitrilotriacetate‡).[6] A model involving a single rate of exchange was not adequate for explaining the temperature dependence of the linebroadening of the free water. A satisfactory fit was obtained, however, with a model involving two rate processes. A similar conclusion was reached in studies of water

---

‡ A comprehensive list of ligand terms used in this report is given in Appendix B.

exchange with 1:1 Ni(II):dien[7], 1:1 Ni(II):tren[8] and 1:1 Ni(II):ida[9] (dien = diethylenetriamine, tren = 2,2',2"-triaminotriethylamine, ida = iminodiacetate). (Water exchange in 1:1 Ni(II):dien was reported to occur via a single rate process in an earlier report[10]).

With all of the complexes above, the arrangement of the non-labile ligand on the hexacoordinated metal ion creates two different environments for water molecules in the first coordination sphere. In the analysis, the two rate processes were assumed to be two different exchange reactions involving waters in different sites. The data were fitted to a model which included the number of different sites and the relative abundance of coordinated water molecules in each, and rate information was obtained for "fast" and "slow" exchange processes (Table 1-1). If the number of water molecules in different sites is unequal (i.e., the octahedral Ni(II):ida complex contains waters in two different environments in relative abundance 1:2[9]) it is possible to identify waters in each site with a particular rate.

The rates in Table 1-1 are consistent with earlier observations, that water exchange is faster in complexes with more coordinated non-labile nitrogens.[10] The difference in exchange rates for water molecules in the same complex can vary greatly. The fast and slow exchange rates differ by a factor of 65 with 1:1 Ni(II):NTA[6], by eleven with 1:1 Ni(II):tren[8], by seven with Ni(II):dien[7] and by four with Ni(II):ida.[9] Regarding the 1:1 Ni(II):ida complex, it was determined that the faster exchanging waters are in the <u>cis</u> positions relative to the bound nitrogen possibly indicating that a carboxylate

oxygen in the non-labile ligand may be more effective in labilizing a bound water via a *trans* effect than is a nitrogen. An argument involving steric effects has also been proposed to explain the faster rate of exchange seen with waters in the *cis* positions.[9]

The rationalization of rate processes based on the number of distinct environments for exchanging ligands has met with some success in studies of solvent exchange with other metal ions and ligands. Two different rates are seen for the exchange of acetonitrile with $Ni(trenol)(CH_3CN)_2^{+2}$ [11] (trenol = 2,2',2''-trihydroxytriethylamine). As expected, only one rate of exchange is seen with $Ni(triol)(CH_3CN)_3^{+2}$ and $Ni(triam)(CH_3CN)_3^{+2}$ (triol = 2,2-di(hydroxymethyl)-1-propanol, triam = 2,2-di(aminomethyl)-1-propylamine).[11] However, only one rate is seen for the exchange of solvent molecules with $Ni(tren)(CH_3CN)_2^{+2}$ where two are expected.[12] With $Ni(diamol)(CH_3CN)_3^{+2}$ (diamol = 2,2-di(aminomethyl)-1-propanol) the solvent molecule *trans* to the ligand nitrogen is exchanging more than 180 times faster than the solvent molecule *trans* to the oxygen in the non-labile ligand, indicating that nitrogen is a better *trans* labilizer.[11] A similar conclusion was reached with solvent exchange in a methanol solution of $Co(CH_3OH)_5py^{+2}$ (py = pyridine), where the solvent molecule *trans* to bound pyridine is exchanging *ca.* three times faster than solvent molecules in the *cis* positions.[13]

The intent of this investigation is to study water exchange by ^{17}O NMR with a series of metal complexes in which only subtle differences exist in the non-labile ligand. The 1:1 Ni(II) complexes

with iminodiacetate (ida), N-methyliminodiacetate (mida) and N-ethyliminodiacetate (eida) were chosen because the substitution of the amine proton in ida for a methyl or ethyl group does not significantly alter the metal ligand configuration. A mechanism involving two rates has been given for the Ni(II):ida complex.[9] A two-rate process is also expected with the mida and eida complexes, with some differences due to the effect of the larger N-substituent group.

THEORETICAL CONSIDERATIONS

A well-known model for solvent (or ligand) exchange is shown in Scheme 1 where A and B represent two possible sites for a solvent molecule. Site A corresponds to a free solvent molecule unassociated with the metal ion complex in solution. Site B corresponds to a coordinated solvent molecules (shown schematically in a hexacoordinated metal ion complex). Exchange is occuring between the two sites with first order rate constants k_{ba} and k_{ab} as indicated. The relative abundance of solvent molecules in the A and B environments is not implicitely given in the scheme as indicated by the brackets around A.

Scheme 1:

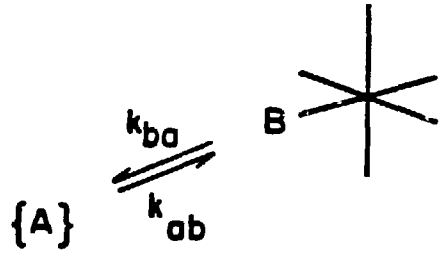

In this study, the metal ion complex (containing site B) is paramagnetic and the effect on the spectrum of the diamagnetic free water molecules (in site A) due to exchange is clearly seen in the chemical shift and the linewidth.[1] In a dilute solution ([B] << [A]), the contribution to relaxation of a spin in a free water molecule due to exchange with the paramagnetic species is given by the Swift-Connick equation:[14]

$$\frac{1}{T_{2p}} = \frac{P_b}{\tau_{ba}}\left[\frac{(T_{2b}^{2})^{-1} + (T_{2b}\tau_{ba})^{-1} + \Delta\omega_b^2}{(T_{2b}^{-1} + \tau_{ba}^{-1})^2 + \Delta\omega_b^2}\right] \qquad [1\text{-}1]$$

The lifetime of the solvent molecule in the complexed state is given by τ_{ba} ($= k_{ba}^{-1}$). The natural transverse relaxation rate of the spin in the B environments is given by T_{2b}^{-1}. The chemical shift difference for a spin in the A and B environments is given by $\Delta\omega_b$. The limiting conditions associated with the Swift-Connick equations[2,14] depend on the relative magnitude of these terms.

The temperature dependence of τ_{ba} is given by an Eyring-type expression:

$$\frac{1}{\tau_{ba}} = \frac{kT}{h} \exp\left(\frac{-\Delta H^{\ddagger}}{RT} + \frac{\Delta S^{\ddagger}}{R}\right) \qquad [1-2]$$

where k is the Boltzmann constant, $\Delta H^{\ddagger}$ is the enthalpy of activation and $\Delta S^{\ddagger}$ is the entropy of activation.

The natural relaxation of a spin in the first coordination sphere of a paramagnetic metal ion is due almost entirely to the scalar interaction of the spin with the paramagnetic electron in the metal.[14] The transverse relaxation rate is described by:[14]

$$\frac{1}{T_{2b}} = \frac{S(S+1)}{3}\left(\frac{A}{\hbar}\right)^2\left[\tau_{c1} + \frac{\tau_{c2}}{1 + \omega_s^2 \tau_{c2}^2}\right] \qquad [1-3]$$

where S is the electron spin quantum number (S = 1 for Ni(II)), A is the electron-nuclear spin scalar coupling constant, ω_s is the Larmor frequency of the electrons and τ_{c1} and τ_{c2} are the effective correlation times:

$$\frac{1}{\tau_{c1}} = \frac{1}{\tau_{ba}} + \frac{1}{T_{1e}} \qquad [1-4]$$

$$\frac{1}{\tau_{c2}} = \frac{1}{\tau_{ba}} + \frac{1}{T_{2e}} \qquad [1-5]$$

The rates T_{1e}^{-1} and T_{2e}^{-1} are the longitudinal and transverse relaxation rates for the paramagnetic electron, respectively. Parameter τ_{ba} has already been defined. Individual correlation times T_{1e} and T_{2e} are seldom known with certainly; therefore it is practical to substitute an effective correlation time τ_e for the expression in brackets in equation [1-3]. The transverse relaxation rate becomes:

$$\frac{1}{T_{2b}} = \frac{S(S+1)}{3}\left(\frac{A}{\hbar}\right)^2\tau_e \qquad [1\text{-}6]$$

The temperature dependence of T_{2b}^{-1} is associated with τ_e in equation [1-6] which is given an Arrhenius-type expression:

$$\tau_e = \tau_e^o \exp\left(\frac{V}{RT}\right) \qquad [1\text{-}7]$$

In this study the preexponential factor τ_e^o and the activation energy V are assigned values 3.8×10^{-12} s and 0.6 kcal mol^{-1}, respectively.[9] The value of τ_e (which equals T_{1e} if $T_{1e} >> T_{2e}$) is 1.0×10^{-11} s at 298 K, which is reasonable based on studies of other Ni(II) complexes.[15,16]

The difference in chemical shift for the free ligand and a coordinated ligand in a diamagnetic metal complex is small compared with $\Delta\omega_b$. Therefore, $\Delta\omega_b$ is set equal to the isotropic shift and is given by:[1]

$$\Delta\omega_b = -\omega S(S+1)\frac{\gamma_S}{\gamma_I}\frac{A}{3kT}$$

The precessional frequency of the spin is given by ω, and γ_S and γ_I are the gyromagnetic ratios of the paramagnetic electron and the observed spin, respectively. In this study the value of γ_S is assumed to be 1.98×10^7 G^{-1} s^{-1} corresponding to $g = 2.25$.[17]

Finally, P_b in equation [1-1] is the ratio of population of spins in the B and A sites:

$$P_b = \frac{(\text{number of spins in B environments})}{(\text{number of spins in A environments})}$$

For water exchange in a dilute aqueous solution:

$$P_b = \frac{N\cdot[\text{complex}]}{55.5 - N\cdot[\text{complex}]} \qquad [1\text{-}8]$$

where N is the number of B sites in the complex. In a dilute solution, the effect of N in equation [1-1] is to multiply the value of T_{2p}^{-1} for one B site by the number of B sites per metal ion undergoing exchange.

In practise, T_{2p}^{-1} is observed as a function of temperature. Relevant parameters are determined from a fit of the data using the expressions above. In this study, parameters A, $\Delta H^{\ddagger}$ and $\Delta S^{\ddagger}$ are determined with the use of this model. The importance of observing

values of T_{2p}^{-1} in both the slow exchange and fast exchange regions has been discussed elsewhere.[1]

A more complicated model for exchange involving a single metal complex is shown in Scheme 2.

Scheme 2:

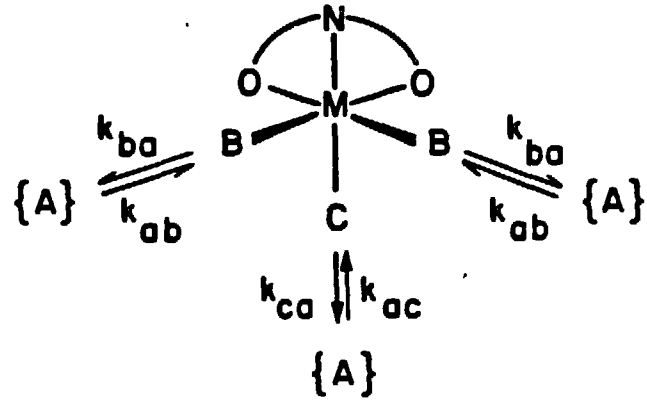

In this case, B and C represent sites for solvent molecules which are different due to the presence of a non-labile ligand in the complex. The facial arrangement of the tridentate iminodiacetate moity is shown in Scheme 2. Two B sites are cis relative to the bound nitrogen and one C site is trans. By the mechanism in Scheme 2, exchange is occuring between the metal sites B and free solvent, and between metal site C and free solvent, with the first order rate constants as indicated in the diagram.

The expression for T_{2p}^{-1} has been derived for the linewidth of the free ligand due to exchange with a paramagnetic metal ion in much less abundance.[14,18] Each exchange process in Scheme 2 contributes independently to the relaxation, and T_{2p}^{-1} is a sum of two terms, each given by equation [1-1] with parameters corresponding to the respective A-B and A-C exchange.

EXPERIMENTAL

Reagent grade iminodiacetic acid was recrystallized twice from methanol and water. N-Methyliminodiacetic acid and N-ethyliminodiacetic acid were synthesized from chloroacetic acid and aqueous solutions of the appropriate alkyl amine,[19] and recrystallized three times from water and methanol. Hydrated nickelous perchlorate, $Ni(ClO_4)_2 \cdot 6H_2O$ (Aldrich) was used without additional purification. Analysis for nickel was done by atomic absorption.

Samples for NMR study were prepared by weighing together the appropriate amount of amine, nickelous perchlorate, water enriched in ^{17}O to about 5% and concentrated NaOH made from $NaOH \cdot H_2O$ (Aldrich) and enriched water, as needed to obtain the desired pH. The total nickel concentration was verified by atomic absorption immediately before and after each run. The analysis before agreed with the formal amount. The analysis after was typically 1% larger probably due to evaporation of water from the sample during the run to the upper end of the NMR tube.

Fourier transformed ^{17}O spectra were obtained with a Chemistry Department spectrometer operating at 27.4 MHz using a Nicolet operating system. In a typical run 32 scans were collected over ca. 10 s using a pulse width of 20 x 10^{-6} s, a sweep width of 5 KHz and a recovery times of 0.001 s. Broadband decoupling was employed at all times to prevent ^{17}O peak broadening due to interaction with the proton.[20]

The temperature was controlled by a heating unit and monitored with a new ^{19}F NMR "thermometer". (It was not possible to use ethylene gycol as a ^{1}H NMR thermometer since the water peak in the proton spectrum is shifted up field by the paramagnetic species and totally obscures the downfield ethylene glycol peak.) Each sample contained a concentrically mounted capillary with a 50:50 by weight mixture of 1,2-difluorotetrachloroethane (Pfaltz & Bauer) and 1,4-di(trifluoromethyl)benzene (Pfaltz & Bauer). The ^{19}F spectrum of the sample was obtained immediately prior to obtaining the ^{17}O data. The temperature was determined from the separation of the two peaks in the ^{19}F spectrum of the mixture.

The separation of peaks in the ^{19}F spectrum was calibrated in a separate experiment by substituting a capillary containing a copper-constantan thermocouple for the fluorocarbon mixture, but without spinning, immediately after observing the ^{19}F spectrum. Linear temperature dependence was observed over the range 273 to 268 K. A least-squares fit produced the following relationship:

$$\text{Temperature } (^{\circ}C) = (-86.154)\delta + 597.916$$

where δ is the peak separation in ppm.

The temperature dependence for the new ^{19}F thermometer is large (0.4 Hz per degress at 200 MHz) compared with other fluorine thermometers. The dependence is unaffected by small changes in the composition of the mixture and the presence of trace amounts of water, making this particular mixture very useful for NMR temperatures studies.

The concentration of the 1:1 Ni(II):ligand species and all other species was calculated with the equilibrium parameters in Table 1-2. Calorimetric parameters for the complexes with ida and mida permitted the calculation of equilibrium constants at each temperature. Calorimetric parameters were not available for the eida complex and the concentrations determined with equilibrium constants for 298 K were used over the entire temperature range. The error introduced by this assumption is probably very small. The same assumption made with the mida and ida complexes produced very little change in the fitted parameters.

RESULTS AND DISCUSSION

The contribution to the transverse relaxation rate due to the interaction with the 1:1 metal ligand, T_{2p}^{-1}, was assumed to be the difference between the observed transverse relaxation rate $T_2(obs)^{-1}$ and other known contributors to the relaxation:

$$\frac{1}{T_{2P}} = \frac{1}{T_2(obs)} - \frac{1}{T_2(H_2O)} - \frac{1}{T_2(Ni(H_2O)_6^{+2})} \qquad [1\text{-}9]$$

The observed transverse relaxation time was obtained from the full linewidth at half height (in units of hertz) of each ^{17}O bulk water peak ($\Delta\nu_{1/2}$) and the following expression:

$$\frac{1}{T_2} = \frac{1}{2}(\Delta\nu_{1/2} \cdot 2\pi)$$

The value of $\Delta\nu_{1/2}$ was obtained from a non-linear least squares fitting to a Lorentzian curve. The range of fitted points from the FT spectrum was at least 10 times $\Delta\nu_{1/2}$ centered about the peak to guarantee an accurate baseline.

In equation [1-9], $T_2(H_2O)^{-1}$ is the natural relaxation rate of the bulk water that occurs while unassociated with the paramagnetic species. It is obtained empirically by observing the linewidth-versus-temperature of a metal:ligand solution in which Zn(II) has been substituted for Ni(II).

The last term in equation [1-9] is the contribution to relaxation of bulk waters by the hexaaquated nickel ion in solution. It includes both exchange and second coordination sphere effects. In this study $T_2((Ni(H_2O)_6^{+2})^{-1}$ was calculated with the Swift-Connick equation using the exchange rate and other parameters reported by Neely and Connick for water in a solution containing metal ion and no complexing ligand.[21] This contribution is usually very small (See Appendix A).

The composition of the solutions is such that an appreciable amount of the 1:2 metal:ligand species is also present. The bis-ligand complexes contribute to the relaxation of the bulk waters by second coordination sphere effects and by direct coordination of a water to the metal during momentary detachment of a ligand carboxylate oxygen. Typical solutions in this study contain 0.25 M 1:2 Ni(II):ligand. If one of the four carboxylate groups is detached 1.5% of the time[9], the linebroadening due to exchange from this site is ca. 0.5% of the linebroadening due to exchange from the mono-ligand complex and is justifiably ignored.

The observed values of T_{2p}^{-1} factored for a hypothetical 0.1 M solution of the 1:1 complex with ida, mida and eida, is plotted as a function of temperature in Figures 1-1, 1-2 and 1-3, respectively. (The practice of factoring the data to produce values corresponding to a particular concentration is useful since data obtained with solutions of different composition can be compared in a single plot. With no prior knowledge of the number of coordinated waters undergoing exchange, the data are distorted slightly since an assumption must be

made about the value of N in equation [1-8]. The distortion is very small with a dilute solution of metal complex.) Both slow exchange and fast exchange regions are seen within the observed temperature range for all the complexes. Good agreement is seen in using samples of different concentration and different pH with each ligand.

1:1 Ni(II):ida. Attempts to fit the data with equation [1-1], i.e., with a single rate of exchange for all the bound waters, produced significant descrepancies, and Scheme 1 was abandoned for modeling water exchange with this complex. A satisfactory fit of the data was obtained using the exchange mechanism given by Scheme 2. The number of B and C aites was assigned N = 2 and N = 1, respectively, consistent with the number of waters in different sites in the 1:1 metal:ligand complex. The six parameters determined in the fit (activation parameters $\Delta H^{\ddagger}$ and $\Delta S^{\ddagger}$, for A-B and A-C exchange, and the scalar coupling constants for a water molecule in the B and C sites) are given in Table 1-3. The calculated curve is shown in Figure 1-1. An excellent fit is seen over most of the temperature range. Some deviation between the data and the calculated curve is seen below 285 K. The difference may be due to error in estimating $T_2(H_2O)^{-1}$ which is a significant portion of the total relaxation at lower temperatures (See Appendix A).

Shown in Figure 1-1 is the contribution to T_{2p}^{-1} at each temperature due to exchange from the individual B and C sites (curves

"B" and "C", respectively). The minimum in the B curve is lower than the minimum in the C curve by a factor of approximately two due to the relative 2:1 abundance of B and C sites in the model. Although the number of B and C sites is fixed in the model, the exchange rate from each site is determined in the fitting of the data. The minimum in the B curve occurs at a lower temperature than the minimum in the C curve indicating that exchange is faster from the B sites.

Results with 1:1 Ni(II):ida show fair agreement with those obtained by Rowland[9] (Table 1-1 and Table 1-3) It is appropriate to compare the values in this study with those obtained by Rowland from a fit of only the linewidth data. The rate of fast exchange (3.2×10^5 s^{-1}, 298 K) is less than the previous reported value (5.3×10^5 s^{-1}, 298 K).[9] Some of the discrepancy can be attributed to uncertainty in the concentration of the mono-ligand species in solution. Values for the rate of slow exchange are nearly equal (ca. 2.4×10^4 s^{-1}, 298 K). This is coincidental since the uncertainty in the parameters associated with the C site is greater than with parameters associated with the B site in as much as exchange from the C site contributes less to the overall shape of the curve.

The number of exchanging waters per metal ion assigned to the two sites was based on the number of waters in different environments in the hexacoordinated 1:1 metal:ligand complex. This assignment is not limited to a facial arrangement of the ligand since a meridional arrangement would also produce the same N = 2 and N = 1 for the B and C sites, respectively. If a carboxylate group were uncoordinated for

an appreciable time, water exchange would also occur at the vacated site. In this case, Scheme 2 would be inadequate for modeling the system and the rates of exchange determined using Scheme 2 would be too large. Assurance that this is not happening to an appreciable extent is given by the satisfactory fit of the data and by the small contribution to relaxation made by detachment of a carboxylate oxygen as seen with the 1:2 metal:ligand complex.[9]

The two waters in the B sites are assigned to waters in the cis position relative to nitrogen, and exchange about 12 times faster than water in the trans C site. The difference has been related to bond strain about the coordinated nitrogen in the bound ligand.[9] Bond angles around the nitrogen are less than ideal for a tetrahedral arrangement.[25] The release of a water in the cis position permits angles closer to 109°, i.e., via the formation of a trigonal bipyramidal transition state. The same reduction in bond strain is not possible with elimination of a water in the trans position.

The use of bond strain to explain the difference in exchange rates for waters in the B and C sites implies that the effect of the inert ligand is felt primarily by waters in the cis position, and that little or no effect is felt by the water in the trans position. Similar rates of exchange (ca. 2×10^4 s^{-1}, 298 K) are seen for the slow rate of exchange with the ida and NTA complexes (Table 1-1 and Table 1-3). The slow rate of exchange is larger by a factor of ca. 10 with the tren and dien complexes which is evidence of an electronic effect associated with the number of non-labile nitrogens in the

complex. The slow exchange rate with the ida complex is approximately equal to the rate of water exchange from the hexahydrated nickelous ion[21] (k_{ex} = 3.2 x 10^4 s^{-1} at 298 K). This suggests that a single bound nitrogen is ineffective in increasing the water exchange rate unless other factors (i.e., bond strain) are involved.

The rate of fast exchange for the complexes in Table 1-1 and 1-3 show considerable variation. Bond strain is expected to be significant with NTA. The coordination of three acetate arms in NTA is more difficult than the coordination two acetate arms in ida, which may account for the 3.4-fold difference in the fast exchange rates seen with these complexes. The fast rates of exchange seen with the dien and tren complexes are larger, again indicating the involvement of electronic effects associated with the number of coordinated nitrogens on the metal ion.

1:1 Ni(II):mida and 1:1 Ni(II):eida. The data in Figures 1-2 and 1-3 were satisfactorily fitted with equation [1-1] for the mechanism of exchange given in Scheme 1. Three exchanging sites per metal ion (N = 3) was assumed in each case. The parameters determined in the fit (A/h, $\Delta H^{\ddagger}$ and $\Delta S^{\ddagger}$) are given in Table 1-4. The calculated curves are shown in Figures 1-2 and 1-3. With the eida complex it was necessary to use a larger value of τ_e^o (= 6.8 x 10^{-1} s) (see Theoretical Considerations) in order to fit the data at higher temperatures (above 355 K). The fit with τ_e^o = 3.8 x 10^{-12} s (used for ida and mida) is

also shown in Figure 1-3 (dotted line) for comparison. Also shown in Figures 1-2 and 1-3 is the contribution to relaxation in the limiting cases associated with the Swift-Connick equation.[1,14]

The line broadening of free water was observed for the 1:1 complex with eida in a higher-strength field (40.7 MHz). The observed T_{2p}^{-1} values are shown in Figure 1-3. The calculated curve through the data is obtained using equation [1-1] and the parameters obtained from fitting the data at lower frequency. Good agreement is seen indicating the frequency dependence is accurately predicted by the Swift-Connick equation.

The results with the mida and eida complexes indicates that all waters are exchanging at the same rate. The possibility of a unique metal:ligand configuration in which all the coordinated waters are in identical environments is very unlikely. The possiblity that waters are exchanging from only the B sites (i.e., exchange from the C site is very slow) was also discounted. A satisfactory fit of the data was obtained using the Swift-Connick equation with N = 2, corresponding to exchange from only the B sites, but the value of the scalar coupling constant obtained in the fit was about 50% greater than any reasonable value for a bound ^{17}O in the first coordination sphere of the nickelous ion.[9,10]

A single rate of exchange for all three coordinated waters in the mida and eida complexes is not expected based on the assumption that waters in different environments exchange at different rates. Two

rates of exchange are seen with the ida complex, therefore the behavior seen with the mida and eida complexes must be related to the substitution of the amine proton in ida for a methyl or ethyl group.

Two approaches will be taken to rationalize the results with mida and eida. The first approach assumes that water molcules are exchanging with the bulk solvent from both the B and C sites, but the rates are comparable and therefore indistinguishable in an NMR linebroadening experiment. The second approach assumes that water molecules are exchanging from only one site, but waters in the second site are involved via a rapid intramolecular rearrangement that interconverts water in the two sites.

If rate constants k_{ba} and k_{ca} in Scheme 2 are equal, Scheme 2 reduces to the more specific case described by Scheme 1 with N equal to the total number of B and C sites involved in exchange. Scheme 1 may be used with similar rates. We estimate that a difference in the rate constants of less than 10% will go unnoticed and result in the reporting of a single rate constant. This depends to some extent on the difference in the scalar coupling constants for water molecules in the B and C sites.

The various effects which influence the exchange rate (i.e., electronic effects, steric effects) are operating differently on the waters in the <u>cis</u> and <u>trans</u> positions. This is very evident with the 1:1 Ni(II):ida complex. The possibility exists that the overall effect with the mida and eida complexes is to produce rates which are

very similar for the exchange for waters from both sites. There is no inherent reason why the rates for the individual processes (according to Scheme 2) should approach a similar value, and the appearance of similar rates with both complexes in this study is highly coincidental

Substitution of the amine proton in ida by a methyl or ethyl group could reduce the difference in exchange rates by increasing the rate of exchange from the slow exchange site, or by decreasing the rate of exchange from the fast exchange site, or both. The results favor an increase in the slow exchange rate (from the C sites) since the observed rate of exchange (ca. 3.2×10^5 s^{-1}) is similar to the fast rate of exchange (from the B sites) seen with the ida complex (Table 1-3). If waters are exchanging from the cis position in all three complexes at nearly the same rate, the bond strain which is responsible for the fast rate of exchange from the cis position in the ida complex, must be present to about the same extent in the mida and eida complexes.

The increase in the rate of exchange from the trans position can be rationalized using electronic effects. In general, an increase in the basicity of the inert ligand is expected to decrease the positive charge on the metal ion and decrease the strength of the bonds to the other groups in the complex. Ligands mida and eida are more basic than ida (See Table 1-2) due to the electron donating properties of the alkyl groups. The metal-oxygen bond to a water in the trans position relative to the non-labile nitrogen is weaker in the mida and eida complexes thus producing an increase in the rate of exchange from

this position. If this is correct, the effect is significant, increasing the water exchange from 2.6×10^4 s^{-1} (the slow exchange rate with ida) to *ca.* 3.2×10^{-5} s^{-1}. The rate of ammonia exchange on the 1:1 Ni(II) complexes with ida and with mida are nearly equal indicating the difference in basicities of the ligands has very little effect on ammonia exchange from the complex.[22] The rate of cyanide exchange on the same complexes is also nearly equal.[23]

The conditions for incoming and outgoing waters in the immediate vicinity of the exchange sites may also be a factor in determining the exchange rates for the different sites. Results with different solvents have shown that exchange rates may depend on outer sphere conditions. In particular, solvent conditions around the complex which interfere with the approach of an incoming ligand are known to be important.[24] A unique feature in the complex with ida in this study is the presence of an amine proton and its propensity to hydrogen-bond to neighboring water molecules. A water in the *cis* position is *ca.* 320 pm from the amine proton while a water in the *trans* position is *ca.* 450 pm away.[25] If the amine proton changes the neighboring solvent structure via hydrogen-bonding the effect will be felt much less at the *trans* sites than at the *cis* site. The effect is not present in the complexes with mida and eida where the amine proton has been replaced. However, this effect should be unimportant in the 1:1 Ni(II):NTA complexes where a large difference in the rate of exchange from the *cis* and *trans* sites was seen.[6]

A very different approach to interpreting the relaxation results is to consider a mechanism that includes both an intramolecular rearrangement process and an exchange process. The two rate processes seen with the ida complex and other complexes (Table 1-1) could correspond to the rearrangement and exchange processes. Only a single rate process may be seen with other complexes (i.e., the mida and eida complexes) if the rate for the rearrangement process is too fast or too slow.

A possible mechanism with the complexes in this study is represented by Scheme 3.

Scheme 3:

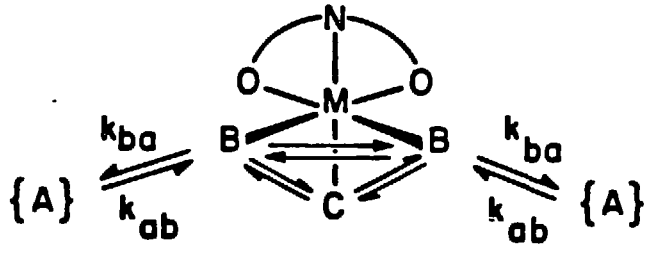

The non-labile iminodiactate moiety is shown with a facial confirmation on the metal. As before, two B sites correspond to waters in the cis position relative to the nitrogen. The C site corresponds to a water in the trans position. Unlike Scheme 2, exchange with bulk solvent is occuring only via the two B sites. In

addition to exchange, an intramolecular rearrangement process interchanges waters in the B and C sites as indicated. In the analysis, it is assumed that water exchange and intramolecular rearrangement are occurring independently.

To investiage the influence of the "twist" mechansism on the relaxation of bulk waters, T_{2p}^{-1} was calculated as a function of temperature. The general expression of Angerman and Jordan,[18] for three-site exchange was used as explained in Appendix C. The rate of exchange was described by an Eyring-type equation with activation parameters previously discussed. The rate of twisting was also described by an Eyring-type equation and an enthalpy and entropy of activation for the intramolecular rearrangment were specified in the calculation.

Calculated curves for T_{2p}^{-1} as a function of temperature are shown in Figure 1-4. Curves (a) through (f) are produced with identical rates of exchange at each temperature. They differ only by the rate of the twist mechanism which is achieved by varying the enthalpy of activation for the twist. Curve (a) corresponds to a very slow twisting rate relative to the exchange rate. Curve (f) corresponds to a rapid twisting rate. Intermediate twisting rates are represented by curves (b) through (e).

The effect of the twisting mechanism on T_{2p}^{-1} is very different in the slow and fast exchange regions. Essentially no effect on T_{2p}^{-1} is seen in the slow exchange region with bulk solvent (below 310 K).

This is reasonable since the rate of relaxation of the bulk water is determined only by the number of bulk solvent molecules which see the metal in the complexed state in a given period of time. The limiting form for the expression of T_{2p}^{-1} is accurate for determining the exchange rate. Evidence for a twist mechanism cannot be seen in this region.

In the intermediate and fast solvent exchange regions (above 310 K) T_{2p}^{-1} is very much affected by the twisting mechanism as seen in Figure 1-4. In the limit of very slow twisting (curve (a)) and very fast twisting (curve (f)) a very simple pattern is seen within the observeable temperature region. With very slow twisting Scheme 3 reduces to Scheme 1 with waters exchanging from only the B sites. The dashed curve in Figure 1-4 was produced with Scheme 1 using the same exchange rate and coupling constant. The difference between curve (a) and the dashed curve reveals that the effect of a finite rate can be seen if it is possible to go to high enough temperatures. In the limit of very fast twisting (curve (f)) waters exchange from only the B sites, but the lifetime of a particular water molecules in the coordinated state is increased by a factor of 1.5. Thus curve (f) lies below curve (a) by a factor of 1.5 in the fast limit.

The effect of the twisting mechanism on T_{2p}^{-1} can be understood by considering the curve (b). This curve clearly shows two minima within the temperature region given in Figure 1-4. In the region of slow solvent exchange (below 310 K) the relaxation of bulk solvent depends on the number of molecules that see the complexed state, as already

mentioned. Above 310 K, however, in the region of fast solvent exchange, solvent molecules are exchanging rapidly and bulk water relaxation depends on the extent of relaxation (dephasing[14]) of each spin while in the complexed state. The extent of relaxation may beaffected by a twisting mechanism which exchanges molecules in the B and C sites, depending on the twisting rate.

With curve (b), it is possible to distinquish two limiting regions associated with the second minimum at higher temperature (450 K). In the region between ca. 400 K and 440 K the additional relaxation caused by introducing the C site depends on the number of molecules in the B sites which will see the C site in a given period of time. A direct relationship between T_{2p} and τ_{cb} is expected as seen by the positive slope in this "slow exchange" region for the twist mechanism in Figure 1-4. Between ca. 460 K and 520 K solvent molecules exchange rapidly between the B and C sites, and the effect on T_{2p} depends on the extent of relaxation of each spin while in the C site. The negative slope within this region in Figure 1-4 is expected under conditions of fast exchange between the C and B sites via the twist mechanism.

The effect of varying the twist rate relative to the rate of solvent exchange is seen with curves (a) through (f). The minimum associated the exchange between the B and C sites (at higher temperature) moves toward the minimum associated with exchange between the A and B sites as the difference in the rates is decreased. With similar rates only a single minimum in an unsymmetrical curve is seen

(curves (d) and (e)). Finally a simple curve with a more narrow minimum (curve (f)) is obtained as previously mentioned.

The relaxation data for the mida and eida complexes (Figures 1-2 and 1-3) resemble curves (a) or (f) in Figure 1-4 in the observed temperature region. The possibility that the twisting mechanism is occuring at a very slow rate (i.e., curve (a)) with the mida and eida complexes has already been discussed and eliminated due to the unreasonably high scalar coupling constants needed to fit the data. The possibility of a very fast rate of twisting (i.e., curve (f)) is considered below.

Scheme 3 was used to fit the data with the mida and eida complexes assuming a fast rate of twisting relative to water exchange. In fitting the data, the scalar coupling constants for water molecules in the B and C sites were set equal to reduce the number of parameters. An excellent fit was obtained with both complexes over the entire temperature range. Parameters associated with the rate of exchange could be determined (Table 1-5), however, only a lower limit could be determined for the rate of twisting. It was also possible to fit the data by assuming that waters exchange from the one C site instead of the two B sites. In this case, the rate of exchange from a single site given in Table 1-4 is increased by a factor of two.

The results with the ida complex (Figure 1-1) resemble curve (d) in Figure 1-4. In fact, curve (d) was produced with the parameters obtained from fitting the data (reproduced in Figure 1-4 for

comparison) using Scheme 3. The parameters are given in Table 1-5. An excellent fit is seen. The small discrepancy at low temperatures in Figure 1-1 does not exist using Scheme 3 (Figure 1-4).

The quality of the fit using Scheme 3 is as good or better than the fit using Scheme 1 with the mida and eida complexes and Scheme 2 for the ida complexes. It is somewhat reassuring that all three complexes can be explained with a single mechanism, the difference in the results being due to the rate of the twisting process. The twisting rate and the rate of exchange are similar in the ida complex. The twisting rate is much larger than the exchange rate by at least a factor of five and six for the mida and eida complexes, respectively. It is reasonable that the substitution of the amine proton in ida for a methyl or ethyl group can affect the rate of twisting as well as the rate of exchange, and that the twist rate relative to the exchange rate may be different.

Another reasonable mechanism can be envisioned which includes features seen in both Scheme 2 and Scheme 3, specifically, exchange from both the B and C sites and intramolecular twisting. Scheme 2 and Scheme 3 may be considered to be two opposite limiting cases. In Scheme 2 exchange occurs between the bulk solvent and the C site (in addition to exchange from the B site) with no internal rearrangement between the B and C sites. In Scheme 3 internal rearrangement is occurring between the B and C sites with no solvent exchange from the C site. A model that includes exchange from both the B and C sites as

well as internal rearrangement is intermediate between these two limiting cases.

The good fit seen with Scheme 2 and Scheme 3 indicates that a mechanism with internal rearrangement and solvent exchange from both the B and C sites will also produce a good fit of the data. With the ida complex it is not possible to determine the extent to which exchange from the C site and intramolecular twisting contribute to the bulk water relaxation. It is possible to assign limits based on the results with Scheme 2 and Scheme 3. The upper limit for the rate of exchange from the C site is obtained using Scheme 2 (Table 1-3) where intramolecular twisting is unimportant. Similarly, a upper limit to the rate of twisting is obtaining using Scheme 3 (Table 1-5) where exchange from the C site is unimportant.

With the mida and eida complexes the rate of twisting is more rapid than exchange, and rate constants for exchange from the individual B and C sites can not be determined. The value obtained using Scheme 3 (Table 1-5) may be considered an upper limit in as much as the introduction of exchange via the C site will reduce the rate of exchange via the B site required to fit the data.

The results in this study suggest that other complexes can be interpreted using mechanisms which include intramolecular rearrangement as well as exchange. If the data reveal more than a single rate-limiting process, than rate information about both processes can be determined. If only a single process is seen, than

limits can be assigned to individual processes in the mechanism. Internal rearrangement in complexes is not limited to a Bailar-twist type processes involving three labile donor groups. With the 1:1 Ni(II):NTA complex, for example, a process can be envisioned which interconverts two different coordinated waters in the complex.

TABLE 1-1

Water Exchange Rate Constants for Ni(II) Species in Which More Than a Single Rate of Exchange is Reported

Complex	k(fast rate) (s^{-1}, 298 K)	k(slow rate) (s^{-1}, 298 K)	Ratio*	Ref.
$[Ni(H_2O)_2NTA]^-$	1.1×10^6 (1)‡	1.8×10^4 (1)	65	6
$[Ni(H_2O)_3dien]^{+2}$	3×10^6 (2)	4.0×10^5 (1)	7	7
$[Ni(H_2O)_2tren]^{+2}$	9×10^6 (1)	8.2×10^5 (1)	11	8
$[Ni(H_2O)_3ida]$**	5.3×10^5 (2)	2.4×10^4 (1)	4	9
$[Ni(H_2O)_3ida]$‡‡	2.9×10^5 (2)	4.3×10^4 (1)	7	9

* Ratio = fast exchange rate/slow exchange rate at 298 K.

‡ Value in parenthesis is the number of equivalent sites in the complex.

** Obtained from fit of linewidth data only.

‡‡ Obtained from fit of both linewidth and shift data.

TABLE 1-2

Equilibrium Constants (298 K, Ionic Strength 0.1 M)

	ida[‡]	mida[**]	eida[‡‡]
log K_{1a}[*]	-9.34	-9.57	-9.68
log K_{2a}	-2.98	-2.12	-2.20
log K_{1f}	8.07	8.67	8.86
log K_{2f}	6.16	7.19	7.26

[*] $K_{1a} = [H^+][L^{-2}]/[HL^-]$

$K_{2a} = [H^+][HL^-]/[H_2L]$

$K_{1f} = [NiL]/([Ni^{+2}][L^{-2}])$

$K_{2f} = [NiL_2^{-2}]/([NiL][L^{-2}])$

[‡] From Reference 26; K_{1a}: ΔH = 8150 cal mol^{-1}, ΔS = -15.4 eu; K_{2a}: ΔH and ΔS uncertain; K_{1f}: ΔH = -5050 cal mol^{-1}, ΔS = 20 eu; K_{2f}: ΔH = -4500 cal mol^{-1}, ΔS = 13.1 eu.

[**] From Reference 26; K_{1a}: ΔH = 6940 cal mol^{-1}, ΔS = -20.5 eu; K_{2a}: ΔH and ΔS uncertain; K_{1f}: ΔH = -4700 cal mol^{-1}, ΔS = 23.9 eu; K_{2f}: ΔH = -2950 cal mol^{-1}, ΔS = 23.0 eu.

[‡‡] From Reference 24.

TABLE 1-3

Rate Parameters with ida According To Scheme 2

ligand		$A/\hbar$ ($\times 10^{-8}$)	$\Delta H^{\ddagger}$ (kcal mol^{-1})	$\Delta S^{\ddagger}$ (eu)	k (s^{-1}, 298 K)
ida*	B site (N = 2):**	1.4 ± .1	12.6 ± .6	8.9 ± 2.1	3.2×10^5
	C site (N = 1):	1.2 ± .3	15.6 ± 1.3	14.0 ± 4.5	2.6×10^4
ida**	B site (N = 2):	1.3	12.1	7.2	5.3×10^5
	C site (N = 1):	1.2	13.8	8.8	2.4×10^4

* This work. $\tau_e^o = 3.8 \times 10^{-12}$ s, V = 0.6 kcal mol^{-1}.

** N = number of exchanging waters per metal ion.

** Reference 9 from fitted linewidth data only. See Table 1-1.

TABLE 1-4

Rate Parameters According to Scheme 1

ligand		A/$\bar{n}$ ($\times 10^{-8}$)	$\Delta H^{\ddagger}$ (kcal mol^{-1})	$\Delta S^{\ddagger}$ (eu)	k (s^{-1}, 298 K)
mida:*	(N = 3)**	1.7 ± .1	12.8 ± .4	8.7 ± 1.1	3.1×10^{5}
eida:‡‡	(N = 3)	1.4 ± .1	13.0 ± .3	10.4 ± 1.0	3.4×10^{5}

* $\tau_e^o = 3.8 \times 10^{-12}$ s, V = 0.6 kcal mol^{-1}.

** N = number of exchanging waters per metal ion.

‡‡ $\tau_e^o = 6.8 \times 10^{-12}$ s, V = 0.6 kcal mol^{-1}.

TABLE 1-5

Rate Parameters According to Scheme 3

ligand		$A/\hbar$ ($\times 10^{-8}$)	$\Delta H^{\ddagger}$ (kcal mol^{-1})	$\Delta S^{\ddagger}$ (eu)	k (s^{-1}, 298 K)
ida*	Exchange (N = 2):**	1.4 ± .2	14.6 ± .5	15.6 ± 1.4	3.2×10^5
	Twist:	-	10 ± 5	0 ± 15	1.6×10^5
mida*	Exchange (N = 2):	1.7 ± 0.2	13.0 ± 0.7	10.0 ± 2.0	3.0×10^5
	Twist:	-	-	-	$> 1.7 \times 10^6$
eida‡‡	Exchange (N = 2):	1.4 ± 0.2	13.0 ± 0.8	10.8 ± 3.0	5.1×10^5
	Twist:	-	-	-	$> 4.7 \times 10^6$

* This work. $\tau_e^o = 3.8 \times 10^{-12}$ s, V = 0.6 kcal mol^{-1}.

** N = number of exchanging waters per metal ion.

‡‡ This work. $\tau_e^o = 6.8 \times 10^{-12}$ s, V = 0.6 kcal mol^{-1}. See Text.

CAPTIONS TO FIGURES

Figure 1-1 Transverse Relaxation T_{2p}^{-1} versus temperature for aqueous solution of Ni(II) and ida at 27.4 MHz; (●) 0.0243 M $Ni(ClO_4)_2$ $6H_2O$, 0.0360 M iminodiacetic acid, pH 5.72; (○) 0.0477 M $Ni(ClO_4)_2$ $6H_2O$, .0755 M iminodiacetic acid, pH 6.18.

Figure 1-2 Transverse Relaxation T_{2p}^{-1} versus temperature for aqueous solution of Ni(II) and mida at 27.4 MHz; (○) 0.0236 M $Ni(ClO_4)_2$ $6H_2O$, 0.0382 M N-methyl iminodiacetic acid, pH 6.11; (●) 0.0562 M $Ni(ClO_4)_2$ $6H_2O$, 0.0900 M N-methyliminodiacetic acid, pH 7.70.

Figure 1-3 Transverse Relaxation T_{2p}^{-1} versus temperature for aqueous solution of Ni(II) and eida. (●) 0.0516 M $Ni(ClO_4)_2$ $6H_2O$, 0.0653 M N-ethyliminodiacetic acid, pH 5.81, at 27.4 MHz; (○) 0.0572 M $Ni(ClO_4)_2$ $6H_2O$, 0.0898 M N-ethyliminodiacetic acid, pH 7.90, at 27.4 MHz; (△) 0.0852 M $Ni(ClO_4)_2$ $6H_2O$, 0.1275 M N-ethyliminodiacetic acid, pH 6.74, at 40.7 MHz.

Figure 1-4 Transerve Relaxation data from Figure 1-1 for aqueous solutions of Ni(II) and ida. Curves calculated with Scheme 3: $A/h = 1.4 \times 10^8$, $\Delta H^{\ddagger}$ (exchange) = 14.6 kcal mol^{-1}, $\Delta S^{\ddagger}$ (exchange) = 15.6 eu, $\Delta S^{\ddagger}$ (twist) = -0.7 eu, $\Delta H^{\ddagger}$ (twist) in kcal mol^{-1} (a) 16.0, (b) 13.5, (c) 12.0, (d) 10.0, (e) 9.0 and (f) 6.0. Dashed curve calculated with Scheme 1 (N = 2) with A/h, $\Delta H^{\ddagger}$ and $\Delta S^{\ddagger}$ for exchange given above.

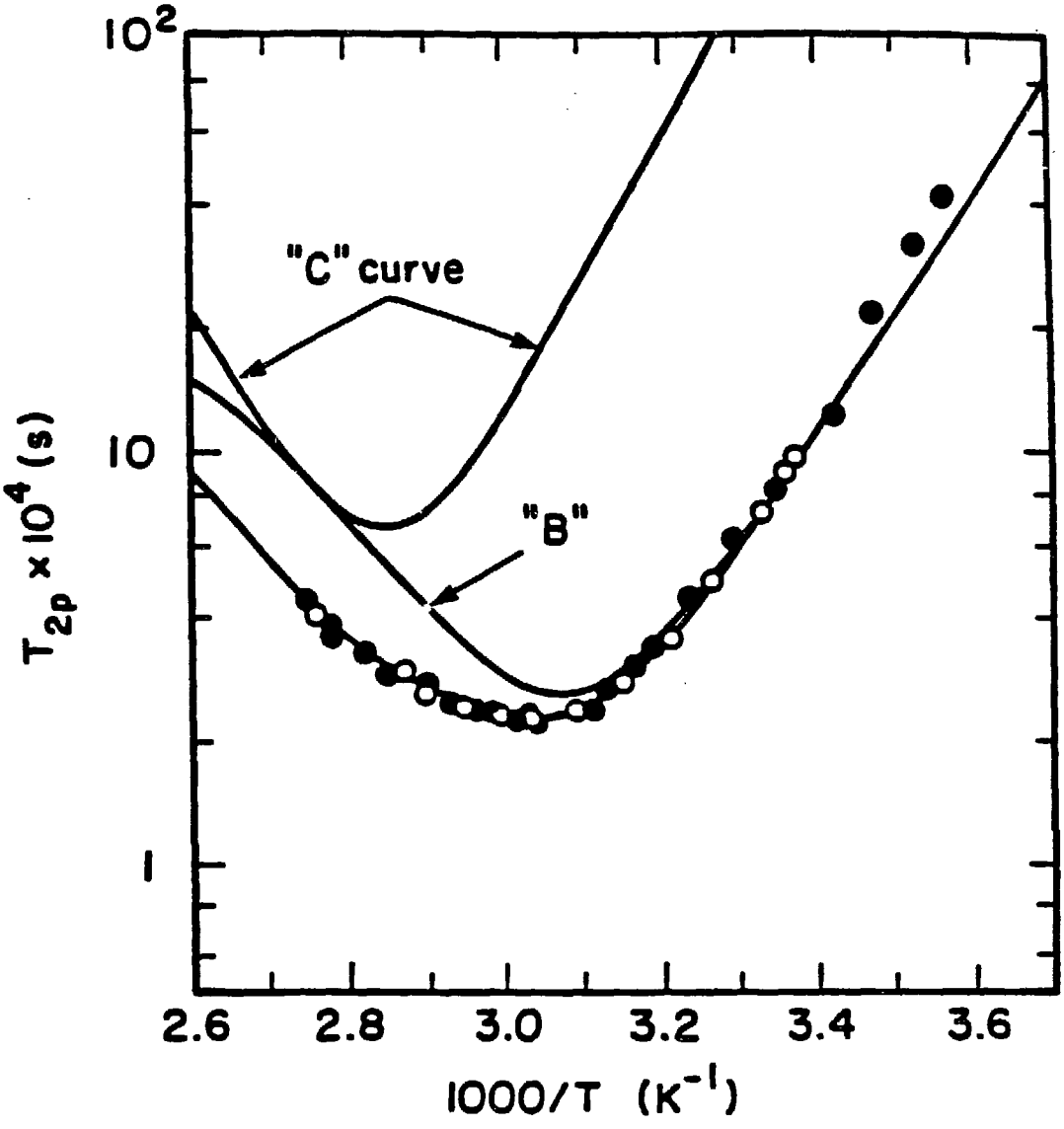

Figure 1-1

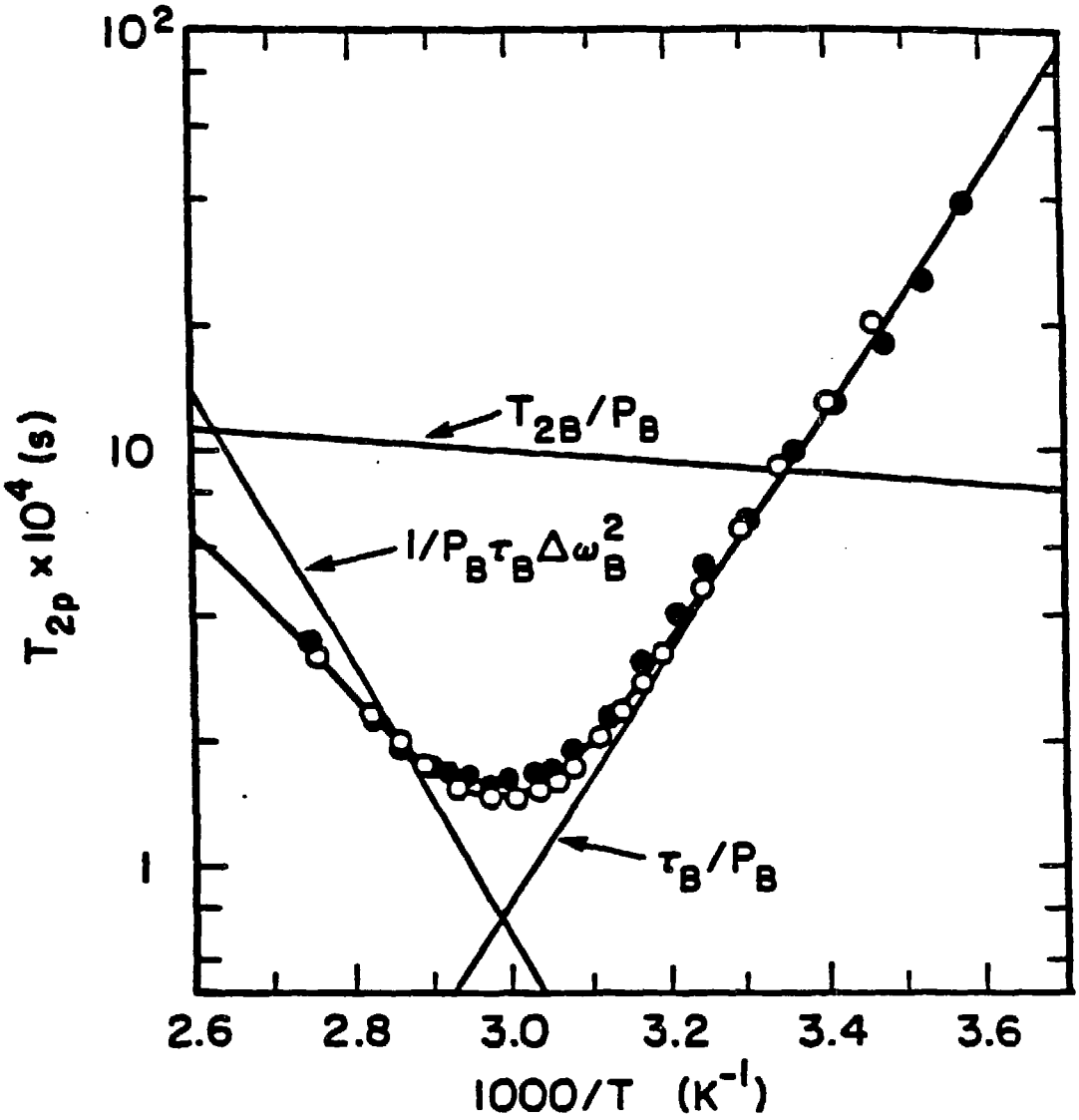
10^2
10
1
$T_{2p} \times 10^4$ (s)
T_{2B}/P_B
$1/P_B\tau_B\Delta\omega_B^2$
τ_B/P_B
2.6
2.8
3.0
3.2
3.4
3.6
1000/T (K^{-1})

Figure 1-2

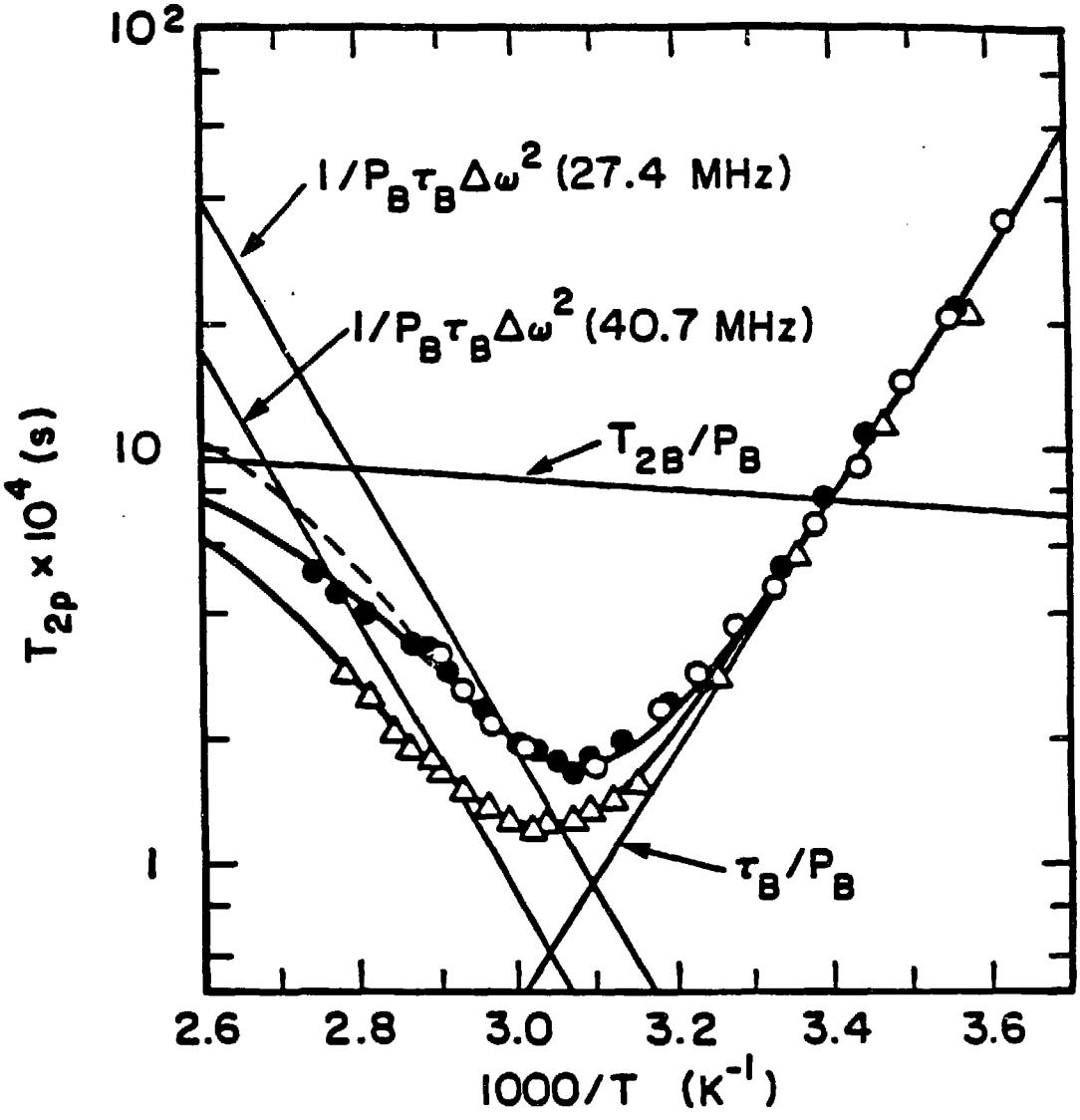
10^2
10
1
$T_{2\rho} \times 10^4$ (s)
$1/P_B\tau_B\Delta\omega^2$ (27.4 MHz)
$1/P_B\tau_B\Delta\omega^2$ (40.7 MHz)
T_{2B}/P_B
τ_B/P_B
2.6
2.8
3.0
3.2
3.4
3.6
1000/T (K^{-1})

Figure 1-3

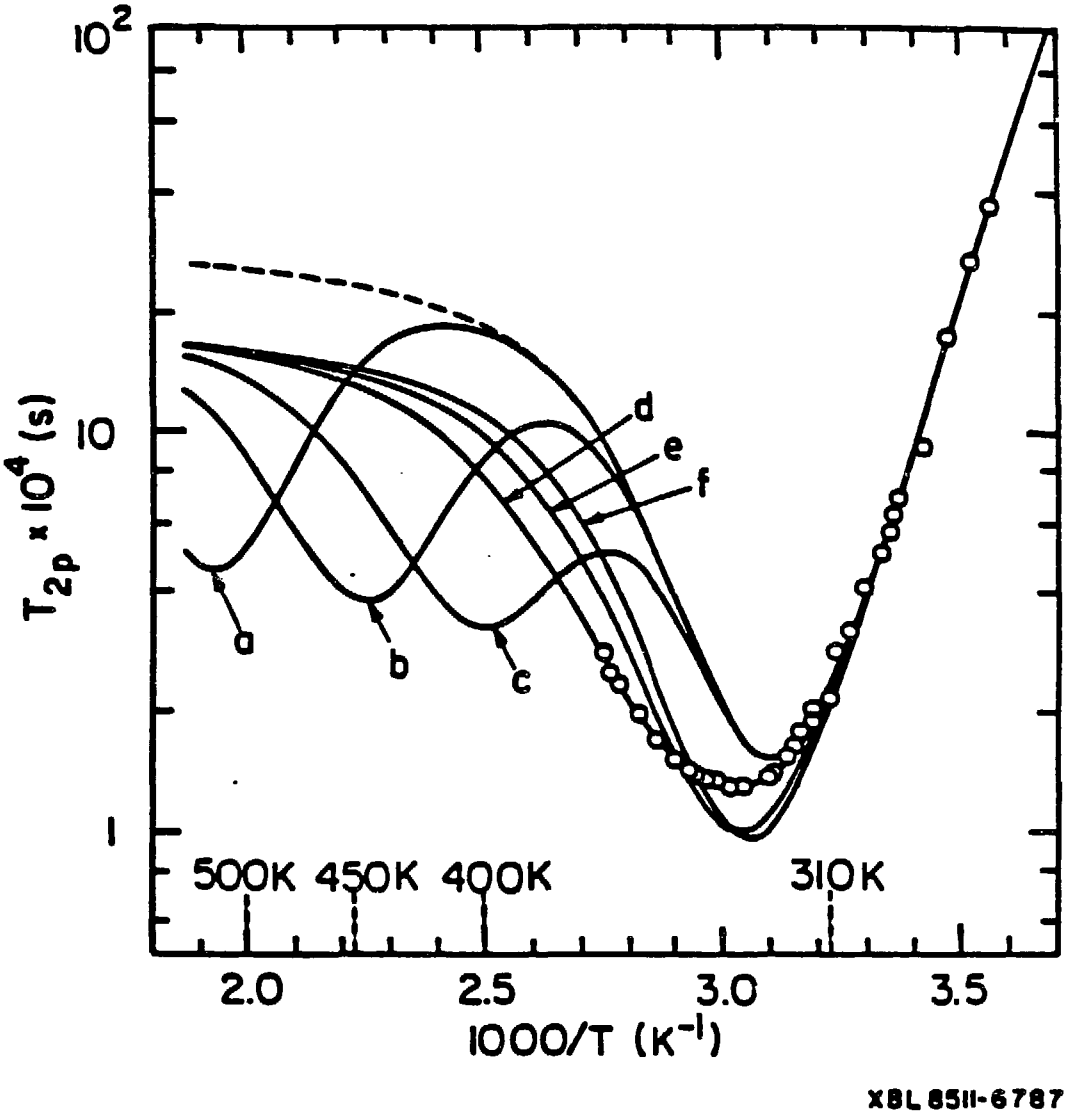
10^2
10
1
$T_{2p} \times 10^4$ (s)
a
b
c
d
e
f
500K 450K 400K
310K
2.0
2.5
3.0
3.5
1000/T (K^{-1})
XBL 8511-6787

Figure 1-4

APPENDIX A-1: Linewidth Data for 1:1 Ni(II):ida at 27.4 MHz

Solution: 0.0243 M $Ni(ClO_4)_2$ $6H_2O$, 0.0360 M iminodiacetic acid and NaOH to pH 5.72

Index:
- Column (4): $T_2(H_2O)^{-1}$
- Column (5): $T_2(Ni(H_2O)_6^{+2})^{-1}$
- Column (6): T_{2p}^{-1} for solution at experimental concentration
- Column (7): T_{2p}^{-1} factored for a 0.1 M Ni(II):ida solution
- Column (8): T_{2p}^{-1} calculated for 0.1 M Ni(II):ida with Scheme 2 and parameters in Table 1-3

Temp (K)	$\Delta\nu^{\ddagger}_{1/2}$ (Hz)	[Ni:ida] ($\times 10^2$,M)	(4) (s^{-1})	(5) (s^{-1})	(6) (s^{-1})	(7) (s^{-1})	(8) (s^{-1})
280.9	95.4	1.471	264.6	0.4	35	236 ± 151	302
283.9	91.0	1.460	240.0	0.5	46	311 ± 135	386
288.1	88.1	1.445	210.3	0.7	66	455 ± 115	540
292.1	95.7	1.431	185.7	1.0	114	796 ± 110	740
298.5	106.1	1.411	160.2	1.7	172	1220 ± 120	1190
303.7	118.2	1.397	143.4	2.5	226	1610 ± 120	1700
309.0	140.5	1.383	128.2	3.7	310	2240 ± 130	2370
313.5	166.5	1.373	117.1	5.1	401	2920 ± 160	3010
315.7	180.5	1.368	112.2	5.9	449	3280 ± 180	3340
319.2	196.9	1.361	104.7	7.5	506	3720 ± 190	3770
321.1	212.6	1.357	100.9	8.6	558	4110 ± 200	3980
328.4	220.7	1.343	88.2	13.3	592	4410 ± 210	4360
331.4	217.2	1.338	83.6	15.6	583	4360 ± 220	4340
329.5	215.4	1.341	86.4	14.1	576	4300 ± 210	4360
337.0	207.1	1.329	75.7	20.0	555	4180 ± 230	4130
335.3	207.0	1.332	78.0	18.7	554	4160 ± 210	4210
337.9	204.6	1.328	74.6	20.7	548	4120 ± 210	4090
340.8	198.7	1.324	71.0	22.6	531	4010 ± 230	3940
344.7	183.9	1.318	66.6	24.3	487	3690 ± 200	3730
350.2	170.4	1.312	60.9	24.6	450	3430 ± 170	3400
353.8	152.0	1.307	57.5	23.5	396	3030 ± 160	3120
359.1	138.3	1.302	53.0	20.7	361	2770 ± 150	2680
359.7	131.6	1.301	52.5	20.3	341	2620 ± 150	2620
363.3	115.4	1.297	49.7	18.0	295	2270 ± 110	2320

‡ Full linewidth at half height.

APPENDIX A-2: Linewidth Data for 1:1 Ni(II):ida at 27.4 MHz

Solution: 0.0477 M $Ni(ClO_4)_2$ $6H_2O$, 0.0755 M iminodiacetic acid and NaOH to pH 6.18

Index:
- Column (4): $T_2(H_2O)^{-1}$
- Column (5): $T_2(Ni(H_2O)_6^{+2})^{-1}$
- Column (6): T_{2p}^{-1} for solution at experimental concentration
- Column (7): T_{2p}^{-1} factored for a 0.1 M Ni(II):ida solution
- Column (8): T_{2p}^{-1} calculated for 0.1 M Ni(II):ida with Scheme 2 and parameters in Table 1-3

Temp (K)	$\Delta\nu^{\ddagger}_{1/2}$ (Hz)	[Ni:ida] ($x10^2$,M)	(4) (s^{-1})	(5) (s^{-1})	(6) (s^{-1})	(7) (s^{-1})	(8) (s^{-1})
296.5	99.6	1.417	167.3	1.4	144	1020 ± 120	1030
297.8	125.5	2.080	162.9	1.3	230	1110 ± 60	1130
300.4	139.8	2.074	153.9	1.6	284	1370 ± 60	1360
306.2	176.3	2.062	136.0	2.5	415	2010 ± 60	2000
311.3	220.9	2.052	122.3	3.7	568	2770 ± 70	2700
317.3	267.7	2.043	108.7	5.7	726	3560 ± 70	3530
322.9	301.9	2.034	97.6	8.4	842	4140 ± 80	4130
329.0	311.4	2.026	87.2	12.2	879	4340 ± 80	4360
333.7	303.1	2.020	80.2	15.7	856	4240 ± 80	4270
339.2	290.8	2.014	72.9	19.7	821	4080 ± 70	4020
344.8	271.8	2.009	66.5	22.5	765	3810 ± 70	3730
348.6	243.2	2.006	62.5	23.1	678	3382 ± 60	3500
361.9	179.1	1.996	50.8	18.0	494	2470 ± 50	2440

‡ Full linewidth at half height.

APPENDIX A-3: Linewidth Data for 1:1 Ni(II):mida at 27.4 MHz

Solution: 0.0561 M $Ni(ClO_4)_2$ $6H_2O$, 0.0900 M N-methyliminodiacetic acid and NaOH to pH 7.70

Index:
- Column (4): $T_2(H_2O)^{-1}$
- Column (5): $T_2(Ni(H_2O)_6^{+2})^{-1}$
- Column (6): T_{2p}^{-1} for solution at experimental concentration
- Column (7): T_{2p}^{-1} factored for a 0.1 M Ni(II):mida solution
- Column (8): T_{2p}^{-1} calculated for 0.1 M Ni(II):mida with Scheme 1 parameters in Table 1-4

Temp (K)	$\Delta\nu^{\ddagger}_{1/2}$ (Hz)	[Ni:mida] (x 10^2,M)	(4) (s^{-1})	(5) (s^{-1})	(6) (s^{-1})	(7) (s^{-1})	(8) (s^{-1})
280.0	104.5	2.167	272.5	0.5	55	254 ± 79	252
283.8	103.5	2.164	241.0	0.8	84	386 ± 71	345
288.2	104.8	2.161	209.7	1.2	118	547 ± 65	493
293.1	110.1	2.157	180.2	1.9	164	760 ± 59	728
297.0	121.7	2.153	163.5	2.8	216	1000 ± 60	1030
302.7	148.0	2.149	146.2	4.5	314	1460 ± 60	1500
307.9	172.1	2.144	131.2	7.0	402	1880 ± 60	2140
311.3	209.0	2.141	122.4	9.3	525	2450 ± 60	2730
315.9	260.1	2.137	111.7	13.5	692	3240 ± 70	3580
320.3	335.7	2.134	102.5	19.0	933	4370 ± 80	4460
327.7	429.5	2.128	89.4	32.0	1230	5770 ± 100	5940
330.3	438.3	2.125	85.3	37.8	1250	5900 ± 100	6320
333.8	454.1	2.122	80.1	46.3	1300	6130 ± 110	6610
336.7	465.0	2.120	76.2	53.6	1330	6280 ± 110	6630
339.3	444.7	2.118	72.8	60.0	1260	5970 ± 110	6500
342.1	440.1	2.115	69.5	65.9	1250	5900 ± 110	6130
344.8	431.5	2.113	66.5	70.3	1220	5770 ± 110	5850
350.0	390.9	2.109	61.1	74.0	1090	5180 ± 110	5010
354.6	330.2	2.105	56.8	71.6	910	4320 ± 100	4250
364.5	228.7	2.097	48.9	56.7	610	2920 ± 70	2960

‡ Full linewidth at half height.

APPENDIX A-4: Linewidth Data for 1:1 Ni(II):mida at 27.4 MHz

Solution: 0.0236 M $Ni(ClO_4)_2\ 6H_2O$, 0.0382 M N-methyliminodiacetic acid and NaOH to pH 6.11

Index:
- Column (4): $T_2(H_2O)^{-1}$
- Column (5): $T_2(Ni(H_2O)_6^{+2})^{-1}$
- Column (6): T_{2p}^{-1} for solution at experimental concentration
- Column (7): T_{2p}^{-1} factored for a 0.1 M Ni(II):mida solution
- Column (8): T_{2p}^{-1} calculated for 0.1 M Ni(II):mida with Scheme 1 and parameters in Table 1-4

Temp (K)	$\Delta\nu^{\ddagger}_{1/2}$ (Hz)	[Ni:mida] ($\times 10^3$,M)	(4) (s^{-1})	(5) (s^{-1})	(6) (s^{-1})	(7) (s^{-1})	(8) (s^{-1})
289.4	78.5	9.024	201.8	0.5	44	491 ± 148	545
294.0	78.0	8.978	175.5	0.8	69	765 ± 134	779
298.9	81.9	8.932	158.7	1.3	97	1090 ± 130	1140
303.7	90.2	8.891	143.3	2.0	138	1550 ± 120	1600
308.3	103.4	8.855	130.0	2.9	192	2170 ± 110	2200
313.2	125.4	8.819	117.9	4.3	272	3080 ± 120	3000
315.9	137.7	8.800	111.7	5.4	316	3590 ± 120	3530
318.6	152.9	8.782	105.9	6.6	368	4190 ± 120	4100
321.5	169.5	8.763	100.3	8.2	424	4840 ± 130	4710
325.0	190.4	8.741	93.8	10.6	494	5650 ± 140	5460
326.9	203.5	8.730	90.7	12.0	537	6150 ± 140	5800
329.6	211.0	8.713	86.3	14.3	562	6460 ± 140	6230
332.7	216.7	8.696	81.7	17.1	582	6700 ± 150	6540
336.0	217.8	8.678	77.1	20.3	587	6760 ± 150	6640
340.9	206.0	8.651	70.9	24.8	551	6370 ± 150	6350
346.0	187.3	8.625	65.2	28.0	495	5740 ± 140	5660
349.8	166.5	8.606	61.3	28.8	433	5030 ± 130	5030
354.2	146.0	8.585	57.1	28.0	374	4350 ± 120	4320
363.2	108.5	8.545	49.9	22.9	268	3140 ± 100	3100

‡ Full linewidth at half height.

APPENDIX A-5: Linewidth Data for 1:1 Ni(II):eida at 27.4 MHz

Solution: 0.0516 M $Ni(ClO_4)_2$ $6H_2O$, 0.0653 M N-ethyliminodiacetic acid and NaOH to pH 5.81

Index:
- Column (4): $T_2(H_2O)^{-1}$
- Column (5): $T_2(Ni(H_2O)_6^{+2})^{-1}$
- Column (6): T_{2p}^{-1} for solution at experimental concentration
- Column (7): T_{2p}^{-1} factored for 0.1 M Ni(II):eida solution
- Column (8): T_{2p}^{-1} calculated for 0.1 M Ni(II):eida with Scheme 1 and parameters in Table 1-4

Temp (K)	$\Delta\nu^{\ddagger}_{1/2}$ (Hz)	[Ni:eida] (x 10^2,M)	(4) (s^{-1})	(5) (s^{-1})	(6) (s^{-1})	(7) (s^{-1})	(8) (s^{-1})
280.8	134.9	3.425	265.7	2.8	155	453	444
286.1	151.2	"	223.7	4.5	247	721	695
290.0	166.9	"	198.0	6.4	320	934	951
294.6	203.6	"	174.7	9.5	455	1330	1360
299.4	267.0	"	157.0	14.1	667	1950	1940
303.9	345.4	"	142.5	20.2	922	2700	2640
308.5	445.4	"	129.6	28.7	1240	3620	3470
312.9	497.2	"	118.6	39.7	1400	4100	4320
318.6	600.5	"	106.0	59.8	1720	5020	5260
322.9	659.3	"	97.7	79.6	1900	5530	5610
325.2	711.0	"	93.6	92.1	2050	5980	5640
327.5	672.8	"	89.7	105.9	1920	5600	5560
330.3	644.0	"	85.2	124.5	1810	5290	5330
333.2	636.2	"	81.0	144.6	1770	5180	5000
336.2	574.2	"	76.9	165.1	1560	4560	4600
338.4	542.0	"	74.0	179.5	1450	4230	4290
342.6	494.6	"	68.9	202.1	1280	3750	3710
343.6	459.9	"	67.8	205.8	1170	3420	3580
346.1	420.2	"	65.1	212.3	1040	3040	3280
348.6	413.0	"	62.4	214.2	1020	2980	3000
355.8	353.5	"	55.8	195.9	859	2510	2380
360.2	316.2	"	52.1	173.7	768	2240	2090
364.1	283.2	"	49.2	152.1	688	2010	1890

‡ Full linewidth at half height.

APPENDIX A-6: Linewidth Data for 1:1 Ni(II):eida at 27.4 MHz

Solution: 0.0572 M $Ni(ClO_4)_2$ $6H_2O$, 0.0898 M N-ethyliminodiacetic acid, and NaOH to pH 7.90

Index:
- Column (4): $T_2(H_2O)^{-1}$
- Column (5): $T_2(Ni(H_2O)_6^{+2})^{-1}$
- Column (6): T_{2p}^{-1} for solution at experimental concentration
- Column (7): T_{2p}^{-1} factored for a 0.1 M Ni(II):eida solution
- Column (8): T_{2p}^{-1} calculated for 0.1 M Ni(II):eida with Scheme 1 and parameters in Table 1-4

Temp (K)	$\Delta\nu^{\ddagger}_{1/2}$ (Hz)	[Ni:eida] (x 10^2,M)	(4) (s^{-1})	(5) (s^{-1})	(6) (s^{-1})	(7) (s^{-1})	(8) (s^{-1})
276.3	120.1	2.376	308.8	0.4	68	287 ± 81	300
281.1	119.2	"	263.1	0.6	111	466 ± 72	456
286.4	124.3	"	221.9	1.0	168	706 ± 64	709
291.0	145.1	"	191.9	1.6	262	1100 ± 60	1030
295.7	170.0	"	170.4	2.3	361	1520 ± 60	1480
300.3	213.7	"	154.1	3.4	514	2160 ± 60	2060
304.8	251.0	"	140.1	4.8	770	2710 ± 60	2780
309.4	306.9	"	127.1	6.9	830	3490 ± 50	3650
313.9	358.7	"	116.1	9.7	1000	4210 ± 80	4520
318.5	416.2	"	106.2	13.3	1190	5000 ± 80	5240
322.5	472.7	"	98.4	17.4	1370	5770 ± 90	5590
331.7	436.5	"	83.1	30.1	1260	5300 ± 90	5180
336.8	381.4	"	76.0	38.1	1080	4560 ± 80	4510
340.9	326.0	"	70.9	43.6	910	3830 ± 100	3960
344.3	274.7	"	67.0	46.8	749	3150 ± 70	3490

‡ Full linewidth at half height.

APPENDIX A-7: Linewidth Data for 1:1 Ni(II):eida at 40.7 MHz

Solution: 0.0852 M $Ni(ClO_4)_2$ $6H_2O$, 0.127 M N-ethyliminodiacetic acid, and NaOH to pH 6.74

Index:
- Column (4): $T_2(H_2O)^{-1}$
- Column (5): $T_2(Ni(H_2O)_6^{+2})^{-1}$
- Column (6): T_{2p}^{-1} for solution at experimental concentration
- Column (7): T_{2p}^{-1} factored for a 0.1 M Ni(II):eida solution
- Column (8): T_{2p}^{-1} calculated for 0.1 M Ni(II):eida with Scheme 2 and parameters in Table 1-3

Temp (K)	$\Delta\nu^{\ddagger}_{1/2}$ (Hz)	[Ni:eida] (x 10^2,M)	(4) (s^{-1})	(5) (s^{-1})	(6) (s^{-1})	(7) (s^{-1})	(8) (s^{-1})
279.6	145.4	4.101	263.8	1.3	190	464 ± 44	403
288.1	183.4	"	211.2	2.8	360	878 ± 41	827
297.9	290.3	"	167.7	6.4	737	1800 ± 40	1780
307.3	511.6	"	137.2	13.4	1460	3550 ± 60	3470
316.8	878.2	"	113.9	27.0	2620	6380 ± 80	5970
320.5	951.9	"	106.6	35.3	2850	6950 ± 90	5950
322.9	994.1	"	102.0	41.8	2980	7260 ± 100	7490
325.4	1054.	"	97.6	49.5	3160	7720 ± 100	7920
329.0	1070.	"	91.9	62.3	3210	7820 ± 110	8210
331.8	1119.	"	87.8	73.7	3350	8180 ± 110	8170
334.4	1053.	"	84.3	85.4	3140	7650 ± 110	7920
337.3	998.7	"	80.6	99.7	2960	7210 ± 110	7470
340.9	929.1	"	76.3	118.1	2720	6640 ± 110	6750
344.6	840.3	"	72.2	135.9	2430	5930 ± 110	5950
345.7	798.9	"	71.1	140.4	2300	5600 ± 100	5720
348.5	755.1	"	68.3	150.7	2150	5250 ± 100	5140
351.2	688.8	"	65.9	157.1	1940	4730 ± 100	4620
355.2	579.3	"	62.4	159.5	1600	3900 ± 90	3950
359.0	517.5	"	59.4	154.0	1410	3440 ± 80	3420

‡ Full linewidth at half height.

APPENDIX B: Ligand Designations

bipy = 2,2'-bipyridine

diamol = 2,2-di(aminomethyl)-1-propanol

dien = diethylenetriamine

EDDA = ethylenediamine-N,N'-diacetate

EDTA = ethylenediamine-N,N,N'N'-tetraacetate

en = ethylenediamine

eida = N-ethyliminodiacetate

HEDTA = monoprotonated EDTA

ida = iminodiacetate

mida = N-methyliminodiacetate

NTA = nitrilotriacetate

1,3-PDTA = 1,3-propylenediamine-N,N'-diacetate

py = pyridine

terpy = 2,2',2''-terpyridine

2,2,2-tet = 1,4,7,10-tetraazacyclododecane

2,3,3-tet = 1,4,7,11-tetraazacyclotetradecane

tetren = tetraethylenediaminepentamine

tren = 2,2',2''-triaminoethylamine

trenol = 2,2'2,''-trihydroxytriethylamine

triam = 2,2-di(aminomethyl)-1-propylamine

trien = triethylenetetraamine

triol = 2,2'-di(hydroxymethyl)-1-propanol

APPENDIX C: Transverse Relaxation with Three-Site Exchange.

A treatment of a completely general three-site system is given by Angerman and Jordan (Chapter 1, Ref. 18). The general exchanging system is designed:

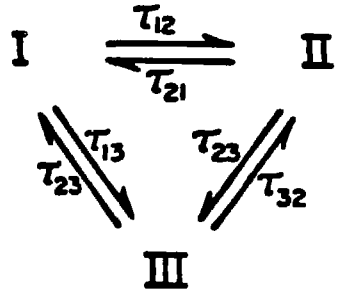

where τ_{ij} represents the lifetime of the nucleus in species i as controlled by the i-to-j site exchange. Under the conditions that [II] and [III] $\ll$ [I], the transverse relaxation for a spin in site I due to exchange is given by equation 1A of references 18.

The equalities below are made in using equation 1A to represent Schemes 1 through Schemes 3 in Chapter 1 where k_{ij} ($= \tau_{ij}^{-1}$) is the rate of transfer from site i to site j. Sites I, II and III in Ref. 18 represent environments A, B, and C, respectively in this work.

Scheme 1:

$$k_{12} = k_{ab} = P_b \cdot k_{ba}$$
$$k_{13} = k_{ac} = P_c \cdot k_{ca}$$
$$k_{21} = k_{ba}$$
$$k_{23} = 0$$
$$k_{31} = k_{ca}$$
$$k_{32} = 0$$

APPENDIX C (Continued)

$$P_b = 2[Ni:L]/(55.5-3[Ni:L])$$
$$P_c = [Ni:L]/(55.5-3[Ni:L])$$

and $k_{ba} = k_{ca}$

Scheme 2:

$k_{12} = k_{ab} = P_b \cdot k_{ba}$
$k_{13} = k_{ac} = P_c \cdot k_{ca}$
$k_{21} = k_{ba}$
$k_{23} = 0$
$k_{31} = k_{ca}$
$k_{32} = 0$

P_b, P_c: same as Scheme 1

Scheme 3:

$k_{12} = k_{ab} = P_b \cdot k_{ba}$
$k_{13} = k_{ac} = 0$
$k_{21} = k_{ba}$
$k_{23} = k_{bc} = k_{cb}/2$
$k_{31} = 0$
$k_{32} = k_{cb}$

P_b, P_c: same as Scheme 1

REFERENCES

1 Swift, T.J., "NMR of Parmagnetic Molecules," Lemar, G.N.; Horrocks, W. DeW. Jr.; Holm, R.H., ed.; Academic Press, New York, 1973, Chapter 2.

2 Lincoln, S.F.; Hounslow, A.M.; Pisaniello, D.L.; Doddridge, B.G.; Coates, J.H.; Merbach, A.E.; Zbinden, D. Inorg. Chem. 1984, 23, 1090-1093.

3 Ikeda, Y.; Tomiyasu, H.; Fukutomi, H. Inorg. Chem. 1984, 23, 1356-1360.

4 Moore, P.; Sachnidis, J.; Willey, G.R. J. Chem. Soc. Dalton 1984, 1323-1327.

5 Summers, M.F.; Marzilli, L.G.; Bresciani-Pahor, N.; Randaccio, L. J. Amer. Chem. Soc. 1984, 106, 4478-4485.

6 Kustin, K.; Vriesenga, J.; "Inorganic Materials Research Division Annual Report, Lawrence Berkeley Laboratory, UCRL-18735, 14 (1968).

7 Rablen, D.P.; Dodgen, H.W.; Hunt, J.P. Inorg. Chem. 1976, 15, 931-933.

8 West, R.J.; Lincoln, S.F. Inorg. Chem. 1973, 12, 495-497.

9 Rowland, T.V.; Ph.D. Dissertation, University of California, Berkeley, 1975.

10 Hunt, J.P. Coor. Chem. Rev. 1971, 7, 1-10, and references therein.

11 Lincoln, S.F.; West, R.J. J. Amer. Chem. Soc. 1974, 96, 400-404.

12 West, R.J.; Lincolm. S.F. Inorg. Chem. 1973, 12, 494-497.

13 Plotkin, K.; Copes, J.; Vriesenga, J.R. Inorg. Chem. 1973, 12, 1494-1498.

14 Swift, T.J.; Connick. R.E. J. Chem. Phys. 1962, 37, 307-320.

15 Boubel, J.C.; Delpuech, J.J. Mol. Phys., 1974, 27, 113-127.

REFERENCES (Continued)

16 Boubel, J.C.; Delpuech, J.J.; Peguy, A. J. Chem. Soc. Dalton, 1978, 1506-1510.

17 Fuentes, R.; Morgan, L.O.; Matwiyoff, N.A. Inorg. Chem. 1975 14, 2774-2779.

18 Angerman, N.S.; Jordan R.B. Inorg. Chem. 1969 8, 1824.

19 Blatt, A.H.; "Organic Synthesis: Volume 2", 1943, Wiley, p 397.

20 Rose, K.D.; Bryant, R.G J. Amer. Chem. Soc. 1980, 102, 21-24.

21 Neely, J.W.; Connick, R.E. J. Amer. Chem. Soc. 1972, 94, 3419-3424.

22 Jones, J.P.; Brillo, E.J.; Margerum. D.W.; J. Amer. Chem. Soc. 1970, 92, 1875-1880.

23 Combs, L.C.; Margerum. D.W. Inorg. Chem. 1970, 9, 1711-1716.

24 Coetzee, J.F.; Karakatsanis, C.G. Inorg. Chem. 1976 15, 3112-3114.

25 Mammano, N.J.; Templeton, D.H.; Zalkin, A. Acta Cryst. 1977, B33 1251-1254.

26 Sillen, L.G.; Martell, A.E.: "Stability Constants of Metal Ion Complexes", The Chemical Society of London, Special Publications No. 17 (1964) and No. 25 (1971).

CHAPTER 2

ANALYSIS OF THE ^{13}C LONGITUDINAL RELAXATION RATES OF THE BIS-LIGAND ZINC(II) COMPLEXES WITH IDA, MIDA AND EIDA

CONTENTS

INTRODUCTION

Increased attention has been given lately to ^{13}C NMR spectra of metal complexes with organic ligands. The ^{13}C shifts and relaxation rates of all the carbons are useful in obtaining relevant parameters about the solution state behavior of the complex. Carbon-13 spectra are usually simpler than proton spectra due to the smaller number of magnetically non-equivalent atoms and the absence of carbon-carbon spin coupling. The typical separation of carbon peaks in frequency units is larger than in the proton spectrum, therefore a larger range of rates is accessible for dynamic processes.

This chapter contains a ^{13}C NMR study of the diamagnetic Zn(II) complexes with ida, mida and eida. The carbon spectra confirm the metal-ligand configuration of the complexes in solution. Longitudinal relaxation rates (T_1^{-1}) and nuclear Overhauser enhancement (nOe) provide information about the relaxation mechanism of the carbons. The temperature dependence of the relaxation rate measurements is analyzed using models for molecular motion to determine the molecular tumbling rate constants which will be used in the complementary ^{13}C study of the paramagnetic Ni(II) complexes in Chapter 3. The extent of rotation about carbon-carbon and carbon-nitrogen bonds in the alkyl chains of the mida and eida complexes is also determined from the longitudinal relaxation measurements.

The primary concern is to relate the effects of the different N-substitutents to the properties and kinetic behavior of the complexes. A brief discussion is also offered on the use of carbon relaxation in ligands with alkyl chains to gain insight into the spacial conditions near the metal center of a complex.

THEORETICAL CONSIDERATIONS

The use of relaxation time to study molecular motions is well established.[1,2,3,4,5] For a carbon in a CH, CH_2 or CH_3 group of a diamagnetic system the primary mechanism of relaxation is the dipole-dipole interaction of the carbon with directly attached proton spins. The interaction is modulated by reorientation of the carbon-hydrogen vector connecting the spins. Any motion in the range 10^8 - 10^{12} s^{-1} can affect the carbon relaxation.[3] Molecular tumbling is of primary important in affecting dipole-dipole relaxation. Internal motions can also be important under appropriate conditions.[3]

The dipole-dipole longitudinal relaxation rates (T_1^{-1}) and the nuclear Overhauser enhancement factor (nOe = 1 + η) may be written:[6,7]

$$\frac{1}{T_{1(DD)}} = \frac{1}{10} N\gamma_C^2\gamma_H^2\hbar^2 r^{-6}[J(\omega_H-\omega_C) + 3J(\omega_C) + 6J(\omega_H+\omega_C)] \qquad [2\text{-}1]$$

$$nOe = 1 + \frac{\gamma_H}{\gamma_C}\left[\frac{6J(\omega_H+\omega_C) - J(\omega_H-\omega_C)}{J(\omega_H-\omega_C) + 3J(\omega_C) + 6J(\omega_H+\omega_C)}\right] \qquad [2-2]$$

Parameter N is the number of directly attached hydrogens, γ_C and γ_H are the gyromagnetic ratios of carbon and hydrogen, respectively, and r is the carbon-hydrogen internuclear distance. The Larmor frequencies of the carbon and proton are ω_C and ω_H, respectively. Cross correlation effects are expected to small and will not be considered in this study.[3] The spectral density functions $J(\omega_I)$ are given by:

$$J(\omega_I) = FT(G(t)) = \int_{-\infty}^{\infty} G(t)\exp(-i\omega_I t)\,dt \qquad [2-3]$$

where FT indicates the Fourier transformation and G(t) is the autocorrelation function.

For a C-H vector in a molecule tumbling isotropically the autocorrelation function is a single exponential and the spectral density function is of a relatively simple form:

$$J(\omega_I) = \frac{\tau_o}{1 + \omega_I^2\tau_o^2} \qquad [2-4]$$

where τ_o is the time constant of the correlation function. Under extreme narrowing conditions ($\omega_I^2\tau_o^2 \ll 1$), $J(\omega_I) = \tau_o$, nOe (= 1.988) is maximal and equation [2-1] reduces to:

$$\frac{1}{T_1(DD)} = N\gamma_C^2\gamma_H^2\hbar^2 r^{-6}\tau_o \qquad [2\text{-}5]$$

The rotational diffusion constant D_o is also used to describe the rate behavior of an isotropically tumbling molecule and is related to τ_o by the expression:

$$\tau_o = \frac{1}{6D_o} \qquad [2\text{-}6]$$

If the molecular tumbling is anisotropic or if internal motion must be considered, the reorientation of the C-H vector is more complex. The autocorrelation function usually involves more than a single exponential and the functional form of the spectral density function depends on the details of all the relevant motions. The case of anisotropic motion will be considered in the discussion section of this chapter. The effects of internal motions on relaxation rates is considered below.

The systematic analysis of spins subject to both molecular tumbling and internal motion has been limited to a few well defined systems. The internal motion must be sizeable since small displacements do not affect T_1, regardless of the rate.[6] The motion must also be described by a reasonable number of parameters. The most well-studied internal motion is methyl rotation which is described by a single rotational diffusion constant. Other internal motions which have been studied are phenyl rotation,[8,9] librational motions in ring

carbons[10] and rotation about carbon-carbon bonds in longer alkyl chains.[11,12]

For ^{13}C spin undergoing methyl rotation in an isotropically tumbling molecule the relaxation rate is given by the expression:[1]

$$\frac{1}{T_1(DD)} = N\gamma_C^2\gamma_H^2\hbar^2 r^{-6}\left(\frac{A}{6D_o} + \frac{B}{6D_o + aD_i} + \frac{C}{6D_o + amD_i}\right) \qquad [2\text{-}7]$$

$$A = \frac{1}{4}(3\cos^2\Delta - 1)^2$$

$$B = \frac{3}{4}(\sin^2 2\Delta)$$

$$C = \frac{3}{4}(\sin^4\Delta)$$

For a stochastic diffusion model (all rotational orientations having equal probability) D_i is the internal methyl rotational diffusion constant in reciprocal seconds. Rotational diffusion constant D_i must be multiplied by statistical factors a = 1 and m = 4 for the stochastic model. For a rapid-jump model (rapid jumps from one position to another) D_i is the jump rate in jumps per second, a = r/2 for an r-jump model and m = 1. A, B and C are geometric factors determined by the angle Δ between the vector connecting the carbon and hydrogen dipoles and the rotation axis which is usually taken to be the carbon-carbon bond connecting the methyl carbon to the remainder of the molecule.

The Woessner method[1,13] of determining methyl rotation rates of carbons in an isotropically tumbling molecule consists of determining

the rotational diffusion constant D_o for the whole molecule from the relaxation of known "rigid" carbons, i.e., those which reorient only with molecular tumbling, then determining D_i for each rotating methyl carbon ("non-rigid" carbons) using D_o and equation [2-7].

Equations [2-5] through [2-7] produce the useful ratio:

$$\theta = \frac{N(i)\cdot T_1(i)}{N(j)\cdot T_1(j)} = A + \frac{B}{1 + a\alpha} + \frac{C}{1 + am\alpha} \qquad [2\text{-}8]$$

$$\alpha = \frac{D_i}{6D_o}$$

where i designates a known rigid carbon in the molecule and j designates another carbon in the same molecule undergoing methyl rotation with rotation diffusion constant D_i. Equation [2-8] assumes equal carbon-hydrogen distances for the two carbons. For illustrative purposes, a plot of $\log(D_i/D_o)$-versus-θ is shown in Figure 2-1 for $\Delta = 109^o$. For both the stochastic and jump models θ has a maximum value of unity when $D_i \ll D_o$ representing highly inhibited methyl rotation. When $D_i \gg D_o$ the ratio is a minimum ($\theta = 0.116$) representing completely uninhibited methyl rotation. Figure 2-1 shows that θ is always equal to or less than one. It also demonstrates that information about the rate of methyl rotation can be obtained from relaxation rates only if D_i is within a reasonable range of D_o ($0.1D_o < D_i < 100D_o$). The information is least reliable near the limits where small changes in θ make a large difference in D_i/D_o.

EXPERIMENTAL

1:2 Zn(II):ligand solutions were made with iminodiacetic acid, N-methyl iminodiacetic acid and N-ethyl iminodiacetic acid (See Chapter 1) to a final concentration of 0.2 M in metal ion. Zinc perchlorate (98.8%), $Zn(ClO_4)_2$ $6H_2O$, was obtained from Alfa Products and used without additional purification. The solutions were adjusted to *ca.* pH 7 with concentrated NaOH. Each sample also contained *ca.* 0.04 M 1,4-dioxane for an internal shift reference. The samples were not degassed since degassing is not necessary for carbons with T_1 values less than 5 s.

Natural abundance Fourier transform ^{13}C spectra were obtained with a Bruker AM-500 spectrometer operating at 125 MHz. Longitudinal relaxation measurements were performed using the $(T-180-\tau-90)_x$ fast inversion recovery pulse sequence, FIRFT,[14] with broad-band decoupling. A total of 32K data points were collected with a sweep width of 30 KHz and radio frequency set mid-way between the C_α and C_N peaks. The 180° pulse was $(25.4 \pm 0.2) \times 10^{-6}$ s and the 90° pulse was assumed to be one-half this value. The recovery time between scans was about two times the longest T_1 (not considering the carboxylate carbons). A total of 96 scans was accumulated for each of eight different τ values by processing one dummy scan then collecting 16 scans at each τ value while rotating through the list of τ values a total of six times. Quadrature phase detection was employed for all experiments.

Nuclear Overhauser enhancement factors were determined using gated decoupling techniques. Experiments were set up to obtain two spectra (280 scans each) at each temperature. One spectrum was acquired with constant broad-band decoupling and another using gated decoupling with the broad-band decoupler on only during acquisition. The recovery time was at least ten times the longest T_1.

The temperature was controlled by a Bruker heat unit. Each 5 mm sample tube contained a concentrically mounted capillary of ethylene glycol. A proton spectrum (8 scans) was taken immediately after collecting each ^{13}C spectrum. The frequency separation of the two ^{1}H ethylene glycol peaks was used to determine the temperature with the calibration curve given in Chapter 1. The temperature values are considered to be accurate within ± 0.2 degrees.

RESULTS

^{13}C chemical shifts and coupling constants are given in Table 2-1 using the carbon designations given on the next page. The assignments are in agreement with other ^{13}C studies of diamagentic complexes with the same ligands.[15] The ^{13}C spectra are consistent with the coordination of two tridentate ligands (ida, mida or eida) per metal ion. The appearance of only one set of carbon peaks for the C_N and C_O carbons with each complex suggests that only the trans isomer is stable in solution. An alternative explanation is the existence of a

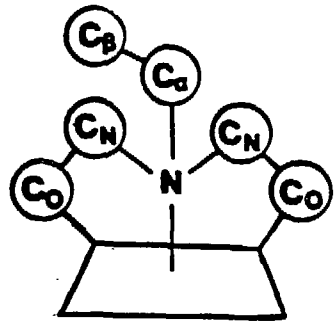

Carbon Labeling

rapid dynamic process which interconverts the trans and cis isomers thus producing a single averaged set of carbon peaks.

The nOe values were calculated with the expression:

$$nOe = \frac{(\text{peak area with decoupling}) - (\text{peak area without decoupling})}{(\text{peak area without decoupling})}$$

The nOe values for all the protonated carbons in the complexes are near 1.988 (± 10%), the value expected for a carbon with relaxation due entirely to the carbon-hydrogen dipole-dipole mechanism. Therefore, $T_1(DD)^{-1}$, the longitudinal relaxation rate due to the C-H dipole-dipole interaction, is set equal to the observed longitudinal relaxation rate in each case.

Relaxation times (Table 2-2) were obtained using the peak intensities from the FIRFT spectra. A three-parameter fit was used:

$$A_\tau = A_3 + A_2 \exp\left(\frac{-\tau}{T_1}\right) \qquad [2\text{-}9]$$

where A_τ is the peak intensity, τ is the delay time and T_1, A_2 and A_3 are the three parameters determined in the fit. T_1 is the longitudinal relaxation rate. A_3 is the relative peak intensity at infinite delay time and A_2 is given by:

$$A_2 = -\left[2 - \exp\left(-\frac{D+Ac}{T_1}\right)\right]$$

where D and Ac are the recovery and acquisition times, respectively. With typical values of (D+Ac) about three times the longest T_1, expected values of A_2 were between -1.9 and -2.0. In practice, values between -1.50 and -1.85 were obtained, probably due to incomplete inversion of the spins with the 180° pulse. Ideally the magnitude of the magnetization vector immediately after the 180° pulse (M_o) equals the magnitude of the magnetization vector after infinite times (M_∞) but of opposite sign:

$$M_o = -M_\infty$$

If the inversion of the spins over the entire sample within the coil of the probe is less than 100% efficient $|M_o|$ will be less than $|M_\infty|$ and a factor for incomplete inversion must be included in the expression for A_2.[16] This factor does not affect the value of T_1 determined in the fit.

A typical fit of the τ-verses-peak intensity data is shown in Figure 2-2. The good fit using the 3-parameter expression (equation [2-9]) is evidence that the protons were sufficiently irradiated and that the cross correlation is negligible, as expected.[17]

Molecular Rotation: The longitudinal relaxation rates of the C_N carbons at each temperature are plotted in Figure 2-3. The error bars represent an estimated 5% error in the T_1 values. In the analysis a 10% error was estimated for the C_α and C_β relaxation times consistent with the one-half relative abundance for these carbons.

The linear pattern in Figure 2-3 is consistent with the behavior predicted with isotropic relaxation (Equation [2-5]) assuming an Arrhenius type equation for the temperature dependence of the rotation correlation time:

$$\tau_o = \tau_r^o \exp\left(\frac{-E_r^o}{RT}\right)$$

A linear least squares fit of the data produced the energies of activation E_r^o (from the slope) and the preexponential τ_r^o (from the intercept) given in Table 2-3. The carbon-hydrogen distance used with equation [2-5] was 109 pm for all complexes.

In using equations [2-5] it is assumed that the C_N carbons are rigid. It is likely that the acetate arms containing the C_N carbons

can be detached for short periods of time from the metal at the oxygen-metal bond, or, to a lesser extent, at the nitrogen-metal bond.[18] It is also possible that an additional intramolecular process responsible for cis-trans interconversion is contributing to the reorientation of the methylene carbons. The former involves the making and breaking of a bond to the metal which is too slow to affect the relaxation rate. The latter process would be indistinquishable from anisotropic molecular tumbling.

The activation energies for molecular tumbling (Table 2-3) are nearly equal for the three complexes and are reasonable compared to values seen with other complexes. Unfortunately, a comparison of the parameters E_r^o and τ_r^o for the purpose of establishing trends was not justified due to the experimental uncertainty in the data and the large correlation between E_r^o and τ_r^o seen in the fitting process. It is not known how each of the parameters is affected by the substitution of the amine proton in ida for a methyl or ethyl groups.

A comparison of tumbling rates at each temperature is justified. The trend in tumbling rates seen over the entire temperature range is

ida > mida > eida

The slower tumbling rate with the bis-mida and bis-eida complexes is readily explained by the increase in size of the complex in going to larger N-substituent groups. For comparison, the tumbling rates may

be calculated by the Stokes-Einstein relationship for rotational diffusion which is generally reliable for a solute molecule at least three times the diameter of the solvent molecule:[19]

$$\tau_r = \frac{4\pi r^3 \eta}{3kT} \qquad [2\text{-}10]$$

Here r is the microscopic radius of the rotating sphere and η is the viscosity of the medium. The viscosity of the solutions in this study do not vary appreciably for the different complexes therefore the only factor in equation [2-10] that differs for each complex is the radius. A value of r = 410 pm is reasonable for the bis-ida complexes based upon the distance from the metal ion to the farthest carboxylate oxygen seen in crystallographic studies.[20] The calculated value of τ_o at 298 K (η ≅ 1.00 cP) for the bis-ida complex using equation [2-10] is 7.1×10^{-11} s.

A modified version of the equation [2-10] includes a microviscosity correction factor f_r:[21]

$$\tau_r = \frac{4\pi r^3 (\mu f_r)}{3kT}$$

The correction factor compensates for the finite thickness of solvent layers around the tumbling molecule. Values of f_r between 1/6 and 1/12 have been determined for the tumbling of a molecules in different pure solvents.[10,21] A value of f = 1/12 was used to describe molecular tumbling of a metal ion complex in solution.[22] In theory, f_r approaches unity as the size of the tumbling molecules increases

relative to the size of a solvent molecules. This is confirmed in studies with large solute molecules in organic solvents.[23] Studies of large molecules in aqueous solutions were not found. The difference in the calculated τ_o using equation [2-10] and the value obtained from relaxation rates warrants the use of a microviscosity correction factor less than unity.

Equation [2-10] predicts a decrease in tumbling rate with an increase in molecular size. An estimate of the relative volume of each complex can be made by considering the number of non-proton atoms. The bis-mida complex is estimated to be 10% larger in volume than the bis-ida complex. The bis-eida complex is about 10% larger than the bis-mida complex. Using the rates obtained in this study at 298 K and the volume dependence given in equation [2-10] (volume = $4\pi r^3/3$), the increase in going from the bis-mida to the bis-eida complex is consistent with this estimate. The difference in the bis-ida and bis-mida complexes is much greater than expected. This suggests that the substitution of an alkyl group for an amine proton is much more disruptive of the tumbling behavior than increasing the length of an alkyl group already attached.

Internal Motion: In examining the relaxation rates for the other carbons (Table 2-2) it is seen that T_1 for the C_α and C_N carbons in the bis-eida complex are nearly equal (N = 2 in both cases). Apparently rotation about the C_α-N bond is highly restricted due to

steric constraints and C_α may be regarded as a rigid carbon. The value of $N \cdot T_1(DD)$ for the C_α carbon in the bis-mida complex and for the C_β carbon in the bis-eida complex, however, is less than the value for the rigid C_N carbons in the respective complexes as indicated by values of Θ less than unity (Table 2-2). It can be concluded that additional motion is operating in the portion of each complex containing these carbons. A reasonable assumption is rotation about the bond attaching each carbon to the remainder of the molecule.

The C_α carbon in the bis-mida complex and C_β is the bis-eida complex were treated by the Woessner method using equation [2-7] with $\Delta = 109^\circ$. The rotational diffusion constants D_1 at each observed temperature are plotted in Figure 2-4. The three-jump model was used to produce these values, since a rapid-jump model is physically more reasonable than a stochastic model for internal rotation in these complexes. John and McClung have shown that modulation of the internuclear distance can also give rise to nuclear relaxation.[4] Their treatment and other more elaborate models[7,24,25] are not warranted in this study due to the accuracy of the results.

The use of equation [2-7] to determine the rate constant for rotation about the C_α-C_β bond in the bis-eida complex was possible only because rotation about the C_α-N bond is highly restricted. Equation [2-7] was derived for rotation about a bond having conformers of equal potential, i.e., methyl rotation. The formulation exists[5,7,11,26,27] for evaluating rates of rotation if rotation is occuring about all the bonds in an ethyl group (as well as in larger

alkyl chains), but the treatment requires knowledge of the energy differences of the possible rotational conformers and their relative occupancy. Since this information is not known, the usual procedure is to assume equal conformer potentials and populations. This appears to be a reasonable assumption in some cases. It would be unreasonable for the bis-eida complex in this study where the carbon chain is subjected to restricted motional freedom. Rotation about the C_α-N bond in the bis-mida complex is rapid whereas rotation about the same bond in the bis-eida complex is highly restricted. The only difference in these two complexes is the additional carbon (C_β) in the latter.

The logarithm of the rotational diffusion constants for the N-C_α bond in the bis-mida complex and the C_α-C_β bond in the bis-eida complex are consistent with a linear dependence on temperature (Figure 2-4). An Arrhenius-type equation was assumed:

$$D_i = D_i^o \exp\left(\frac{V^o}{RT}\right)$$

and a least squares fit of the data gives the energy barrier for rotation V^o and the preexponential D_i^o reported in Table 2-3.

DISCUSSION

In regard to ^{13}C NMR spectroscopy, the overwhelming occurence in nature of the CH, CH_2 and CH_3 arrangements in their natural isotopic abundances is particularly fortunate. The carbons in a molecule are relaxed largely by the interaction with their own set of directly attached protons and with little involvement of other CH_n groups. Each relaxation time reveals motional information about that particular portion of the molecule and relaxation times for several carbons in a molecule can provide a fairly complete picture of motions operating throughout the molecule. The problem, of course, is relating the relaxation data with the use of a suitable model which contains a reasonable number of meaningful parameters.

The tumbling motion of the complexes in this study is not completely isotropic, yet the assumption of isotropic molecular tumbling was necessary in order to determine both the molecular tumbling rates and the rates of methyl rotation. The effect of anisotropic motion depends upon the position of each carbon relative to the principle diffusion axis and upon the diffusion rate constants (D_x,D_y,D_z) about each axis.[9,13,28,29,30,31,32] Since internal motions also cause the relaxation rates to vary, the investigations of internal motion and anisotropic behavior are interrelated and frequently unsolvable.

The assumption of isotropic tumbling in this study is not unreasonable since the overall shape of the bis-complexes is largely

spherical. In general, the shape of a molecule must be appreciable distorted from a spherical form in order to warrant an anisotropic interpretation.[10] Relevant to the investigation of internal motions, studies of molecules with known anisotropic motion and internal methyl rotation show that the deduced barriers to methyl rotation did not differ appreciably when the isotropic and anisotropic models were used.[33,34] Validation of the isotropic assumption in this study is also given by the near equal relaxation rates of the C_N and C_α carbon in the mida complex. Their rates could be equal due to a highly coincidental combination of atom placement, rotational diffusion rates and rate of internal motion for the C_α carbon. It is more likely that both atoms are rigidly bound and that molecular tumbling is adequately described as isotropic.

There are very few data for comparing the rates of methyl rotation in other metal complexes where the motion is affected by the metal-ligand structure. With organic molecules, in general, methyl group rotation is considered to uninhibited if the activation energy is less than ca. 2 kcal mol^{-1}. The activation energies obtained with the mida and eida complexes in this study indicate that very little inhibition exists with methyl rotation. The value of D_i^o for methyl rotation is usually assumed equal to the jump rate or diffusion rate of a freely rotating methyl group:[1]

$$D_i^o = \left(\frac{kT}{I}\right)^{1/2} = 8.7 \times 10^{12}\ s^{-1} \qquad (298\ K)$$

where I is the moment of inertia of the methyl group. The value of D_i^o

obtained for the bis-eida complex in this study shows reasonable agreement. The value obtained with the bis-mida complexes is much smaller, but considerable uncertainty exists in its determination.

The results in this study indicate that considerable information can be obtained about the internal motion of alkyl groups in metal complexes, particularly if the alkyl group is only a few carbons long and secured directly to the rigid portion of the complex. Conditions related to freedom of motion, such as steric crowding, can be assessed. If the alkyl group is near the metal ion it is conceivable that motion could be related to activity at the metal ion including ligand exchange and other substitution reactions.

The results are most meaningful when compared to values obtained with other complexes containing alkyl groups. Complexes which already contain alkyl groups are excellent candidates for further relaxation studies. It is also possible to attach an alkyl group to an existing ligand at an appropriate site, for example, at a primary or secondary nitrogen, or to add a second "spy" ligand to an existing metal-ligand complex. In each case, a study of ^{13}C relaxation rates can provide a useful method of studying dynamic behavior in the complex.

TABLE 2-1

^{13}C Chemical Shifts (ppm)[†]

Complex	C_o	C_N	C_α	C_β
1:2 Zn(II):ida	115.53	-10.26	-	-
1:2 Zn(II):mida	114.52	-1.83	-18.80	-
1:2 Zn(II):eida	115.33	-4.34	-12.02	-54.09

[†] 25 °C, relative to internal 1,4-dioxane. Positive chemical shift is downfield.

TABLE 2-2

T_1 Measurements with Broadband Decoupling

Complex	T, °C	T_1, s (θ)*		
		C_N	C_α	C_β
1:2 Zn(II):ida	30.5	0.79		
	51.5	1.24		
	72.4	1.86		
1:2 Zn(II):mida	31.0	0.54 (1.0)	0.60 (0.68)	
	53.0	0.91 (1.0)	0.79 (0.77)	
	72.6	1.36 (1.0)	1.11 (0.82)	
1:2 Zn(II):eida	29.8	0.47 (1.0)	0.48 (.98)	1.23 (.25)
	52.0	0.74 (1.0)	0.72 (1.0)	1.87 (.26)
	72.7	1.10 (1.0)	1.12 (.98)	2.40 (.31)
	93.5	1.63 (1.0)	-	-

* Value in parenthesis is the ratio $\theta = N(i) \cdot T_1(i) / N(j) \cdot T_1(j)$ where atom i is the C_N carbon in each complex and j is the other carbon atom in the same complex.

TABLE 2-3

Molecular Tumbling and Methyl Rotation Rate Parameters

A. Molecular Tumbling

Complex	E_r^o (kcal mol^{-1})	τ_r^o ($x10^{14}$, s)	τ_r (s, 298 K)
1:2 Zn(II):ida	4.2 ± 0.3	3 ± 1	3.3×10^{-11}
1:2 Zn(II):mida	4.6 ± 0.3	2 ± 1	5.0×10^{-11}
1:2 Zn(II):eida	4.3 ± 0.3	4 ± 1	5.7×10^{-11}

B. Methyl Rotation

Complex	V^o (kcal mol^{-1})	D_1^o ($x10^{-10}$, s^{-1})	D_1 (s^{-1}, 298 K)
1:2 Zn(II):mida†	1 ± 2	1 ± 20	9×10^9
1:2 Zn(II):eida‡	2 ± 1	400 ± 300	7×10^{10}

† Rotation about the C_α-N bond.

‡ Rotation about the C_α-C_β bond.

CAPTIONS TO FIGURES

Figure 2-1: The function $\Theta = N(i)\ T_1(i)/N(j)\ T_1(j)$ for the three-jump and the stochastic models. Only values for D_1 within a reasonable range of D_o will be detectable as a reduction in the relaxation rate.

Figure 2-2: Peak intensity-verses-delay time for the C_N carbon (○), C_α (□) and C_β (■) in the 1:2 Zn(II):eida complex. Calculated curves are for the C_N and C_β carbons as indicated

Figure 2-3: Longitudinal relaxation rate-verses-temperature for the C_N (○) and C_α (●) carbons in 1:2 Zn(II):eida, the C_N carbon in 1:2 Zn(II):mida (□) and the C_N carbon in 1:2 Zn(II):ida (△).

Figure 2-4: Rotational diffusion constants as a function of temperature for rotation about the C_α-C_β bond in the 1:2 Zn(II):eida complex (●) and about the N-C_α bond in 1:2 Zn(II):mida (■).

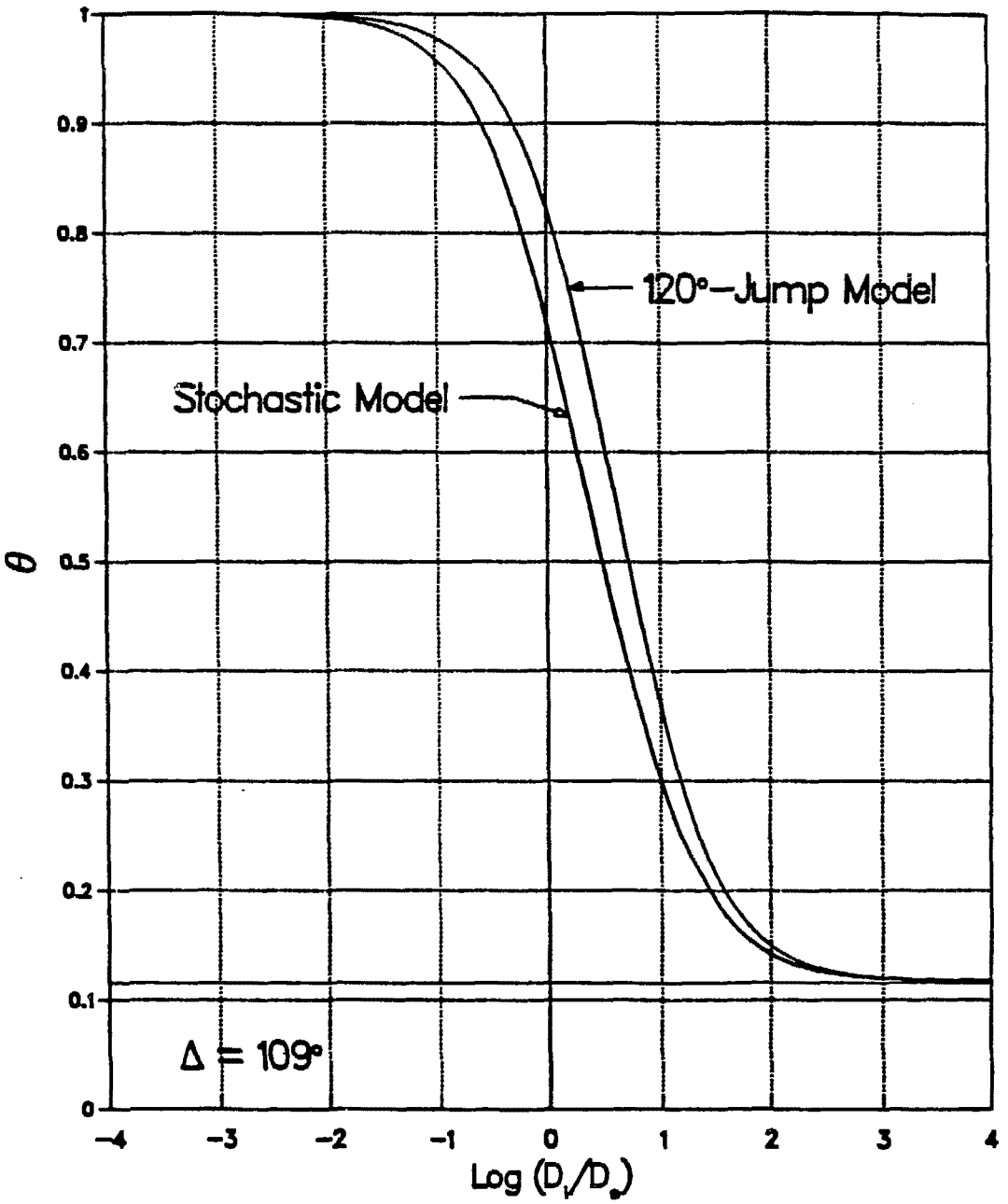
1
0.9
0.8
0.7
0.6
0.5
0.4
0.3
0.2
0.1
0
θ
120°–Jump Model
Stochastic Model
Δ = 109°
−4
−3
−2
−1
0
1
2
3
4
Log (D_v/D_e)

Figure 2-1

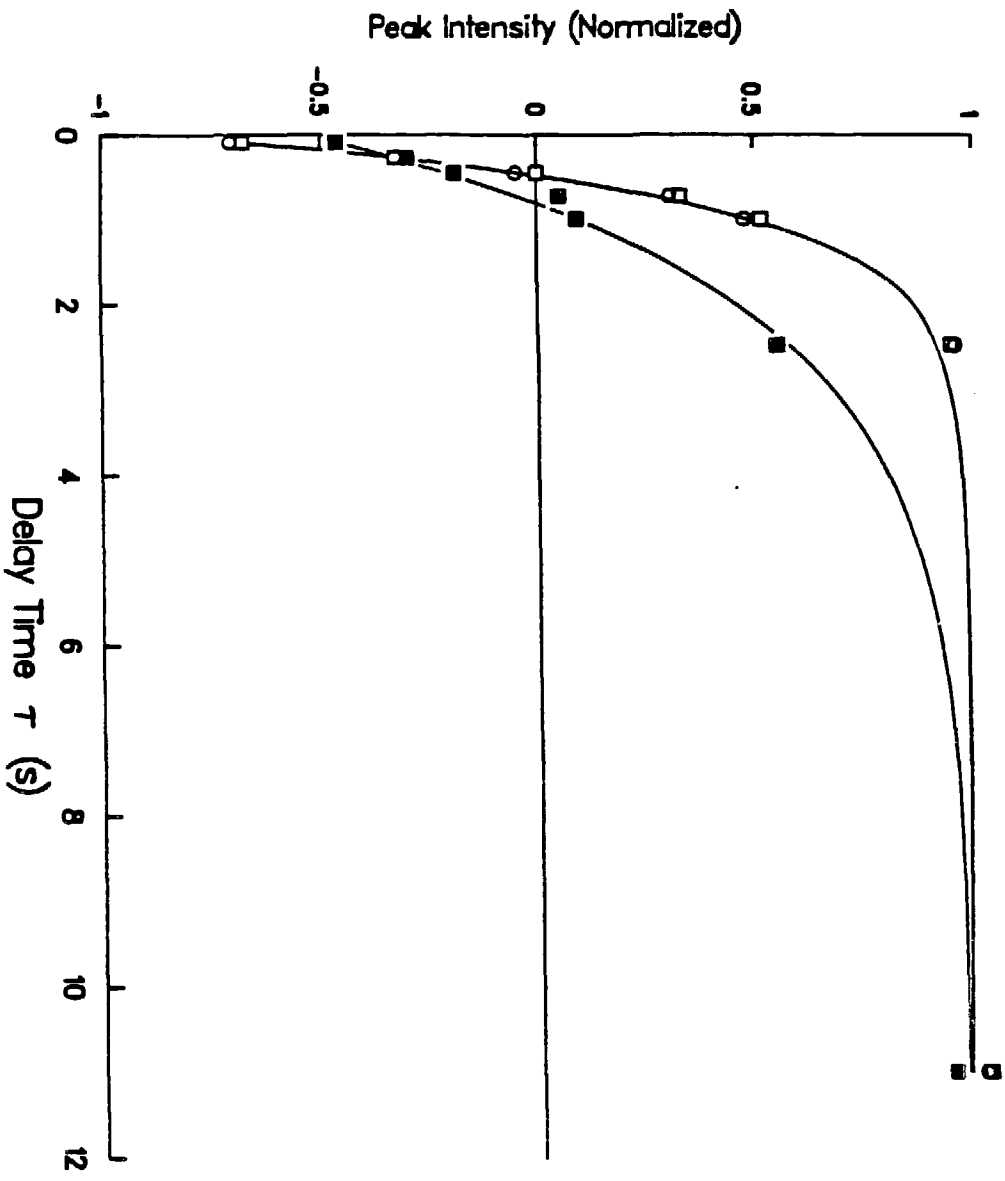
Peak Intensity (Normalized)
-1
-0.5
0
0.5
1
0
2
4
6
8
10
12
Delay Time τ (s)
a
b

Figure 2-2

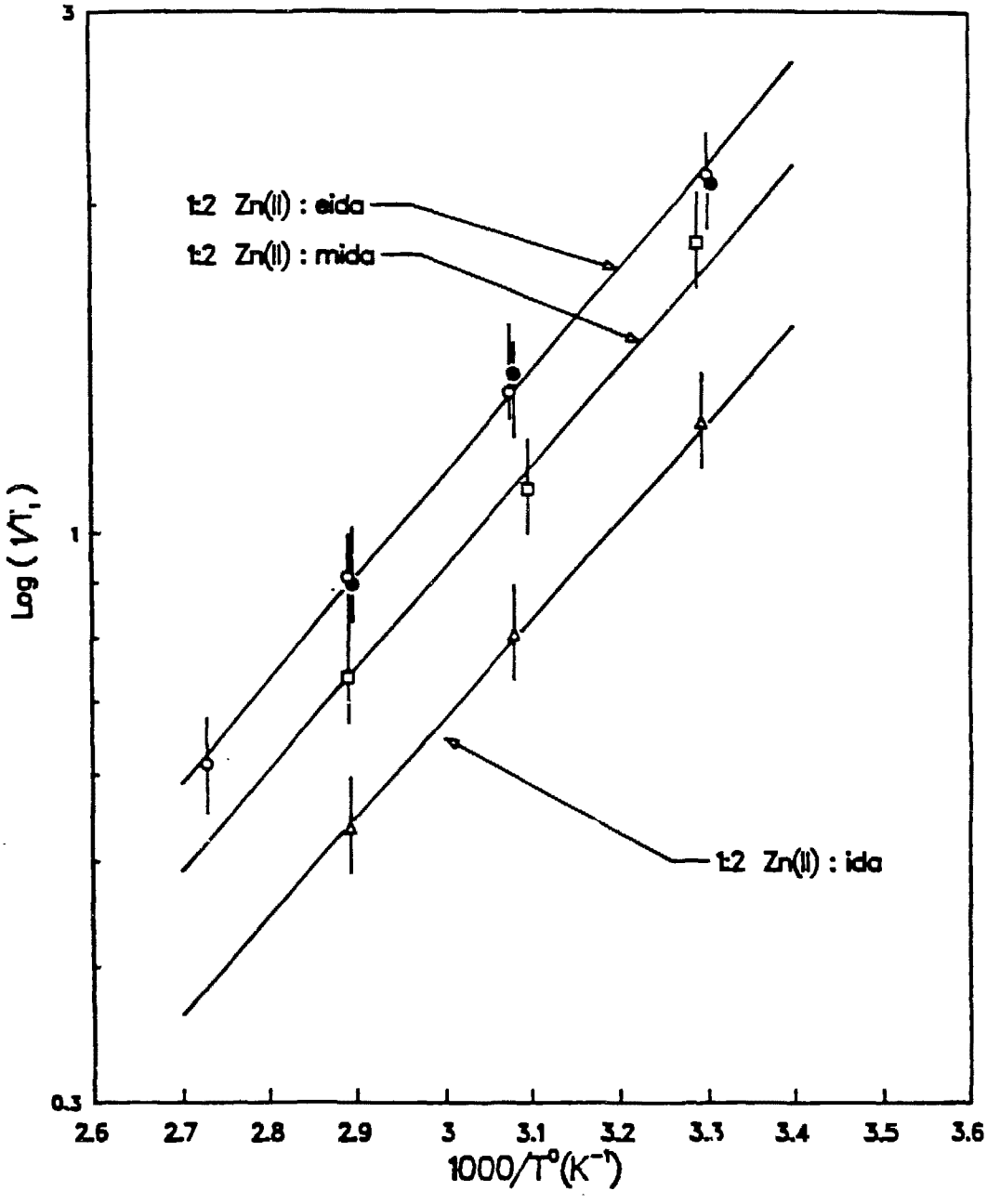
3
1
0.3
Log (1/T1)
1:2 Zn(II) : eida
1:2 Zn(II) : mida
1:2 Zn(II) : ida
2.6
2.7
2.8
2.9
3
3.1
3.2
3.3
3.4
3.5
3.6
1000/T°(K⁻¹)

Figure 2-3

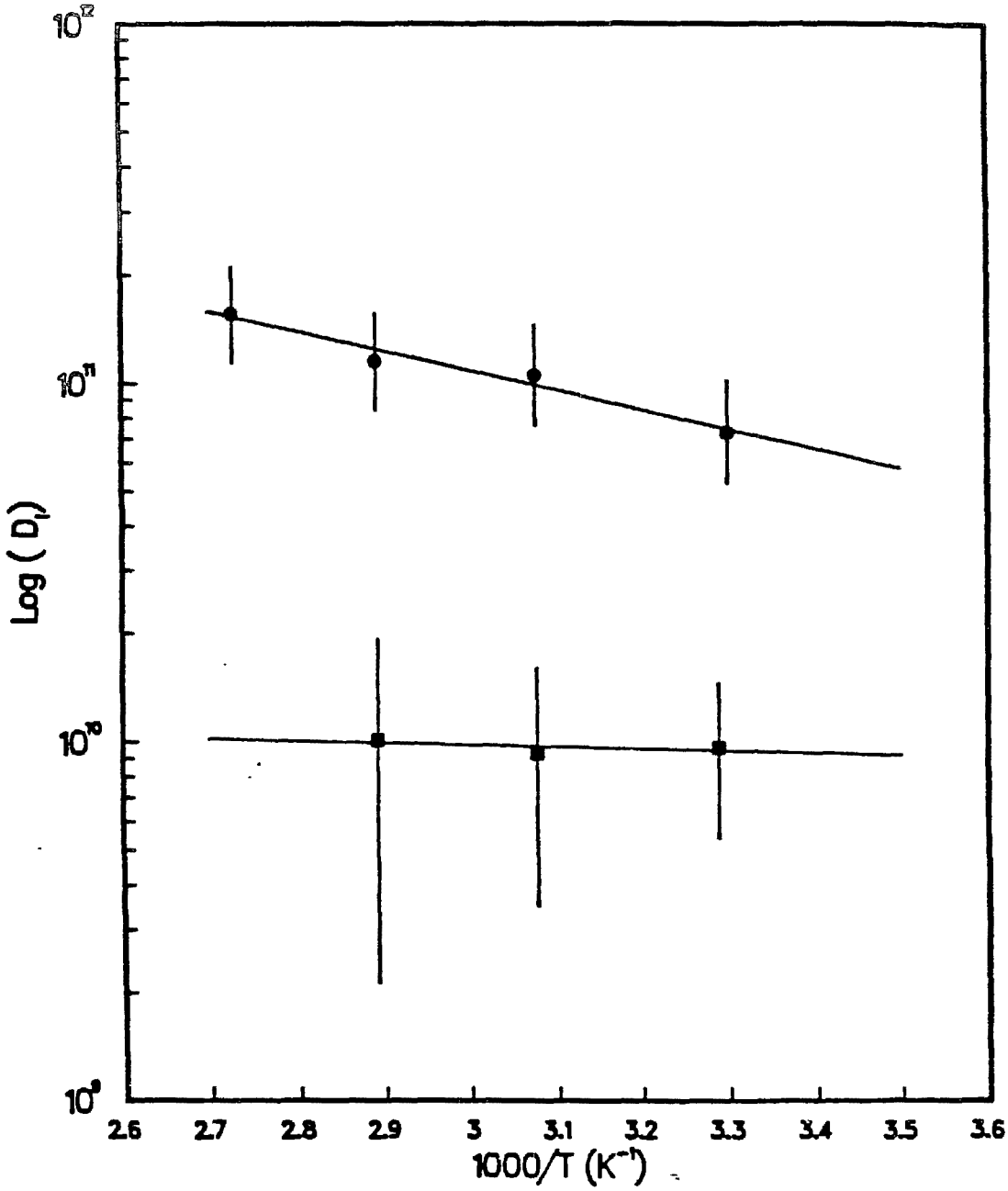

Figure 2-4

REFERENCES

1 Lambert, J.B.; Nienhuis, R.J.; Keepers, J.W. Angew. Chem. Int. Engl. 1981, 20, 487-500.

2 Lyerla, J.R., Jr.; Grant, D.M.; "Topics in Carbon-13 NMR Spectroscopy", G.C.Levy, Ed., J. Wiley, 1974, 79-149.

3 Brietmaier, E.; Spohn, K.-H.; Bergen, S. Angew. Chem. Int. Ed. Engl. 1975, 14, 144-159.

4 John, B.K.; McClung, R.E.D. J. Magn. Res. 1982, 50, 267-273.

5 Levy, R.M.; Karplus, M.; Wolynes, P.G. J. Amer. Chem. Soc. 1981, 103, 5998-6011.

6 London, R.E.; Avitabile J. Amer. Chem. Soc. 1978, 100, 7159-7165.

7 Levy, G.C.; Axelson, D.E.; Schwartz, R.; Hochman. J. Amer. Chem. Soc. 1978, 100, 410-424.

8 Llort, F.M.; Mislow, K.L.; Wooten, J.B.; Beyerlein, A.L.· Savitsky, G.B.; Jacobus, J. J. Amer. Chem. Soc. 1979, 101, 292-220.

9 London, R.E.; Phillippi, M.A. J. Magn. Res. 1981, 45 476-489.

10 Komoroski, R.A.; Levy, G.C. J. Phys. Chem. 1976, 80, 2410-2416.

11 Levine, Y.K.; Birdsall, N.J.M.; Lee, A.G.; Metcalfe, J.C.; Partington, P.; Roberts, G.C.K. J. Chem. Phys. 1974, 60, 2890-2899, and references therein.

12 Levine, Y.K.; Partington, P.; Roberts, G.C.K.; Birdsall, N.J.M.; Lee, A.G.; Metcalfe, J.C. FEBS Lett. 1972, 23, 203.

13 Woessner, D.E.; Snowden, B.S., Jr.; Meyer, G.H. J. Chem. Phys. 1969, 50, 719-721.

14 Canet, D.; Levy, G.C.; Peat, I.R. J. Magn. Res. 1975, 18, 199-204.

15 Freeman, M.A.; Van Der Vaart, D.R.; Schultz, F.A., Reilley, C.N. J. Coor. Chem. 1981, 11, 81-90.

REFERENCES (continued)

16 Hanssum, H. J. Magn. Res. 1981, 45, 461-475.

17 Campbell, I.D.; Freeman, R. J. Magn. Res. 1973, 11, 143-162.

18 Rowland, T.; Ph.D. Thesis, University of California, Berkeley, 1975.

19 Mitchell, R.W.; Eisner, M. J. Chem. Phys. 1960, 33, 86-91.

20 Mammano, N.J.; Templeton, D.H.; Zalkin, A. Acta Cryst. 1977, B33, 1251-1254.

21 Woessner, D.E.; Snowden, B.S., McKay, R.A.; Strom, E.T. J. Mag. Res. 1, 105-118.

22 Nordenskiold, L.; Kowalewski, J.; Benetis, N. J. Phys. Chem., 1980, 84, 3646-3652.

23 Meakin, R.J. Faraday Soc. Trans. 1958, 54, 1160-1165.

24 Gordon, R.G. J. Chem. Phys. 1966, 44, 1830-1836.

25 McClung, R.E.D. J. Chem. Phys. 1972, 57, 5478.

26 Wallach, D. J. Chem. Phys. 1967, 47, 5258-5268.

27 Levine, Y.K.; Partington, P.; Roberts, G.C.K. Mol. Phys. 1973, 25, 497-514.

28 Woessner D.E. J. Chem. Phys. 1962, 36, 1-4.

29 Levy, G.C.; Kumar, A.; Wang J. Amer. Chem. Soc. 1983, 105, 7536-7540, and references therein.

30 Beierbeck, H.; Martino, R.; Saunders, J.K. Can. J. Chem. 1980, 58, 102-109.

31 Chung, D.S.; Kim, E.M.; Shin, K.J. Chem. Phys. Lett. 1984, 108, 283-287.

32 Komoroski, R.A.; Levy, G.C. J. Phys. Chem. 1976, 80, 2410-2417.

33 Platzer, N. Org. Magn. Reson. 1978, 11, 350.

34 Lambert, J.B.; Nienhuis, R.J.; Finzel, R.B. J. Phys. Chem. 1981, 85, 1170-1178.

CHAPTER 3

^{13}C ISOTROPIC SHIFT AND LINEWIDTH ANALYSIS OF THE BIS-LIGAND NICKEL(II) COMPLEXES WITH IDA, MIDA AND EIDA

CONTENTS

INTRODUCTION

Previous studies of paramagnetic metal complexes with organic ligands fit both the ^{13}C relaxation rate and isotropic shifts of the carbon atoms to theoretical formulas.[1,2,3,4,5,6,7,8,9,10,11,12] Several parameters are involved in the fit. Some parameters, such as the electron-nuclear coupling constant for the scalar interaction, are specific for each carbon. Other parameters associated with molecular tumbling and electron relaxation are specific for the entire molecule. Fitting both types of data for several carbons in a complex can yield values for these parameters and verify the interpretation. If a chemical process is also involved then information can be gained about the chemical exchange rates. (For example see references 1,2,3,4.) The longitudinal relaxation rate will be different than the transverse relaxation rate, thus providing a third type of data for the fitting process.

The Bloembergen-Solomon expression is used to describe relaxation rates.[13] The Fermi contact expression is used for the isotropic shift if Curie behavior is seen.[14] If non-Curie behavior is observed other expressions are used.[15,16] Different expressions produce different values for the scalar coupling constants which always leaves some question as to the accuracy of reported scalar coupling constants in

describing the distribution of electron spin density at the various atoms.

In this chapter the ^{13}C isotropic shifts and transverse relaxation rates (T_2^{-1}) are reported for the carbons in the bis-ligand complexes of Ni(II) with ida, mida and eida over the temperature range 275 to 368 K. Non-Curie behavior was seen in the isotropic shifts of all the carbons. Two different interpretations were used to obtain scalar coupling constants from the shifts. The interpretations were evaluated by attempting to use the different scalar coupling constants to fit the transverse relaxation rates. The exact cause of the non-Curie behavior was not determined, but some criteria were established for choosing between the different interpretations of the isotropic shift.

THEORETICAL CONSIDERATIONS

A good approximation to the isotropic shift is:[14]

$$\Delta\omega/\omega_o = \frac{g\beta \langle S_{eff} \rangle (A/\hbar)}{3\gamma_I kT} \qquad [3\text{-}1]$$

The origin of this expression is the contact interaction where g and $\langle S_{eff} \rangle$ are the effective g-value and effective spin quantum number, respectively, and include both electron spin and orbital effects. The scalar coupling constant is given by A (in units of ergs) and γ_I is

the gyromagnetic ratio of the observed spin. For Curie behavior $\langle S_{eff} \rangle$ is independent of temperature and a plot of $\Delta\omega/\omega_o$ as a function of T^{-1} is a straight line with intercept $\Delta\omega/\omega_o = 0$ at infinite temperature.

For Ni(II) in an octahedral environment with no thermally accessible excited states $\langle S_{eff} \rangle$ is given by S(S+1) and Curie behavior is expected. With a slightly distorted octahedral environment this expression for $\langle S_{eff} \rangle$ is still a good approximation and the effect on the isotropic shift due to the anisotropic magnetic behavior ($g_{xx} \neq g_{yy} \neq g_{zz}$) is to introduce a pseudocontact term.[17]

General expressions for the contact shift ($\Delta\omega_F/\omega_o$) and pseudocontact shift ($\Delta\omega_M/\omega_o$) which allow for moderate magnetic anisotropy are:[18]

$$\Delta\omega_F/\omega_o = \frac{(A/\hbar)}{3\gamma_I\beta}\left[\frac{\chi_{xx}}{g_{xx}} + \frac{\chi_{yy}}{g_{yy}} + \frac{\chi_{zz}}{g_{zz}}\right] \qquad [3\text{-}2]$$

$$\Delta\omega_M/\omega_o = \frac{-1}{2R^3}\left[(1-3\cos^2\Omega)(\chi_{zz}-\bar{\chi}) + \sin^2\Omega\cos 2\psi\,(\chi_{yy}-\chi_{xx})\right] \qquad [3\text{-}3]$$

where $\bar{\chi} = (\chi_{xx}+\chi_{yy}+\chi_{zz})/3$. The equations of Van Vleck[19] are used in describing the magnetic susceptibility ($\chi_{xx}, \chi_{yy}, \chi_{zz}$). Parameter R is the length of the vector between the paramagnetic center and the spin. Angles ψ and Φ describe the orientation of the vector in the principal axis system.[18] Equation [3-2] still requires no thermally accessible excited states. Equation [3-3] considers only unpaired electrons occupying orbitals centered at the metal ion and ignores

unpaired electrons occupying orbitals centered at ligand nucleii, an assumption which may be reasonable for proton shifts but unacceptible for carbons.[4,11]

Expressions for the axially symmetric case ($\chi_{xx}=\chi_{yy}\neq\chi_{zz}$ and $g_\perp=g_{xx}=g_{yy}$ and $g_\parallel=g_{zz}$) are obtained using an effective spin Hamiltonian which characterizes the interaction in the absence of an applied field by the zero field splitting parameter D:[17,18]

(for S = 1)

$$\chi_{zz} = \frac{2g_\parallel^2\beta^2 e^{-X}}{kT(1+2e^{-X})} \qquad [3\text{-}4]$$

$$\chi_{xx} = \chi_{yy} = \frac{2g_\perp^2\beta^2(1-e^{-X})}{kTX\ (1+2e^{-X})} \qquad [3\text{-}5]$$

where X = D/kT. Equations [3-2] through [3-5] may be used as written or expanded in a power series:

$$\Delta\omega_P/\omega_o = \frac{2g\beta(A/\hbar)}{3k\gamma_I}\frac{1}{T} - \frac{2\beta(A/\hbar)(g_\parallel-g_\perp)D}{27k^2\gamma_I}\frac{1}{T^2} + \text{H.O.} \qquad [3\text{-}6]$$

$$\Delta\omega_M/\omega_o = \frac{2\beta^2(g_\parallel^2-g_\perp^2)}{9k}\left[\frac{3\cos^2\Omega-1}{R^3}\right]\frac{1}{T} + \frac{-2\beta^2(g_\parallel^2+g_\perp^2/2)D}{27k^2}\left[\frac{3\cos^2\Omega-1}{R^3}\right]\frac{1}{T^2} + \text{H.O.} \qquad [3\text{-}7]$$

These expressions show that magnetic anisotropy affects both the contact and pseudocontact interactions. The first term in [3-6] is equivalent to equation [3-1] for S = 1. Equation [3-7] and the second

term in [3-6] (and all higher order terms) go to zero as $(g_{\parallel}-g_{\perp})$ and D go to zero. Thus, the additional terms may be considered a correction to Curie behavior for the introduction of moderate magnetic anisotropy.

The transverse relaxation rate (T_{2P}^{-1}) for the carbons due to the presence of the paramagnetic electron can be expressed by the modified Solomon-Bloembergen equation[13]:

$$\frac{1}{T_{2P}} = \frac{1}{15}S(S+1)g^2\beta^2\gamma_I^2 r^{-6}\left[4\tau_{c1} + \frac{3\tau_{c1}}{1+\omega_I^2\tau_{c1}^2} + \frac{13\tau_{c2}}{1+\omega_s^2\tau_{c2}^2}\right] + \frac{1}{3}S(S+1)\left(\frac{A}{\hbar}\right)^2\left[\tau_{e1} + \frac{\tau_{e2}}{1+\omega_s^2\tau_{e2}^2}\right] \qquad [3\text{-}8]$$

The first term is due to the electron-nuclear dipole-dipole interaction $(T_2(DD)^{-1})$. The second term is the scalar interaction $(T_2(SC)^{-1})$. The Larmor frequency of the nucleus and the electron are given by ω_I and ω_S, respectively, and r is the electron-nuclear distance. The effective correlation times are:

$$\frac{1}{\tau_{c,k}} = \frac{1}{\tau_r} + \frac{1}{T_{k,e}} + \frac{1}{\tau_j} \qquad [3\text{-}9]$$

$$\frac{1}{\tau_{e,k}} = \frac{1}{T_{k,e}} + \frac{1}{\tau_j} \qquad [3\text{-}10]$$

Here, τ_r^{-1} is the isotropic rotational reorientation rate (τ_o^{-1} in Chapter 2). The electron longitudinal and transverse relaxation rates are given by $T_{k,e}$ for k = 1 and 2, respectively. Equations [3-9] and

[3-10] include the effect of chemical exchange between two different sites for the relaxing atom, where τ_j^{-1} is the reciprocal lifetime of the spin in each site occupied by the atom. The carbons in the Ni(II) complexes in this study are assumed to be non-exchanging and the τ_j^{-1} term in equations [3-9] and [3-10] is ignored.

The Ni(II) ion with triplet ground state has only one T_{1e} and T_{2e} relaxation time given by:[5,20]

$$\frac{1}{T_{1e}} = \frac{2D^2}{75}[4S(S+1)-3]\left[\frac{\tau_v}{1+\omega_s^2\tau_v^2} + \frac{4\tau_v}{1+4\omega_s^2\tau_v^2}\right] \qquad [3\text{-}11]$$

$$\frac{1}{T_{2e}} = \frac{D^2}{75}[4S(S+1)-3]\left[3\tau_v + \frac{5\tau_v}{1+\omega_s^2\tau_v^2} + \frac{2\tau_v}{1+4\omega_s^2\tau_v^2}\right] \qquad [3\text{-}12]$$

where τ_v is a time characteristic for the random field modulation responsible for the electron relaxation, and D is the zero-field splitting parameter. Equations [3-11] and [3-12] are independent of the physical origin of the relaxation. The zero-field splitting parameter is known to have a small temperature dependence which will be ignored in this study.[21] The conditions for rigorous application of [3-11] and [3-12] are:[22]

$$\tau_v \ll T_{1e}, T_{2e}$$

These conditions are not necessarily fulfilled over the entire temperature range for the complexes in this study.

Finally, the temperature dependence of the relaxation rates

appears in the correlation times τ_r and τ_v which are given Arrhenius-type expressions with each characterized by an energy of activation and preexponential:

$$\tau_r = \tau_r^o \exp[\frac{E_r^o}{RT}]$$

$$\tau_v = \tau_v^o \exp[\frac{E_v^o}{RT}]$$

EXPERIMENTAL

The 1:2 Ni(II):ligand solutions were prepared with the appropriate reagents (See Chapter 1) with a final concentration of about 0.20 M metal ion. Each sample was neutralized to *ca.* pH 7 with concentrated NaOH and contained *ca.* 0.04 M 1,4-dioxane for an internal shift reference.

Natural abundance ^{13}C NMR spectra were obtained at 50 MHz and 75 MHz in the Fourier transform mode using Nicolet 1180 and 1280 operating systems, respectively. Proton decoupling was not employed. In a typical run 100,000 scans were collected over about 25 minutes with 1K data points per scan and a spectrum width of 25 KHz. The pulse width was 16×10^{-6} s. The acquisition time plus recovery time was about 22×10^{-3} s which assured complete relaxation of allthe carbon spins (T_2 *ca.* 0.001 s, maximum). Quadrature phase detection was used for all experiments.

The temperature was controlled by a heating unit and monitored with the use of the ^{19}F NMR thermometer discussed in Chapter 1. The ^{19}F spectrum was taken immediately before and after each carbon spectrum. The average separation of the fluorine peaks was used with the temperature calibration curve given in Chapter 1. The accuracy of the temperature measurements was estimated to be $\pm 0.2^{o}$.

RESULTS

Isotropic Shift Analysis: The room temperature ^{13}C spectra are shown in Figure 3-1. The assignments were made using the peak intensities and spectra seen with similar complexes.[2,5,10,23,24] The peak locations of the corresponding diamagnetic Zn(II) complexes (from Chapter 2) are also shown in Figure 3-1. The isotropic shift of a paramagnetic Ni(II) complex is taken as the difference between the shifts of the Ni(II) and the corresponding Zn(II) complexes.[17] The isotropic shift of the C_o, C_N and C_α carbons in all the complexes in Figure 3-1 is negative (toward higher field strength) which signifies a negative net electron spin density on these atoms. Their similar positions in the complex, directly attached to a donor atom, suggests that a spin polarization mechanism originating from positive net electron density on the donor atoms is overwhelming the effect of a direct delocalization mechanism.[17] The latter distributes positive electron density originating on the donor atom onto the ligand through

the σ-orbitals of the complex and produces a positive contribution to the isotropic shift.

The C_β carbon in the bis-eida complex shows an isotropic shift of the opposite sign. The positive isotropic shift is due to the delocalization mechanism and to some extent to the spin polarization mechanism operating on an atom two bonds away from a donor atom.[17] In general, more remote carbons show only a positive isotropic shift due to the delocalization mechanism.[23,24]

The ^{13}C spectra of the bis-ligand Co(II) complexes with ida, mida and eida are also shown in Figure 3-1. If the pattern of electron spin distribution in the Co(II) and Ni(II) complexes is alike, their isotropic shifts are related by a constant of proportionality and a pseudocontact term present only in the Co(II) complexes.[17] The differences in isotropic shift seen in Figure 3-1 show that the additional shift in the Co(II) complexes is of the same sign and about the same magnitude for the C_O carbons with all three ligands. The C_N and C_α carbons also show about the same magnitude of additional shift. These results suggest that the metal-ligand configuration and the electronic structure are alike in the complexes with all three ligands.

All of the spectra in Figure 3-1 show only one peak for each type of carbon except the spectrum of the 1:2 Ni(II):ida complex. No additional structure was seen in spectra taken at a higher frequency (125 MHz). These results may be due to the presence of only the trans

isomer in solution. An equally acceptible explanation is the presence of both isomers in rapid equilibrium such that only the averaged peaks are seen in the spectrum. The presence of only the trans isomer is reasonable for the bis-mida and bis-eida complexes since one effect of replacing the N-substituted proton in ida with the larger methyl or ethyl group is to destablize the cis configuration (See Chapter 1). The appearance of only one set of carbon peaks seen with the 1:2 Co(II):ida complex cannot be explained by destablization of the cis isomer. The Co(II) ion is larger than the Ni(II) ion and should accommodate both the cis and trans configuration seen with nickel, although, some differences in structure may exist related to the difference in d electron configuration. Spectra taken at the high end (365 K) and low end (275 K) of the temperature range did not reveal any dynamic behavior.

The 1:2 Ni(II) complex with ida shows three C_O carbon peaks due to the presence of both cis and trans isomers. This is contrary to the behavior seen with the corresponding Zn(II) complex (See Chapter 2). The two large C_O peaks of near equal size are attributed to carbons in the two different environments of the cis isomer. The smaller C_O peaks is the trans isomer. The C_N carbons show a small peak for the trans isomer and a single large peak for the two cis isomers. Apparently the isotropic shift mechanisms responsible for two cis peaks with the carboxylate carbons are ineffective in separating the two C_N peaks in the same isomer. The spectra of the 1:2 Ni(II):ida complex are examined in more detail in Chapter 4 where possible mechanisms for cis-trans interconversion are investigated.

The frequency shifts-versus-temperature for the bis-ligand complexes are plotted in Figure 3-2. The lines through the data were obtained by a least-squares fit and show a linear dependence on the reciprocal of temperature. No evidence of curvature is seen within the observed temperature region. The shift of the C_O, C_N and C_α carbons for the bis-mida and bis-eida complexes are very similar and indicate similar ligand coordination in these complexes. The isotropic shifts for the bis-eida complex at 50 MHz and 75 MHz (see Figure 3-2) are also alike which indicates no frequency dependence in the fractional shift.

The carboxylate carbons (C_O^1,C_O^2,C_O^3) of the bis-ida complex are located downfield compared with the carboxylate carbon in the bis-mida and bis-eida complexes indicating more positive electron spin density for ida. The C_N carbons (C_N^1,C_N^2) are located slightly upfield indicating less positive electron spin density. The explanation may lie with structural differences that affect the various mechanisms for electron spin distribution. One effect of replacing the N-substituted proton in the ida complex with a methyl or ethyl group is to produce a more uniform arrangement of the groups around the nitrogen. This is seen in crystallographic data[25,26] and is also seen with the Zn(II) complexes as a decrease in chemical shift differences (δ_{AB}) between the outer(A) and inner(B) protons in the series (See Chapter 5)(at 500 MHz):

ida (δ_{AB} = 325 Hz) > mida (≈ 70 Hz) > eida (= 17 Hz)

A smaller δ_{AB} indicates the A and B proton environments are more alike. While a more perfect tetrahedral arrangement at the nitrogen would decrease the transmission of electron density through the σ-structure (i.e., producing less positive spin density on the C_N carbon), the spin polarization mechanism would also be affected.[17] Detailed energy calculations which incorporate both spin polarization and direct delocalization effects are necessary to relate more clearly the changes in the structure to changes in the isotropic shifts.[17] From the effect seen on the carboxylate carbon shifts (Figure 3-2) it can be concluded that the isotropic shifts of the C_O carbons are influenced by spin distribution through both the nitrogen and oxygen donor atoms. Structural changes due to different N-substituents is confined largely to the nitrogen end of the ligand and would not produce the large difference seen with the C_O carbon shifts if spin distribution to this carbon occured via only the donor oxygen atom.

The displaced ^{13}C shifts seen with the bis-ida complex could also be due to an equilibrium in which the donor carboxylate oxygens are momentarily detached from the metal ion. The C_O and C_N carbon nuclei gain negative electron spin density via the spin polarization mechanism operating through the donor oxygen and nitrogen atoms, respectively. The C_O and C_N nuclei receive negative spin density by the same mechanism from the opposite direction in the ring due to

their position one atom from the donor nitrogen and oxygen atoms, respectively. The cancelling effect which occurs when the acetate arm is attached at the oxygen atom is nullified when the acetate arm is detached. An equilibrium between complexes with attached and unattached acetate arms is expected to shift the C_O to lower field and C_N to higher field, as seen, compared to the species with no carboxylate detachment.

Equation [3-1] predicts that a plot of $T\cdot(\Delta\omega/\omega_o)$ as a function of temperature produces a line of zero slope if Curie behavior is observed. The data produced the lines shown in Figure 3-3 with zero set equal to the diamagnetic value obtained with the Zn(II) complexes for each carbon. Non-zero slopes are clearly seen for all the carbons. The slope of each line is given in Table 3-1 and indicates the extent of deviation from Curie behavior. The slopes are opposite the sign of the isotropic shift which shows that the shifts are approaching the diamagnetic value too quickly with increasing temperature. The non-Curie behavior has been seen in the ^1H [15,16,27] NMR spectra and ^{13}C [15] spectra of other complexes. Very little is known about the origin of this behavior, although several explanations have been offered.[15]

Two different treatments were used with the isotropic shift data in this study. In the first treatment the data were fitted to equation [3-1] plus a constant. The scalar coupling constant and the additional constant (the intercept at $\Delta\omega/\omega_o = 0$) are given in Table 3-

i. In a second treatment the isotropic shift data were fitted to an expression of the form:

$$\Delta\omega/\omega_o = \frac{B_1}{T} + \frac{B_2}{T^2} \qquad [3\text{-}13]$$

B_1 and B_2 are temperature-independent constants. McGarvey has shown that this form is justified if the origin of the non-zero behavior is due to a pseudocontact term in the isotropic chemical shift.[18] Using equations [3-6] and [3-7], B_1 and B_2 are given by:

$$B_1 = \frac{2g\beta(A/\hbar)}{3k\gamma_I} \qquad [3\text{-}14]$$

$$B_2 = \frac{-2\beta^2(g_\parallel^2+g_\perp^2/2)D}{27k^2}\left[\frac{3\cos^2\Omega-1}{R^3}\right] \qquad [3\text{-}15]$$

The second term in equation [3-6], the first term in [3-7] and all terms higher than second order are ignored because they will always contribute much less than the terms in equations [3-14] and [3-15]. The term B_1 represents the contact interaction and depends on the magnitude and sign of the scalar coupling constant, while B_2 represents the pseudocontact interaction and is directly proportional to the zero-field splitting parameter and a geometric term containing Ω. The latter determines the sign of this term which can be either positive or negative. Although equation [3-13] predicts a non-linear temperature dependence it has been stated[18] that curvature in a plot of isotropic shift-versus-temperature may be undetectable over the accessible temperature region but still show a non-zero intercept at infinite temperature.

A non-linear least squares fit of the data to equation [3-13] produced the scalar coupling constants (using [3-14]) and B_2 values in in Table 3-2. Knowledge of the geometric factor ($3\cos^2\Omega-1$) and the electron-nuclear distance is required to obtain the zero-field splitting parameter D. Using distances taken from crystallographic studies[25,26] (r = 282, 289 and 306 pm, for C_o, C_N and C_α, respectively) and the maximum possible value for the geometric factor, the values for D given in Table 3-2 were obtained. A value r = 310 pm was assumed for the C_β carbon of the bis-eida complex based upon the linewidth analysis.

The negative value for the C_β carbon in the bis-eida complex (Table 3-2) is, of course, meaningless. A positive value can be obtained with an appropriate geometric factor. Regardless, all the D values in Table 3-2 are much larger than reasonable for octahedral Ni(II) complexes (typically [D] = 0.1 - 5 cm^{-1}). Assuming a moderate value for D = 5 cm^{-1} the pseudocontact contribution to B_2 is 5% or less than the observed value in Table 3-2. In addition, the geometric factors are probably less than the maximum thus reducing the actual pseudocontact contribution even further.

Other studies with near-octahedral Ni(II) complexes reached similar conclusions about the importance of a pseudocontact interaction in explaining non-Curie behavior.[1,15,16] In spite of this, equation [3-13] has been used to fit the isotropic shift data with the scalar coupling constants obtained from the B_1 expression given above and B_2 remaining a constant of unknown origin.[1,16] The

form given by equation [3-13] has been justified on fundamental grounds,[16] that the actual interaction responsible for the behavior can always be described as a summation of Boltzmann energies and expanded to first order in T^{-1}. Using this interpretation, B_2 may be non-zero (non-Curie behavior) with some complexes and zero for the same carbons (Curie behavior) with similar complexes.[1] Even in the same complex, the isotropic shift of some carbons required a significant non-zero B_2 term while other nearby atoms required only a B_1 term.[1] These results shed doubt on any scalar coupling constant reported in the literature where the origin of non-Curie behavior cannot be clearly determined. Even values for A/ħ given when a B_2 term was clearly zero are questionable since the origin of the B_2 term could also contribute to the T^{-1} term thus completely invalidating equation [3-1].

Other possible origins of non-Curie behavior are a Curie-Weiss dependence of the magnetic susceptibility on temperature,[15] temperature independent paramagnetism (TIP)[15] and chemical exchange. Behavior due to TIP can be eliminated in this study since the sign of the intercept is opposite the sign of the observed shift.[15] It has been shown with a few Ni(II) and Co(II) complexes that Curie-Weiss behavior is unimportant[15] but generalization to other complexes is not possible from only the known studies. Chemical exchange is a possiblity for complexes in this study and is discussed below.

A condition for the use of equations to describe the contact and pseudocontact shifts is that one is looking at the same species at

each temperature. With a temperature-dependent equilibrium between two or more species, the shift depends on the relative distribution as well as the contact and pseudocontact interactions. Non-zero slopes are expected as seen in Figure 3-3. The magnitude of the slopes has been used as an indicator of the free energy change (ΔG^{o}) between the equilibrium states, a lower slope indicating a larger ΔG^{o}.[28]

The equilibrium shown below may be relevant to the complexes in this study:

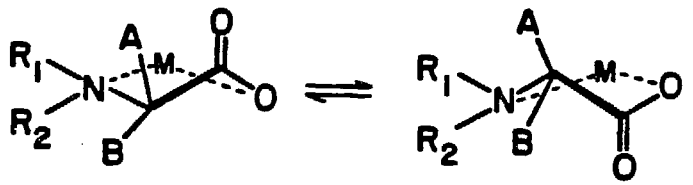

In this case, the aminocarboxylate ligand is bound to the metal via both the donor nitrogen and oxygen atoms. If A is a proton and B is a proton[28] or other group,[29] the methylene proton environments are different in each state and interconversion is possible via a twisting motion. The ^{1}H spectrum of Ni(II):L complexes where L is an amino acid shows a single peak indicating a rapid equilibrium. Non-Curie behavior is seen in the proton isotropic shift which is attributed to the above equilibrium.[29]

If the R_1 and R_2 groups are different (i.e., ida, mida or eida)

the methylene carbon and carboxylate carbon will also differ for the two states and non-Curie behavior is expected for the ^{13}C isotropic shifts according to the temperature dependence of the equilibrium. Two different states possible for the C_O and C_N carbons in solution are clearly seen in the solid state structure of the complexes in this study.[25,26] One ring in each complexed ligand is puckered while the other ring is nearly planar. Although a twisting motion in solution could interconvert the conformation of each ring, this twisting mechanism cannot be responsible for the non-Curie behavior seen with the isotropic shift since the relative abundance of the carbon in the two environments would remain equal at all temperatures.

An important equilibrum relevant to the results in Chapter 1 is the rapid interconversion between the cis and trans isomers of each complex. By assuming Curie behavior at each temperature for the carboxylate carbon in the bis-eida complex, the effective $A/\hbar$ changes from $-5.6 \times 10^6\ s^{-1}$ at 275 K to $-5.5 \times 10^6\ s^{-1}$ at 368 K according to the observed isotropic shifts at these temperatures. This small change is reasonable if the scalar coupling constants for the cis and trans isomers of the bis-eida complex are similar to the values seen with the bis-ida complex (Table 3-1). To investigate this possibility further, the isotropic shifts of the 1:1 Ni(II):ligand complexes were observed as a function of temperature. If the non-Curie behavior with the 1:2 complexes is due to shifts of the cis-trans equilibrium with temperature, Curie behavior can be expected with the 1:1 complexes where this equilibrium is not present. Results with the 1:1 Ni(II):mida and Ni(II):eida complexes (not reported here) also showed

non-Curie behavior, therefore, the cis-trans equilibrium cannot be eliminated or confirmed with the corresponding bis-ligand complex.

Other types of chemical exchanges are ion-pair formation and hydrogen-bonding. Ion-pair formation could affect the isotropic shift if the degree of formation is significantly altered over the observed temperature range. The effect on the shift is primarily through the magnetic anisotropy (the pseudocontact interaction) which will never be important for the Ni(II) complexes in this study.[15] The value of the isotropic shift for each carbon did not differ with solutions of different metal-ligand concentration, suggesting that ion-pair formation is also not important in determining the isotropic shift.

The effect of hydrogen-bonding on the isotropic shift is significant with some complexes as shown by comparing isotropic shifts for the same complexes in two solvent systems which differ in their hydrogen-bonding capabilities.[15,30] Less hydrogen-bonding is expected at higher temperatures for an exothermic interaction. In any case, a linear-reciprocal temperature dependence with a non-zero intercept is expected. This explanation is possible for the 1:1 and 1:2 complexes in this study, although, it is not obvious why the C_β carbon in the bis-eida complex should experience a much greater deviation than the other carbons as a result of this effect.

Linewidth Analysis: The transverse relaxation rates (T_{2P}^{-1}) of the carbons were obtained from the linewidth at half height ($\Delta\nu_{1/2}$) assuming a Lorentzian lineshape and the equation:

$$\frac{1}{T_{2P}} = \Delta\nu_{1/2} \cdot \pi$$

The linewidth for each carbon in the absence of the paramagnetic electron was less than a few hertz and justifiably ignored. Accuracy and reproducibility of the T_{2P}^{-1} values were ± 10% or better. This was limited primarily by the quality of the spectra taken with the natural abundance ^{13}C samples in a reasonable amount of time. Unfortunately, the size and proximity of the C_α peak next to the larger C_N peak in the bis-mida complex did not permit an accurate determination of the relaxation rates of this carbon.

Relaxation rates as a function of temperature are plotted in Figures 3-4 through 3-6 for carbons in the bis-eida and bis-mida complexes. The general appearance of the data in the plots is similar to that seen with carbons in other paramagnetic complexes.[2]

The theoretical expression for the isotropic shift (equations [3-6] and [3-7]) and for the transverse relaxation rate (equations [3-8] through [3-12]) contain $A/\hbar$ and the zero-field splitting parameter D. The shifts and relaxation rates could be simultaneously fit to the equations to determine these parameters. An alternative method employed in this study is to fit the relaxation data using the two choices for scalar coupling constants given in Table 3-1 and 3-2, and to evaluate the choices based upon the fit to the relaxation data and the reasonableness of the other parameters. Relaxation rates for the

bis-eida complex taken at a higher field strength (75 MHz) were also used which provides an additional test of the interpretation.

Certain parameters in equation [3-8] are assigned reasonable values. The effective g-value was set equal to 2.25 for all the complexes. The electron-nuclear distance r was set equal to the metal-carbon distance seen in crystallographic studies.[25,26] The other parameters are E_r^o, τ_r^o, E_v^o, τ_v^o, and already mentioned D. These parameters are highly correlated due to the form of their involvement in the equations. Each is seldom determined with certainty without additional input.

In order to obtain a manageable number of parameters, E_r^o and τ_r^o for the Ni(II) complexes were assigned the values obtained for the corresponding Zn(II) complexes (Chapter 2). This is a reasonable assumption since the macromolecular properties of the Zn(II) and Ni(II) complexes are expected to be alike.

The value of E_v^o, τ_v^o and D were determined for the bis-eida complex by fitting the C_O, C_N and C_α relaxation rates at 50 MHz to the expression above. The complete set of parameters shown in Table 3-3 produced the curves in Figure 3-4. A suitable curve for the C_β carbon was obtained using an electron-nuclear distance of 310 pm and the scalar coupling constant in Table 3-1. The data for all the carbons are probably within experimental error of the calculated curves.

An equally good fit of the C_O, C_N and C_α relaxation data for the bis-eida complex at 50 MHz was obtained using the alternative set of scalar coupling constants in Table 3-2. The value for E_v^o, τ_v^o and D determined in the fit were only slightly different than the values in Table 3-3. An inconsistency did appeared in attempting to fit the relaxation rate of the C_β carbon. The much smaller value of $A/\hbar$ (4.35×10^6 s^{-1}) seen with this set for the C_β carbon required a larger dipole-dipole contribution and an electron-nuclear distance of 260 pm for this carbon was necessary in order to fit the data. Based upon this unrealistic electron-nuclear distance the second set of scalar coupling constants could be eliminated.

Relaxation for the carbons in the bis-eida complex at 75 MHz is shown in Figure 3-5. The calculated curves were obtained using all the parameters in Table 3-3 except for the value of D which was 4.46 cm^{-1} for the data at the higher frequency. A frequency dependence in the value of D has already been noted.[21] It has also been suggested that equation [3-8] through [3-12] may be too simple and that another expression with two characteristic time constants for electron relaxation may be needed.[31]

The relaxation rates for the C_O and C_N carbons in the bis-mida complex at 50 MHz did not provide a single best fit of the parameters E_v^o, τ_v^o and D. The calculated curves in Figure 3-6 were obtained using the value of E_v^o = 4.9 kcal mol^{-1} seen with the bis-eida complex and fitting the data to determine τ_v^o and D. The complete set of parameters is given in Table 3-4. An equally good fit was obtained

using the alternative set of scalar coupling constants in Table 3-1; thus no evidence favoring either interpretation of the isotropic shifts is found with this complex.

DISCUSSION

A satisfactory fit of the transverse relaxation rates was possible using equation [3-8]. The fit could be improved further with small changes in the scalar coupling constants and electron-nuclear distances, but the importance of these results lies with the fact that acceptable values for the coupling constants could be obtained for all the carbons from only the isotropic shift data. The correlation time for electron relaxation remains a parameter determined in the fit of the data. An independent determination of τ_v is needed to more accurately fix the scalar coupling constants. The satisfactory use of metal-nuclear distance from crystallographic data confirms that the solution state and solid state structures of the complexes are similar.

Evidence for distinctly different behavior of the bis-ida complex compared with the bis-mida and bis-eida complexes is clearly seen in the value of the isotropic shifts of the C_O and C_N carbons (Figure 3-2). The possibility of structural differences causing this effect has already been discussed. It is interesting that the carboxylate carbons in all the complexes approach approximately the same value at

infinite temperature, about 15 ppm downfield from the diamagnetic value. No single explanation can be offered with any assurity.

In the presence of chemical exchange the observed $A/\hbar$ values are actually an effective scalar coupling constant and reflect the average electron spin density based upon the relative abundance of the various equilibrium states. The scalar coupling constants in Table 3-1 can be compared with the values below for other Ni(II) complexes containing the acetate group:

$A/\hbar$ ($\times 10^{-6}$, s^{-1})	Complex	References
Carboxylate carbon (C_o):		
-1.9 to -2.2	$[Ni(H_2O)_5(CH_3COOH)]^+$	10
2.7	$[Ni(histidine)_2]^{-2}$ (carboxylate bound)	2
-0.94	$[Ni(histidine)_2]^{-2}$ (carboxylate unbound)	2
Methylene carbon (C_N):		
-8.7	$[Ni(histidine)_2]^{-2}$ (carboxylate bound)	2
-2.3	$[Ni(histidine)_2]^{-2}$ (carboxylate unbound)	2

The values for the bis-histidine Ni(II) complex were obtained indirectly by observing the free ligand exchanging with complexed ligand.[2] The positive in sign for the C_o carbon in the carboxylate-bound and carboxylate-unbound forms are just opposite the signs expected from the mechanisms discussed earlier. The values were not obtained directly, but were obtained from a fit of data involving at least two different species. Thus, more uncertainty exists with these values. Including the values seen in this study, the (-1 to 6) x 10^6 s^{-1} range for the carboxylate carbons is larger than the (7 to 8) x 10^6 s^{-1} range for the methylene carbons indicating much more possible variation for the C_o carbon. In addition to chemical exchange and hydrogen-bonding, ionic strength can vary the effective scalar coupling constants by as much as 20%.[10]

The percent contribution of the dipole-dipole mechanism to the total transverse relaxation in the bis-eida complex decreases in the order (at 298 K):

$$C_o\ (53\%) > C_N\ (31\%) > C_\alpha \approx C_\beta\ (24\%)$$

The most signficant difference is seen between the carboxylate carbon and the other carbons. In the former both the dipole-dipole and scalar coupling relaxation mechanisms are important due to a smaller electron-nuclear distance and smaller scalar coupling constant. In the latter the scalar coupling relaxation mechanism is clearly dominant. For all the carbons the dipole-dipole contribution becomes less important with increasing temperature over the observed range.

This over-all pattern is also seen with the bis-mida complex as well as the bis-histidine[2] and acetate[10] nickel complexes.

The results in this study offer some insight on the nature of electron relaxation in paramagnetic complexes. According to existing theory[1,3,31] two origins for electron relaxation are distinquished. In one, electron relaxation is caused by collision with solvent molecules which creates a transient zero-field splitting component (ZFS) and modulates the interaction. In the second, the complex possesses a sizeable static ZFS component due to low molecular symmetry which is modulated by molecular rotation. A transient ZFS interaction is identified with complexes such as the hydrated nickelous ion[20] where a static ZFS component is not possible due to molecular symmetry. Studies with other complexes conclude that a transient ZFS interaction must be important because reasonable estimates of the molecular rotation rate and the static ZFS parameter (usually taken from solid state studies) cannot account for the observed relaxation.[1]

In other studies a static ZFS interaction is assumed which has the advantage of reducing the number of parameters to be determined since electron relaxation is now modulated by molecular rotation ($\tau_e = \tau_r$). With the complexes in this study it was not possible to fit the relaxation data while requiring $\tau_e = \tau_r$. This is clearly seen in the large difference in τ_e and τ_r at each temperature. The rotational correlation time is much smaller than the electron relaxation correlation time over most of the observed temperature region

indicating that modulating of electron relaxation is due almost entirely to a transient ZFS interaction. The T_{1e} and T_{2e} electron relaxation times at 298 K (Tables 3-3 and 3-4) are longer than those seen with other Ni(II) complexes.[32] Longer relaxation times were also seen with the 1:2 Ni(II):histidine complex.[2]

TABLE 3-1

^{13}C Isotropic Shifts and Parameters with Equation [3-1]*

Complex	Carbon	$\Delta\omega/\omega_o$ ‡ (ppm, 298 K)	$A/\hbar$* ($\times 10^{-6}$, s^{-1})	Intercept (ppm)
1:2 Ni(II):eida	C_o	-165.7	-5.8	125
	C_N	-389.1	-8.7	25
	C_α	-411.1	-8.4	45
	C_β	+269.6	+8.3	-148
1:2 Ni(II):mida	C_o	-174.7	-6.1	130
	C_N	-409.1	-8.6	22
	C_α	-388.1	-7.8	3
1:2 Ni(II):ida	C_o^1	-62.0	-3.7	122
	C_o^2	-104.0	-4.7	133
	C_o^3	-140.0	-6.0	162
	C_N^1	-426.2	-8.9	20
	C_N^2	-449.0	-10.5	77

* Obtained with equation [3-1] plus a constant. See Text.

‡ Relative to 1,4-dioxane.

TABLE 3-2

^{13}C Isotropic Shift Parameters with Equation [3-13]*

Complex	Carbon	A/ħ ($\times 10^{-6}$, s^{-1})	B_2 (ppm K^2)	D (cm^{-1})	C‡‡ ($\times 10^2$, ppm)
1:2 Ni(II):eida	C_o	-5.3	-0.9	+21	+0.9
	C_N	-7.4	-2.9	+70	+2.9
	C_α	-6.2	-5.6	+160	+5.7
	C_β	+4.3	+9.3	-273	-9.4
1:2 Ni(II):mida	C_o	-5.4	-1.6	+35	+1.6
	C_N	-7.6	-2.3	+55	+2.4
	C_α	-6.8	-2.2	+64	+2.1
1:2 Ni(II):ida	C_o^1	-3.4	-0.6	+13	+0.6
	C_o^2	-4.0	-1.6	+36	+1.7
	C_o^3	-4.1	-4.3	+96	+4.6
	C_N^1	-7.6	-2.8	+68	+3.0
	C_N^2	-6.9	-8.3	+198	+8.7

* Obtained with equations [3-12] through [3-14]. See Text.

‡‡ Slope of line in Figure 3-3. See Text.

TABLE 3-3

Parameters for Relaxation Rates with 1:2 Ni(II):eida*

E_r^o **	4.3 kcal mol^{-1}
τ_r^o **	3.9×10^{-14} s
E_v^o	4.9 kcal mol^{-1}
τ_v^o	3.4×10^{-16} s
$D^{\ddagger}$ (at 50 MHz)	4.1 cm^{-1}
τ_r (298 K) (calc)	5.6×10^{-11} s
τ_v (298 K) (calc)	1.4×10^{-12} s
T_{1e} (298 K) (calc)	2.5×10^{-11} s
T_{2e} (298 K) (calc)	8.4×10^{-12} s

* See Table 3-1 for A/ħ values. Electron-nuclear distances are 282, 289, 306 and 310 pm for C_O, C_N, C_α and C_β, respectively.

** From Table 2-3 of Chapter 2 for 1:2 Zn(II):eida.

‡ D = 4.5 cm^{-1} at 75 MHz. See Text.

TABLE 3-4

Parameters for Relaxation Rates with 1:2 Ni(II):mida*

E_r^o **	4.6 kcal mol^{-1}
τ_r^o **	2.1 x 10^{-14} s
E_v^o ‡	4.9 kcal mol^{-1}
τ_v^o	2.1 x 10^{-16} s
D	3.7 cm^{-1}
τ_r (298 K) (calc)	4.9 x 10^{-11} s
τ_v (298 K) (calc)	8.3 x 10^{-13} s
T_{1e} (298 K) (calc)	2.5 x 10^{-11} s
T_{2e} (298 K) (calc)	1.3 x 10^{-11} s

* See Table 3-1 for A/ħ values. Electron-nuclear distances are given in Table 3-3.

** From Table 2-3 of Chapter 2 for 1:2 Zn(II):mida.

‡ From Table 3-3 for 1:2 Ni(II):eida.

CAPTIONS TO FIGURES

Figure 3-1: Room temperature ^{13}C spectra of bis-ligand Ni(II) and Co(II) complexes with ida, mida and eida at 50 MHz. Peak locations for corresponding Zn(II) complexes are represented schematically.

Figure 3-2: Isotropic shift-versus-reciprocal temperature for C_o, C_N and C_α carbons relative to 1,4-dioxane.

Figure 3-3: Absolute value of $T\cdot(\Delta\omega/\omega_o)$ as a function of temperature for ^{13}C isotropic shifts. Dashed lines for 1:2 Ni(II):ida indicate extrapolated isotropic shift assuming no exchange.

Figure 3-4: Transverse relaxation rate of C_o, C_N, C_α and C_β carbons of 1:2 Ni(II):eida at 50 MHz. Calculated values: total (———), scalar coupling only (- - - - -) and dipole-dipole only (—·—·—).

Figure 3-5: Transverse relaxation rate of C_o, C_N, C_α and C_β carbons of 1:2 Ni(II):eida at 75 MHz. Calculated values: total (———), scalar coupling only (- - - - -) and dipole-dipole only (—·—·—).

Figure 3-6: Transverse relaxation rate of C_o and C_N carbons of 1:2 Ni(II):mida at 50 MHz. Calculated values: total (———), scalar coupling only (- - - - -) and dipole-dipole only (—·—·—).

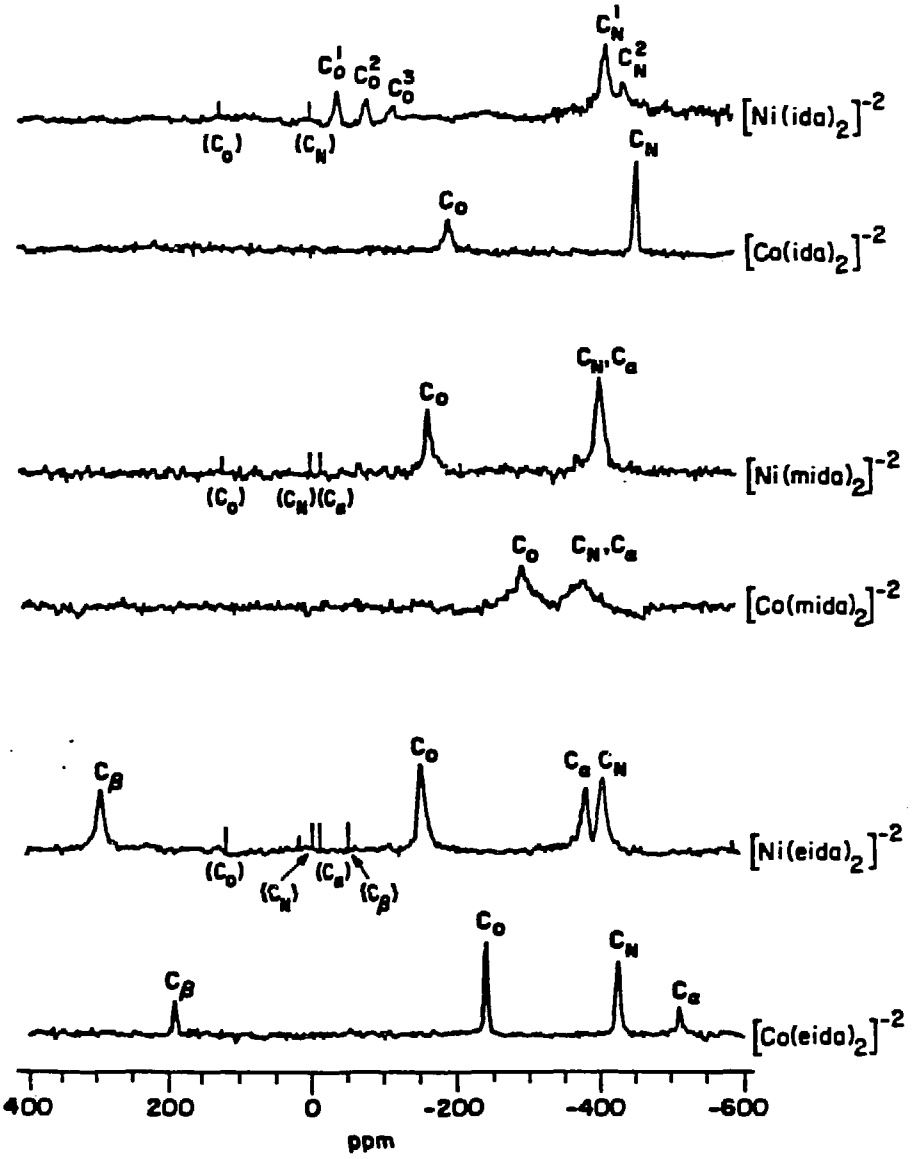
C_N^1
C_O^1 C_O^2 C_O^3
C_N^2
(C_O) (C_N)
$[Ni(ida)_2]^{-2}$
C_N
C_O
$[Co(ida)_2]^{-2}$
C_N, C_α
C_O
(C_O) $(C_N)(C_\alpha)$
$[Ni(mida)_2]^{-2}$
C_O C_N, C_α
$[Co(mida)_2]^{-2}$
C_β
C_O
C_α C_N
(C_O) (C_N) (C_α) (C_β)
$[Ni(eida)_2]^{-2}$
C_O
C_N
C_β
C_α
$[Co(eida)_2]^{-2}$
400 200 0 -200 -400 -600
ppm

Figure 3-1

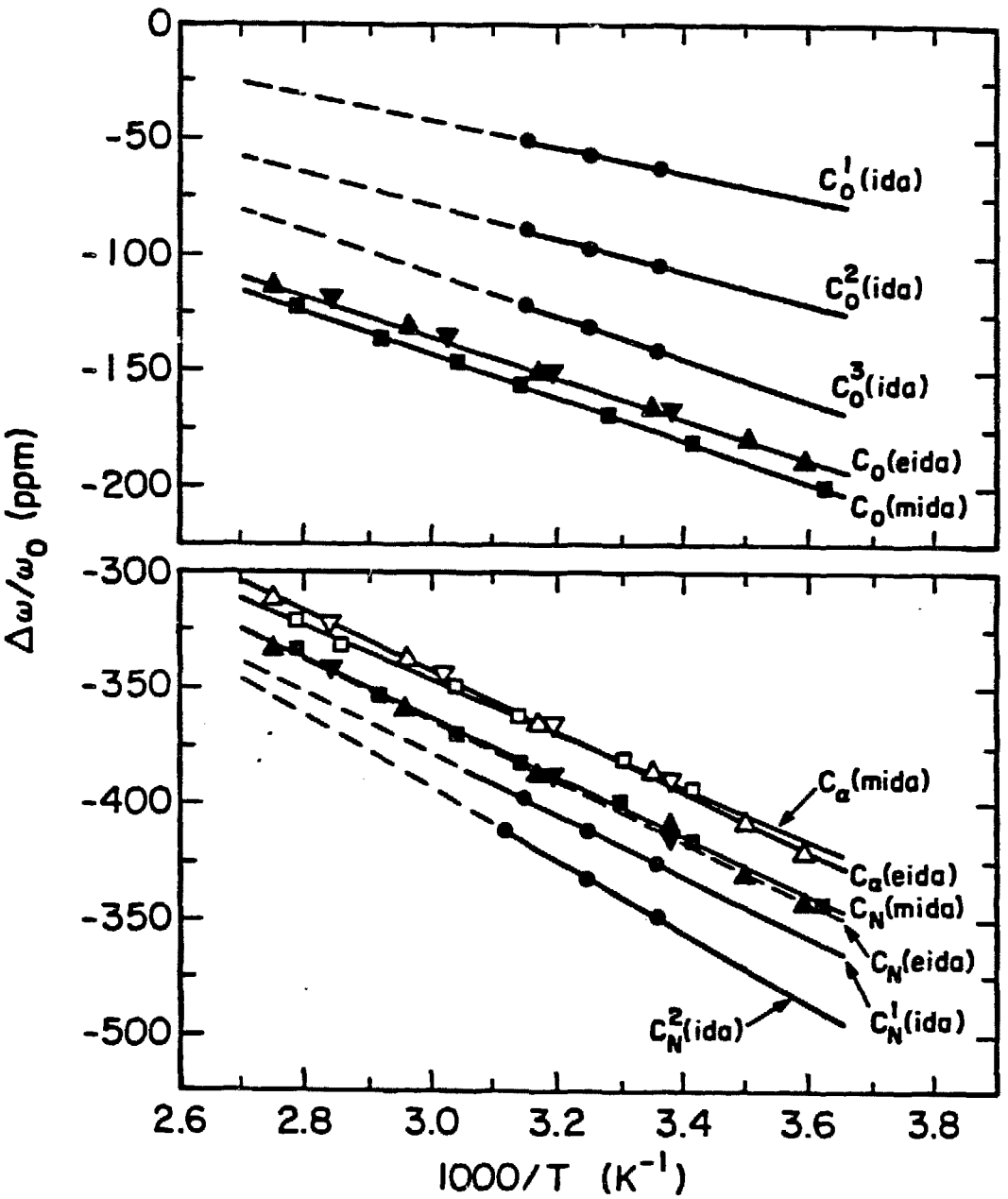
0
-50
-100
-150
-200
-300
-350
-400
-350
-500
$\Delta\omega/\omega_0$ (ppm)
C_0^1(ida)
C_0^2(ida)
C_0^3(ida)
C_0(eida)
C_0(mida)
C_α(mida)
C_α(eida)
C_N(mida)
C_N(eida)
C_N^1(ida)
C_N^2(ida)
2.6
2.8
3.0
3.2
3.4
3.6
3.8
1000/T (K^{-1})

Figure 3-2

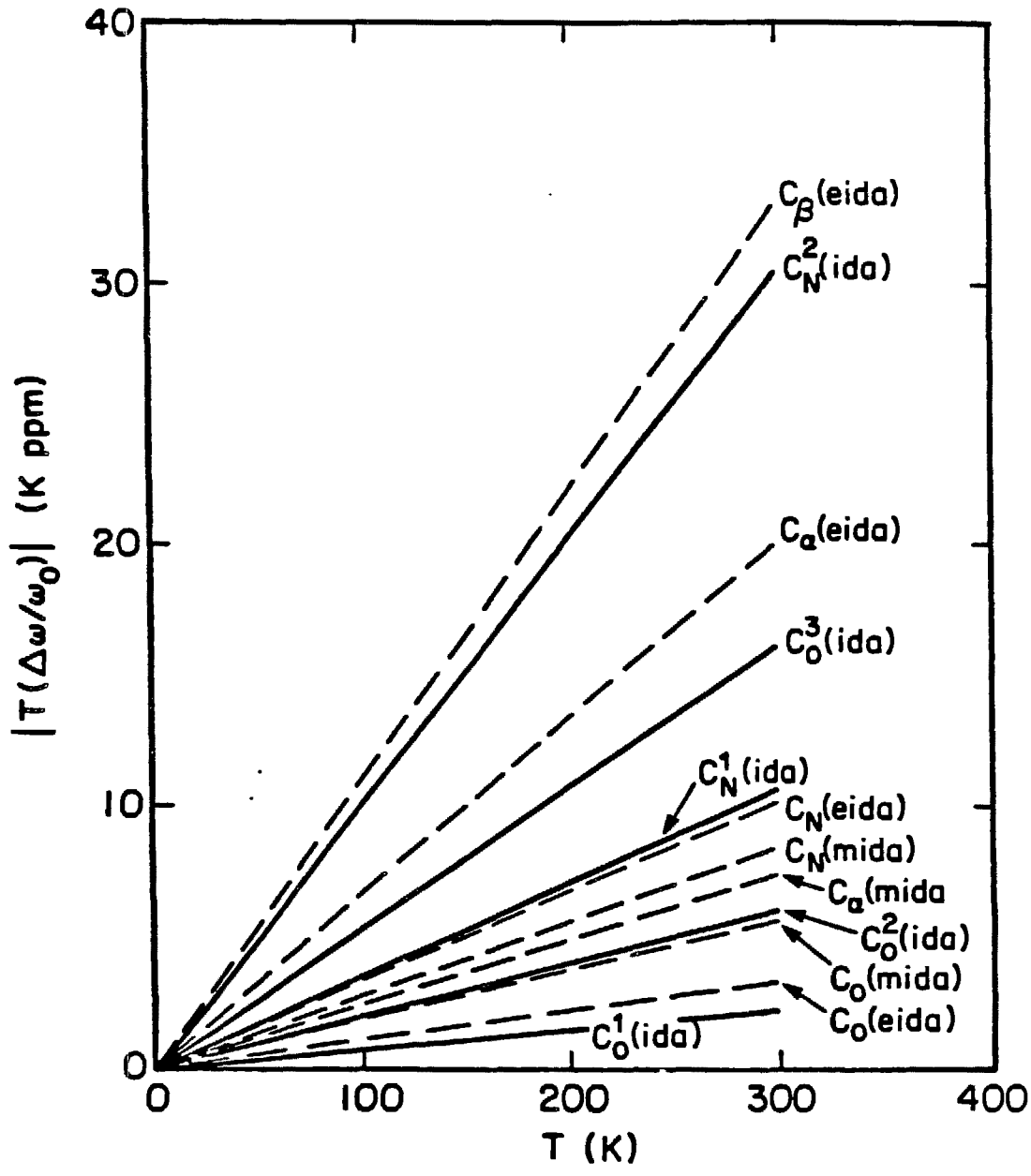
40
30
20
10
0
0
100
200
300
400
T (K)
|T(Δω/ω0)| (K ppm)
Cβ(eida)
C2N(ida)
Cα(eida)
C3O(ida)
C1N(ida)
CN(eida)
CN(mida)
Cα(mida
C2O(ida)
CO(mida)
CO(eida)
C1O(ida)

Figure 3-3

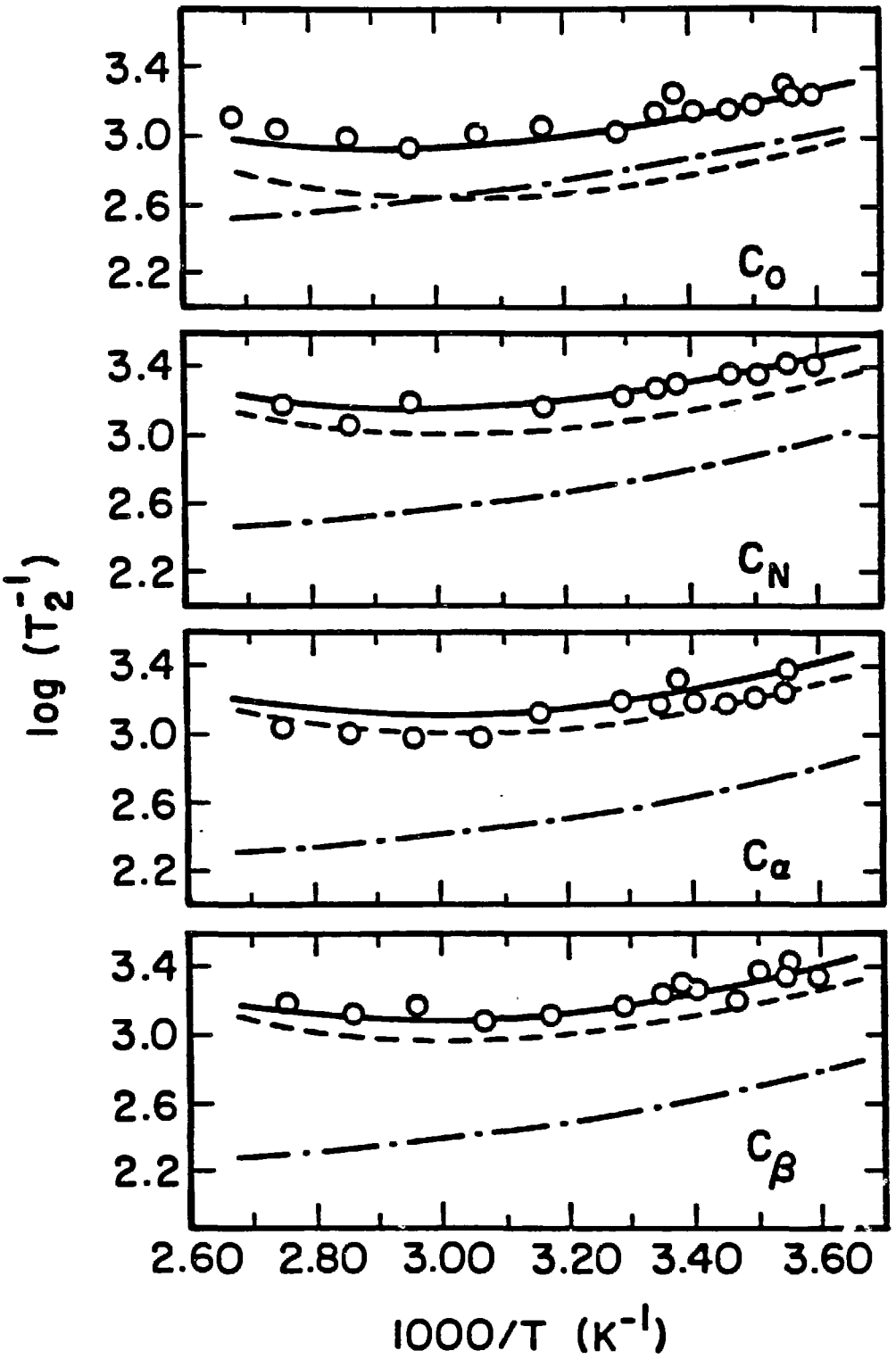
3.4
3.0
2.6
2.2
C_O
C_N
C_α
C_β
log (T_2^{-1})
2.60 2.80 3.00 3.20 3.40 3.60
1000/T (K^{-1})

Figure 3-4

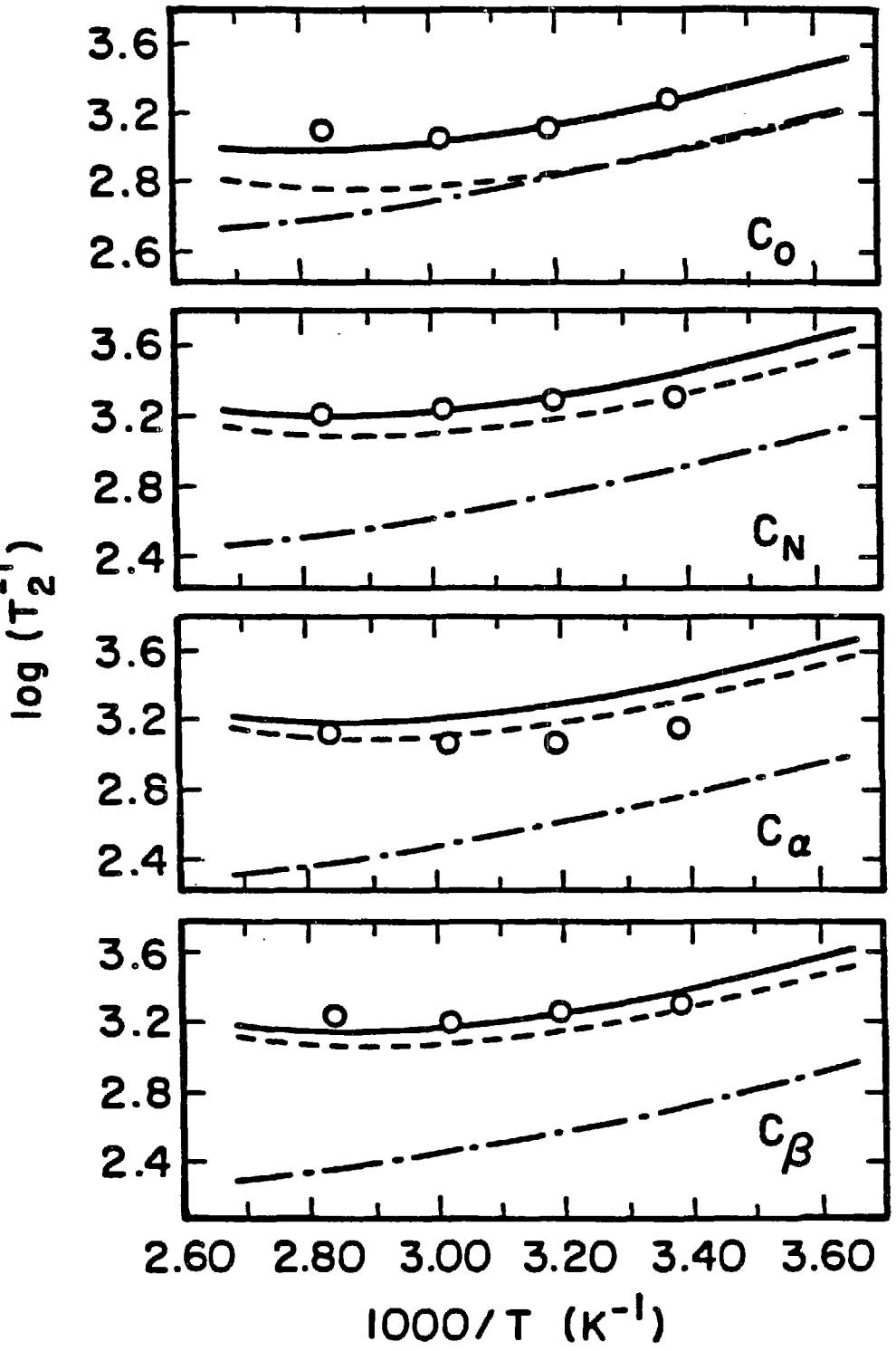
3.6
3.2
2.8
2.6
C_O
3.6
3.2
2.8
2.4
C_N
3.6
3.2
2.8
2.4
C_α
3.6
3.2
2.8
2.4
C_β
log (T_2^{-1})
2.60 2.80 3.00 3.20 3.40 3.60
1000/T (K^{-1})

Figure 3-5

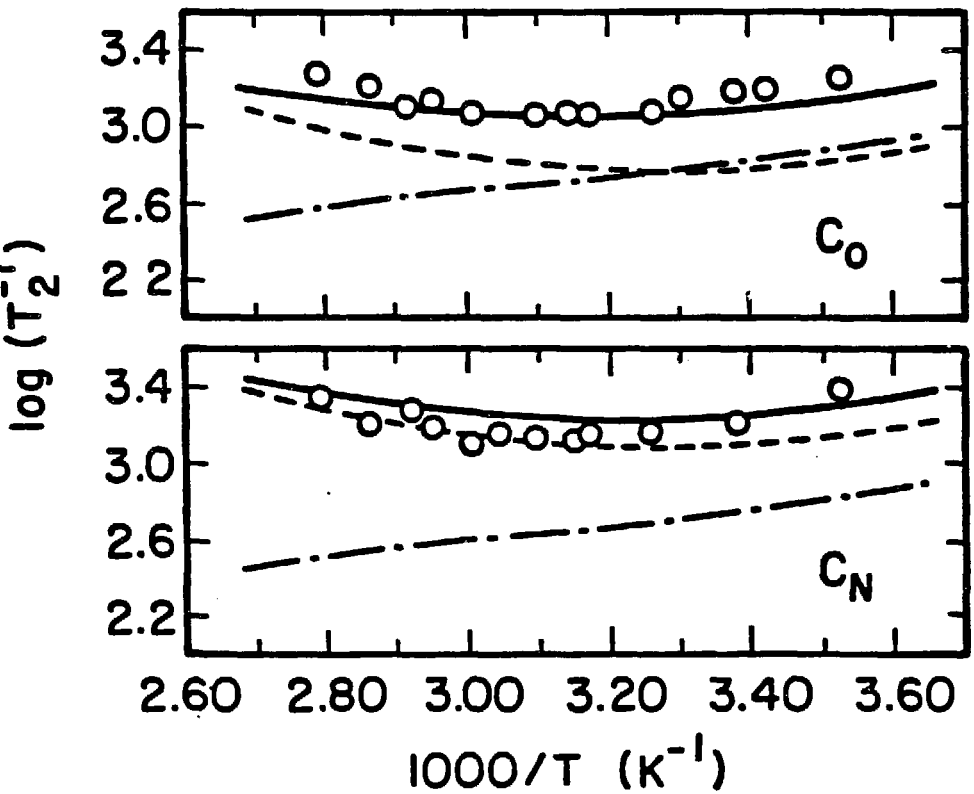
3.4
3.0
2.6
2 2
C_O
3.4
3.0
2.6
2.2
C_N
log (T_2^{-1})
2.60 2.80 3.00 3.20 3.40 3.60
1000/T (K^{-1})

Figure 3-6

REFERENCES

1 Nordenskiöld, L.; Kowalewshi, J.; Benetis, N. J. Phys. Chem. 1980, 84, 3646-3652.

2 Led, J.J.; Grant, D.M. J. Am. Chem. Soc. 1977, 99, 5845-5858; Led, J.J. Mol. Phys. 1980, 40, 1293-1313.

3 J.C., Ronfard-Haret; Chachaty, C. J. Phys. Chem. 1978, 82, 1541-1547.

4 Quaegebieur, J.-P.; Chachaty, C.; Yasukawa, T. Mol. Phys. 1979, 37, 409-424.

5 Kitagawa, S.; Yoshikawa, K.; Morishima, I. J. Phys. Chem. 1978, 82, 89-97.

6 Henry, B.; Boubel, J.-C., Delpuech, J.-J. Polyhedron 1982, 1, 113-121.

7 Hartman, J.S.; Kelusky, E.C. Can. J. Chem. 1979, 57, 2118-2122.

8 Benetis, N.; Holmen, K.; Kowalewski, J.; Nordenskiöld, L.; Wahlberg, D. Acta. Chem. Scand. 1981, A35, 513-520.

9 Yasukawa, T.; Chachaty C. Chem. Phys. Lett. 1977, 29, 311-314.

10 Fuentes, R. Jr.; Morgan, L.O.; Matwiyoff, N.A. Inorg. Chem. 1975, 14, 2774-2779.

11 Doddrell, D.M.; Healy, P.C.; Bendall, M.R. J. Magn. Res. 1978, 29, 163-166.

12 Eperson, W.G.; Martin, R.B. J. Amer. Chem. Soc. 1976, 98, 40-44.

13 Solomon, I. Phys. Rev. 1955, 99, 559-565; Bloembergen, N. J. Chem. Phys. 1957, 27, 572-573.

14 McConnell, H.M.; Robertson, R.E. J. Chem. Phys. 1958, 29, 1361-1365.

15 Perry, W.D.; Drago, R.S. J. Am. Chem. Soc. 1971, 93, 2183-2189. And references therein.

REFERENCES (continued)

16 Newman, K.E.; Meyer, F.K.; Merbach, A.E. J. Am. Chem. Soc. 1979, 101, 1470-1476.

17 LeMar, G.N.; "NMR of Paramagnetic Molecules", LeMar, G.N.; Horrocks, W. DeW Jr.; Holm R.H., eds.; Academic Press, New York, 1973, Chapter 3.

18 Kurland, R.J.; McGarvey, B.R. J. Magn. Reson. 1970, 2, 286-301.

19 Van Vleck, J.H.; "Theory of Electric and Magnetic Susceptibilities", Oxford Univ. Press, London, 1933.

20 Bloembergen, N; Morgan, L.O. J. Chem. Phys 1961, 34, 842-850.

21 Boubel, J.C.; Delpuech, J.J. Mol. Phys. 1974, 27, 113-127.

22 Redfield, A.G. Adv. Magn. Reson. 1965, 1, 1.

23 Strouse, C.E.; Matwiyoff, N.A. Chem. Commun. 1970, 439-440.

24 Matwiyoff, N.A.; Strouse, C.E.; Morgan, L.O. J. Amer. Chem. Soc. 1970, 92, 5222-5224.

25 Mammano, N.J.; Templeton, D.H.; Zalkin, A. Acta Cryst. 1977, B33, 1251-1254.

26 Wagner, M.R.; Beach, D.B. Acta Cryst. 1985 C41, 669-671.

27 Waysbort, D.; Navon, G. J. Chem. Phys. 1973, 59, 5585-5590.

28 Ho. F.F.-L.; Erickson, L.E.; Watkins, S.R.; Reilley, C.N. Inorg. Chem. 1970, 9, 1139-1153.

29 Jezowska-Trzebiatowska, B.; Latos-Grazynski, L. J. Inorg. Nucl. Chem. 1980, 42, 1079-1082.

30 Wayland, B.B.; Drago, R.S. J. Am. Chem. Soc. 1965, 87, 2372-2378.

31 Dwek, R.A.; "Nuclear Magnetic Resonance in Biochemistry" Clarendon Press, Oxford, 1973, p 185.

32 Neely, J.W.; Connick, R.E. J. Amer. Chem. Soc. 1972, 94, 3419-3423.

CHAPTER 4

ANALYSIS OF THE ^{13}C ISOTROPIC SHIFT OF THE 1:2 NICKEL(II):LIGAND COMPOUND WITH IDA TO EVALUATE POSSIBLE MECHANISMS FOR CIS-TRANS ISOMER INTERCONVERSION

CONTENTS

INTRODUCTION

Several coordination complexes of aminopolycarboxylate ligands are known to undergo intramolecular rearrangement in solution.[1,2,3,4,5] These have been investigated primarily by observing the temperature dependence of the proton NMR spectrum. Various mechanisms have been proposed and in some cases the free energy of activation at the coalescence temperature has been determined. Some factors that may be important are (1) the strength of the donor–metal bonds, (2) the ligand structure and the ability of the ligand to bond the maximum number of donor atoms, (3) the presence of a free acetate arm, (4) the availability of sites on the metal for additional reactivity and (5) the choice of metal.

Complexes with tridentate iminodiacetate (ida) and N-alkyl substituted analogues are interesting because of their simple and more symmetrical ligand–metal arrangements compared with other aminopolycarboxylate complexes. Unlike most others, two ida ligands can completely fill the available sites on the hexacoordinated metal. The two ligands are not attached to each other, thus affording more flexibility for rearrangement. Possible mechanism are not limited to a facial arrangement of the ligand since the meridional arrangement also exists with ida in some octahedral compounds.[6,7]

Most of the NMR spectra and other types of spectroscopic data with bis-ida complexes and analogues has been interpreted assuming a rigid solution state structure (Co(III)[6,8,9,10,11], Ni(II)[2,3,4,12,13] Cr(III)[14,15,16], Zn(II)[7,17,18], Mo(VI)[19,20,21], Mo(V)[22], Co(II)[1,23,24], Rh(III)[11], Pt(II)[25], Pd(II)[26], W(VI)[27]). With the 1:2 Ni(II):ida complex, all three possible isomers (Δ-cis, Λ-cis and trans) are present based on the peak assigment in the proton spectrum.[2] (An earlier assignment[13] is incorrect. Proof of the correct assignment was given by the ^{13}C spectrum of the same complex.[28]) Dynamic behavior with the 1:2 Ni(II):ida complexes was reported by Everhart and Evilia[3]. Four proton peaks assigned to the A and B methylene protons in the Λ-cis and Δ-cis isomers collapsed to two peaks at higher temperatures presumably due to interconversion between the two isomers. The same four proton peaks are seen with the Co(III)[8,11] and Rh(III)[11] complexes indicating both isomers are present. With the faster reacting Co(II) complex,[1] however, the room temperature spectra showed only two peaks corresponding to the already collapsed set. Pratt and Smith observed some ^{1}H peak broadening with a decrease in temperature with the bis-mida Co(II) complex indicating the presence of a slow exchanging process.[13] Recently, Gennaro and Mirti[7] reported an intramolecular rearrangement with the 1:2 Zn(II):ida complexes based on the coalescence at higher temperature of the AB pattern of the methylene protons.

The involvement of the trans isomer in the interconversion of the cis isomers with the 1:2 Ni(II):ida complex is not obvious from the proton spectrum since the trans peaks are beneath the much larger cis

peaks.[2] A possible mechanism for Λ-cis-Δ-cis interconversion that does not involve the trans isomer has been considered.[11] A more likely mechanism is similar to Bailar twist mechanism[29] and involves interconversion between all three possible geometric isomers. Recently, the temperature dependence of the ^{13}C spectrum was observed[28] which confirmed that both cis and trans isomers are involved in the rearrangement process.

In this chapter a ^{13}C shift-versus-temperature analysis is presented for the carboxylate and methylene carbon peaks of the 1:2 Ni(II):ida complex. A model based on the Bailar twist is used to fit the data. Evidence is given that interconversion between the two cis isomers is occuring via two pathways, one involving the direct interconversion between the two isomers, the other involving the formation of the trans isomer as an intermediate.

EXPERIMENTAL

The natural abundance ^{13}C spectrum of the 1:2 Ni(II):ida solution from Chapter 3 (0.2 M in metal ion) was observed over the temperature range from 290 K to 365 K. The FT spectra were collected on a Bruker AM-500 spectrometer operating at 125.7 MHz.

Each 5 mm NMR tube contained a concentrically mounted capillary containing ethylene glycol. The temperature was monitored by taking

the ^{1}H spectrum (8 scans) immediately before and immediately after the ^{13}C collection. The average separation of the ethylene glycol peaks was used to determine the temperature as described in Chapter 2.

RESULTS

The room temperature ^{13}C spectrum shows three peaks in the carboxylate region at room temperature (See Figure 3-1). The two large downfield peaks (C_o^1,C_o^2) have been assigned to carboxylate carbons in the two different environments of the cis isomers. The third smaller peak (C_o^3) is assigned to carbons in the trans isomer. All three peaks are clearly coalesced into a single peaks above 360 K.

The frequency maximum of each peak is plotted as a function of temperature in Figure 4-1. Carbon peaks C_o^2 and C_o^3 coalesce at about 345 K. Coalescence with C_o^1 occurs at a higher temperature (about 353 K. The higher temperature for the second coalescence is consistent with the larger separation of these peaks.

The model in Scheme 1 was used to analyze the results. All three isomers are included. (The acetate arm in the lower coordinated ligand in each species in Scheme 1 is not drawn to simplify the drawing.) Interconversion between any two isomers is achieved by rotating one ida ligand 120° relative to the other ligand about the axis perpendicular to the O-N-O planes of the ligands. The first

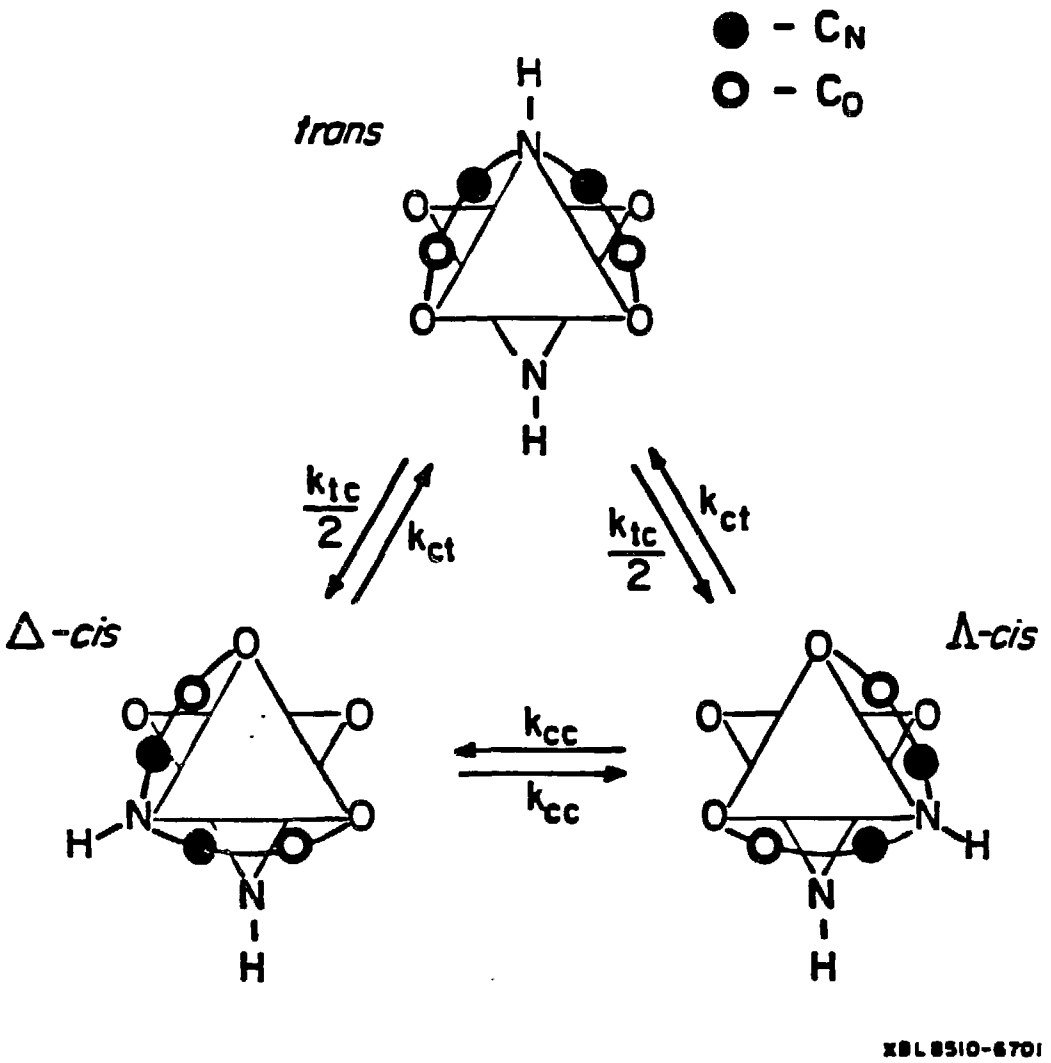
● - C_N
○ - C_O
trans
$\frac{k_{tc}}{2}$
k_{ct}
$\frac{k_{tc}}{2}$
k_{ct}
Δ-cis
Λ-cis
k_{cc}
k_{cc}
XBL8510-6701

SCHEME 1:

order rate constants, k_{cc}, k_{ct} and k_{tc}, correspond to the interconversion between the possible isomers as indicated. Rate constants k_{cc} and k_{ct} are not necessarily equal since the transition state of the direct Λ-*cis*-Λ-*cis* interconversion may involve appreciable overlap of the amine protons which would inhibit this process.

The rate constant for *cis*-to-*trans* interconversion k_{ct} is related to the rate constant for *trans*-to-*cis* interconversion k_{tc} by the equilibrium constant:

$$K_{eq}(\textit{trans} \rightleftharpoons \textit{cis}) = k_{tc}/k_{ct}$$

K_{eq} was determined from the areas of the *cis* and *trans* peaks at room temperature and equals 4.0 ± 0.2. This equilibrium distribution agrees with an earlier report based on peak areas in the proton spectrum.[2]

The temperature dependence of the *cis*-*trans* equilibrium was determined by extrapolating the low temperature isotropic shifts to the high end of the temperature range. By assuming complete collapse at 370 K, a value of K_{eq} = 2.0 at this temperature was determined. The temperature dependence is given by the parameters in Table 4-1 which indicate a small energy difference in the *cis* and *trans* configurations. The *cis* configuration is more favored as indicated by the negative enthalpy. The small entropy is reasonable for this isomerization process. Within the region of slow exchange from 298 K

to 313 K a small decrease (about 4%) is predicted in the area of the *cis* peaks and a small increase (about 15%) with the *trans* peak. These changes were not seen partly due to the quality of the natural abundance spectra. The observed value for the equilibrium constant may be compared to a statistical value of $K_{eq} = 2$ based on the number of ways a second ida ligand can attached itself to the mono-ida complex.

Scheme 1 represents two pathways for interconversion between the Λ-*cis* and Δ-*cis* conformers, a direct pathway (*i*)

$$\Lambda\text{-}\underline{cis} \rightleftharpoons \Delta\text{-}\underline{cis} \qquad (\underline{i})$$

and an indirect route (*ii*) involving the formation of the *trans* isomer as an intermediate

$$\Lambda\text{-}\underline{cis} \rightleftharpoons \underline{trans} \rightleftharpoons \Delta\text{-}\underline{cis} \qquad (\underline{ii})$$

It is convenient to define a parameter α:

$$\alpha = \frac{k_{cc}}{k_{ct}}$$

The value of α will be zero or larger depending upon the importance of the direct pathway (*i*) compared to pathway (*ii*) for interconversion of the Λ-*cis* and Δ-*cis* isomers.

The temperature dependence of k_{ct} is described by an Eyring-type equation:

$$k_{ct} = \frac{kT}{h} \exp\left(\frac{-\Delta H^{\ddagger}}{RT} + \frac{\Delta S^{\ddagger}}{R}\right)$$

where the parameters have their usual meaning.

It will be assumed that k_{ct} and k_{cc} have the same temperature dependence ($\Delta H^{\ddagger}$ is the same for both processes), therefore the rate behavior for all the interconversions in Scheme 1 are described by only three parameters, α, $\Delta H^{\ddagger}$ and $\Delta S^{\ddagger}$, where the activation parameters pertain to the expression above for k_{ct}.

The ^{13}C spectra were simulated at several temperatures using the equation of Reeves and Shaw[30] for the absorption spectrum under conditions of low saturation. The equation and the required transfer-exchange matrix representing Scheme 1 are described in Appendix D. The transverse relaxation rates were taken from the linewidths of the carboxylate and methylene carbons of the 1:2 Ni(II):mida complex (Chapter 3). Parameters α, $\Delta H^{\ddagger}$ and $\Delta S^{\ddagger}$ were varied while comparing a plot of the calculated peak maxima to the observed values in Figure 4-1. A good fit was obtained with the values given in Table 4-2. The calculated values are plotted in Figure 4-1 for comparison. Because of the high correlation between $\Delta H^{\ddagger}$ and $\Delta S^{\ddagger}$, other sets of enthalpy and entropy of activation values produced equally good fits (See Table 4-2). In each case, the value of α remained unchanged.

Confirmation of the kinetic parameters was obtained by using the parameters in Table 4-2 to predict the temperature dependence of the methylene carbon peaks. The cis carbon peak (C_N^1) (See Figure 3-1) coalesces with the trans carbon peak at about 344 K. The calculated peak maxima are plotted with the observed values in Figure 4-2 which show very good agreement.

DISCUSSION

The Bailar twist mechanism has been investigated primarily with tris-bidentate compounds where interconversion of equatorial and axial methylene protons is accomplished at a rate faster than ligand exchange.[31,32,33,34] In these systems the ligands are limited to rearrangement between two states involving at least two ligands. Evidence for the Bailar twist mechanism with other Ni(II) compounds has also been seen with the 1:1 compound with EDTA and analogues containing additional carbons in the $>N-(CH_2)_n-NK$ backbone where the twist is blocked for $n > 3$.[24]

The satisfactory fit of the data in Figures 4-1 and 4-2 is consistent with the Bailar twist mechanism with the bis-ida complex. From the coalescence pattern seen in Figure 4-1 it is obvious that the indirect pathway (ii) for interconversion is operating. The temperature of coalescence of the C_O^2 and C_O^3 peaks alone is sufficient to determine the rate of cis-trans interconversion. The importance of

the direct pathway (i) is seen in the value of α. For comparison the calculated coalescence patterns for (a) $\alpha = 0.6$, (b) $\alpha = 1.0$ and (c) $\alpha = 1.6$ have also been drawn in Figure 4-1. As expected, the coalescence of C_o^1 and the combined C_o^2 and C_o^3 peaks moves to lower and higher temperatures as the direct pathway (ii) becomes more or less important, respectively.

The value of $\alpha = 1.0$ seen in this study indicates that the Λ-*cis*-to-Δ-*cis* and *cis*-to-*trans* interconversions occur at similar rates. Since the former involves some overlap of the amine protons, it can be concluded that this overlap is small. No overlap of amine protons is seen in the ground state configuration of the *cis* isomers. Several bis-ida complexes are known to exist in the *cis* configuration which may be more stable than the *trans* configuration as seen in this study. Direct evidence of minimal overlap is also seen in the solid state structure of *cis*-$K[Cr(III)(ida)_2]\cdot 3H_2O$ where distortion of the ligand on the metal due to overlap is not apparent.[35] The distance between the amine protons in this *cis*-configuration complex is about 300 pm.

The formation of the transition state, possibly a trigonal prismatic structure, during the Λ-*cis*-to-Δ-*cis* interconversion is a more severe test for overlap of the amine protons. The distance between the amine protons in this configuration is estimated to be about 240 pm for the bis-ida Cr(III) compound[35] assuming the twist is an angular function only and bond lengths are unchanged. This distance is expected to be slightly larger for the Ni(II) compound due

to the larger ion radius. Some overlap may exists with each protons which has a Van der Waals radius of 120 pm, but the overlap is apparently small and does not affect the rate of direct interconversion of the cis isomers.

The activation free energy for the racemization of $[Ni(II)(en)_3]^{+2}$ via a twist mechanism is $\Delta G^{\ddagger}_{coal}$ (374 K) = 15.7 kcal mol^{-1}.[36] For the racemization of tris(meso-butylenediamine)nickel(II) $\Delta G^{\ddagger}_{coal}$ (323 K) = 14.0 kcal mol^{-1}.[37] These values can be compared directly with the activation free energy for the twist mechanism in this study ($\Delta G^{\ddagger}$ = 14.8 kcal mol^{-1}), if the temperature dependence of $\Delta G^{\ddagger}$ is small ($\Delta S^{\ddagger}$ = 0) for all the processes. The larger value of $\Delta G^{\ddagger}$ seen with the tris-ethylenediamine complex may be due to considerable distortion of the ligand structure which occurs in forming a trigonal prismatic configuration. Very little distortion of the ligand is necessary to form the same configuration with the ligands in this study.

The activation energy for racemization of $[Ni(II)(EDTA)]^{-2}$ at coalescence (353 K) is 14.2 kcal mol^{-1}.[3] For the racemization of $[Ni(II)(1,3\text{-PDTA})]^{-2}$ $\Delta G^{\ddagger}$ = 14 kcal mol^{-1} at coalescence (352 K).[3] For racemization of $[Ni(II)(NTA)]^{+1}$ $\Delta H^{\ddagger}$ = 9 kcal mol^{-1} and $\Delta S^{\ddagger}$ = -13 eu,[2] giving an activation free energy of 13.6 kcal mol^{-1} at 353 K. The free energies of activation are all within ca. 1.0 kcal mol^{-1} of the values seen in this study even though a different mechanism involving detachment of an acetate arm (the "$\Lambda \rightleftharpoons \Delta$ mechanism")[3,5] is presumably operating with these compounds.

The ^{13}C room temperature spectra of the bis-ida compounds of Co(II) and Zn(II) (See Figure 2-1) show only a single set of peaks for the carboxylate carbons, presumably the average of the cis and trans isomers. The activation energies of the Bailar twist have been calculated by both Wentworth[38] and Larsen et al.,[39] for transition metal compounds on the basis of ligand field theory and the number of d electrons.[40] Co(II) and Zn(II) show virtually no preference for an octahedral configuration compared to the trigonal prismatic configuration, while Ni(II) shows a strong preference.[38] This calculation is consistent with the observed dynamic behavior of the bis-ida compounds.

The strong resistence to twist with Ni(II) complexes compared to Zn(II) and Co(II) complexes is also seen with other ligands. With ligands NTA,[2] 1,3-PDTA[3,41] and EDDA[1,3] proton peaks are resolved in the proton spectra of the Ni(II) compounds indicating more than a single isomer present. The same resolution is not seen with the Co(II) and Zn(II) complexes possibly indicating a much faster rearrangement process in the latter.

TABLE 4-1

Parameters for Cis-Trans Equilibrium with 1:2 Ni(II):ida

ΔH_{eq}	-2.1 kcal mol^{-1}
ΔS_{eq}	-4.4 eu
K_{eq} (298 K) (calc)*	4.0 ± 0.2

* $K_{eq} = k_{tc}/k_{ct}$, trans $\rightleftharpoons$ cis

TABLE 4-2

Activation Parameters for Cis-Trans Isomer Interconversion with 1:2 Ni(II):ida

$\Delta H^{\ddagger}$	(14.8 ± 0.2) kcal mol^{-1}*
$\Delta S^{\ddagger}$	0.0 eu
α**	1.0 ± 0.2
k_{cc} (298 K) (calc)	88 s^{-1}
k_{ct} (298 K) (calc)	88 s^{-1}
k_{tc} (298 K) (calc)	350 s^{-1}

* The following sets of $\Delta S^{\ddagger}$ and $\Delta H^{\ddagger}$ values produced equally good fits with no change in α: ($\Delta S^{\ddagger}$ = 5.0 eu, $\Delta H^{\ddagger}$ = 16.5 kcal mol^{-1}) ($\Delta S^{\ddagger}$ = 10 eu, $\Delta H^{\ddagger}$ = 18.0 kcal mol^{-1})

** $\alpha = k_{cc}/k_{ct}$. See Scheme 1, Chapter 4.

CAPTIONS TO FIGURES

Figure 4-1: Carbon-13 peak maxima-versus-temperature for the carboxylate carbons (C_O) of 1:2 Ni(II):ida relative to 1,4-dioxane. The curves are the calculated patterns for $\Delta H^{\ddagger}$ = 14.8 kcal mol^{-1}, $\Delta S^{\ddagger}$ = 0.0 eu and (a) α = 0.6, (b) α = 1.0 and (c) α = 1.6

Figure 4-2: Carbon-13 peak maxima-versus-temperature for the methylene carbons (C_N) of 1:2 Ni(II):ida relative to 1,4-dioxane. The curves are the calculated patterns for $\Delta H^{\ddagger}$ = 14.8 kcal mol^{-1}, $\Delta S^{\ddagger}$ = 0.0 and α = 1.0.

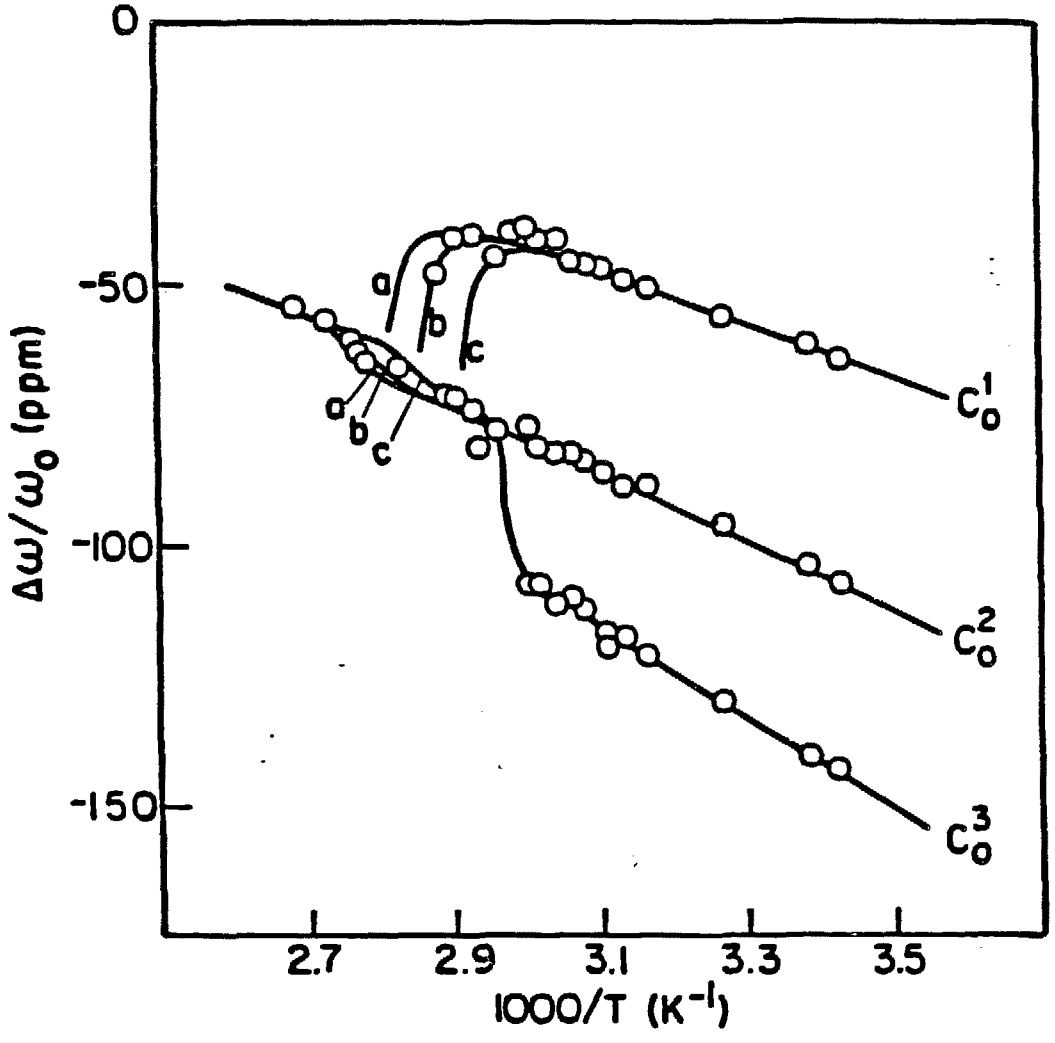
0
-50
-100
-150
Δω/ω₀ (ppm)
a
b
c
a
b
c
C₀¹
C₀²
C₀³
2.7
2.9
3.1
3.3
3.5
1000/T (K⁻¹)
XBL 8510-6700

Figure 4-1

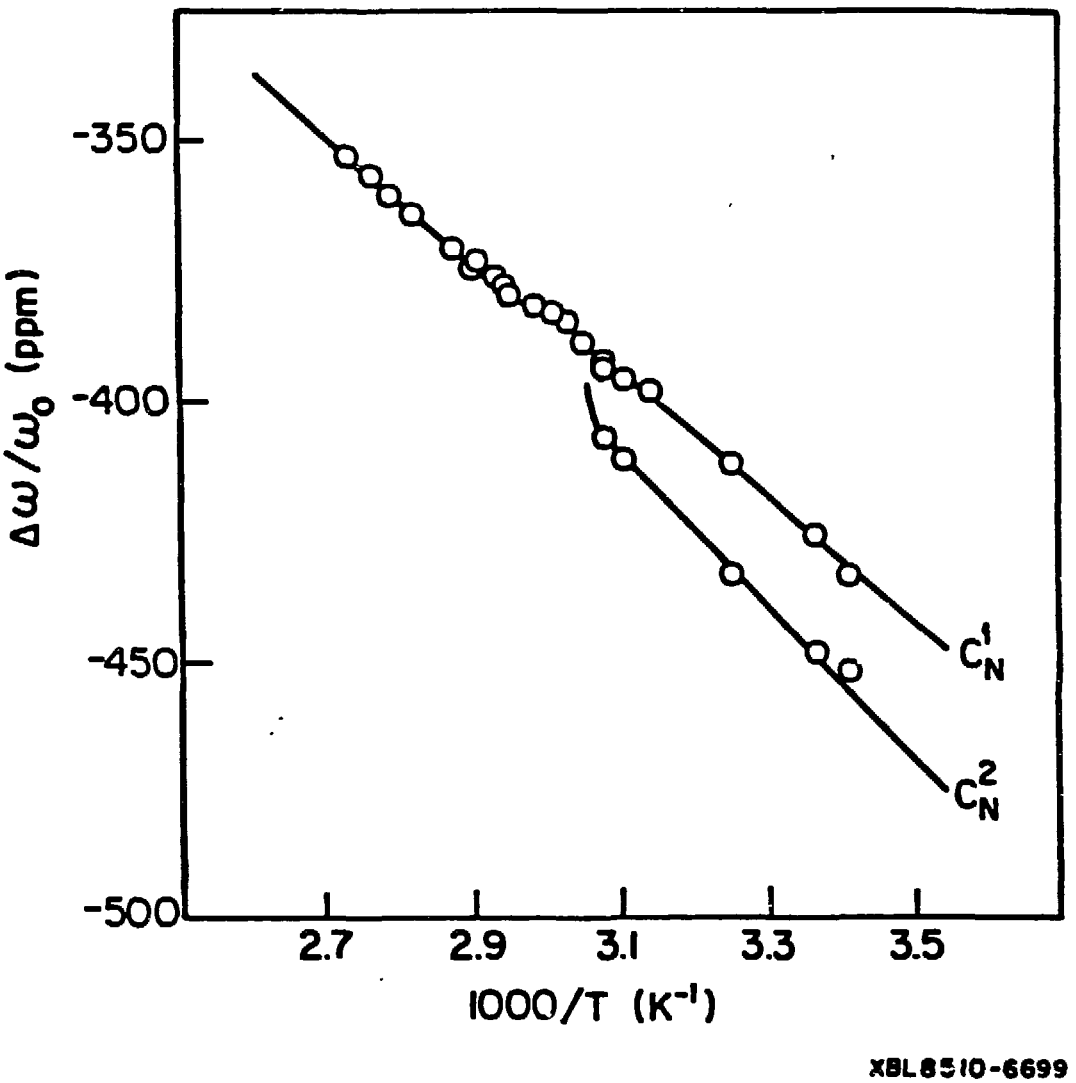
-350
-400
-450
-500
Δω/ω0 (ppm)
2.7
2.9
3.1
3.3
3.5
1000/T (K-1)
C1N
C2N
XBL8510-6699

Figure 4-2

APPENDIX D: Derivation of the Transfer-Exchange Matrix Representing Scheme 1 of Chapter 4

For a system of n distinct sites the steady-state absorption-mode magnetization V(ω) is given by Reference 30 of Chapter 4:

$$V(\omega) = -\omega_1 M_o \underline{C}^{-1} \cdot \underline{P}$$

where

$$\underline{C} = \underline{R}_2 + \underline{w} \cdot \underline{R}_2^{-1} \cdot \underline{w}$$

$$\underline{R}_2 = \underline{T}_2 + \underline{K}$$

M_o is the thermal equilibrium value for z-mode magnetization and ω_1 is the radio frequency. The matrix $\underline{w}$ is a diagonal matrix of dimension (n x n) whose elements are $\Delta\omega_i = \omega - \omega_i$ for each site i with Larmor frequency ω_i. Matrix $\underline{P}$ is a column matrix of dimension (n x 1) with elements equal to the fractional population for the respective site. Matrix $\underline{T}_2$ is a diagonal matrix of dimension (n x n) whose elements are the transverse relaxation rates T_2^{-1} of each site.

$\underline{K}$ is the transfer-rate matrix of dimension n x n. For a completely general three site system with sites A, B and C, $\underline{K}$ is defined:

APPENDIX D (Continued)

$$\underline{K} = \begin{vmatrix} -(k_{ab} + k_{ac}) & k_{ba} & k_{ca} \\ k_{ab} & -(k_{ba} + k_{bc}) & k_{cb} \\ k_{ac} & k_{bc} & -(k_{ca} + k_{cb}) \end{vmatrix}$$

where k_{ij} is the first order rate constant for exchange from site i to site j.

In accordance with Scheme 1 of Chapter 4, sites A and B are assigned the two different environments for the carboxylate carbon (or two identical environments for the methylene carbon) in the cis isomers. Site C is assigned to the trans isomer. The following first order rate constants can be assigned and substituted in the above expression for K:

$$k_{ab} = k_{cc}$$
$$k_{ac} = k_{ct}$$
$$k_{ba} = k_{cc}$$
$$k_{bc} = k_{ct}$$

$$k_{ca} = \frac{1}{2} k_{tc}$$
$$k_{cb} = \frac{1}{2} k_{tc}$$

APPENDIX D (Continued)

The rate constant k_{tc} and k_{ct} are related by the equilbrium constant K for the cis-trans equilibrium:

$$K = \frac{k_{tc}}{k_{ct}}$$

Rate constants k_{cc} and k_{ct} are related by the ratio α ($= k_{cc}/k_{ct}$). With these relationships the useful form of the transfer-exchange matrix becomes:

$$\underline{K} = k_{ct} \begin{vmatrix} -(\alpha+1) & \alpha & K/2 \\ \alpha & -(\alpha+1) & K/2 \\ 1 & 1 & -K \end{vmatrix}$$

The population matrix $\underline{P}$ used in the analysis is:

$$\underline{P} = \begin{vmatrix} \frac{K}{2(1+K)} \\ \frac{K}{2(1+K)} \\ \frac{1}{1+K} \end{vmatrix}$$

It can be shown that:

$$\sum_{i=1}^{n} P_i = 1$$

and $\underline{K} \cdot \underline{P}$ equals the zero matrix consistent with the steady state assumption.

REFERENCES

1 Everhart, D.S.; Evilia, R.F. Inorg. Chem. 1977, 16, 120-125.

2 Erickson, L.E.; Ho, F. F.-L.; Reilley, C.N.; Ho, F.F.-L. Inorg. Chem. 1970, 9, 1148-1153.

3 Everhart, D.S.; Evilia, R.F. Inorg. Chem. 1975, 14, 2755-2759.

4 Erickson, L.E.; Young, D.C.; Ho, F. F.-L., Watkins, S.R.; Terrill, J.B.; Reilley, C.N. Inorg. Chem. 1971, 10, 441-453.

5 Gennaro, M.C.; Mirti, P.; Casalino, C. Polyhedron 1983, 2, 13-18.

6 Legg, J.I.; Cooke, D.W. Inorg. Chem. 1966, 5, 594-601.

7 Gennaro, M.C.; Mirti, P. J. Inorg. Nucl. Chem. 1981, 43, 1711-1717.

8 Cooke, D.W. Inorg. Chem. 1966, 5, 1141-1145.

9 Mori, M.; Shibata, M.; Kyuno, E.; Maruyama, F. Bull. Chem. Soc. Jap. 1962, 35, 75-77.

10 Van Saun, C.W.; Douglas, B.E. Inorg. Chem. 1969, 8, 1145-1149.

11 Smith, B.B.; Sawyer, D.T. Inorg. Chem. 1968, 7, 922-92**8.

12 Jones, M.B.; Pratt, L. J. Chem. Soc. Dalton 1976, 1207-1212.

13 Pratt, L.; Smith, B.B. Trans. Faraday Soc. 1969, 65, 915-927.

14 Weyh, J.A.; Hamm, R.E. Inorg. Chem. 1968, 7, 2431-2435.

15 Israily, N. Bull. Soc. Chim. 1966, 1141-1144.

16 Vieles P.; Israily, N. Bull. Soc. Chim. 1967, 139-144.

17 Gennaro, M.C.; Mirti, P. J. Inorg. Nucl. Chem. 1977, 39, 1259-1264.

REFERENCES (Continued)

18 Rabenstein, D.L.; Blakney, G.; Fuhr, B.J. Can. J. Chem. 1975, 53, 787-791.

19 Chan, S.I.; Kula, R.J.; Sawyer, D.T. J. Amer. Chem. Soc. 1964, 86, 377-379.

20 Kula, R.J. Anal. Chem. 1966, 38, 1382-1388.

21 Kula, R.J. Anal. Chem. 1967 39, 1171-1175

22 Haynes, L.V.; Sawyer, D.T. Inorg. Chem. 1967, 6, 2146-2150.

23 Pratt, L.; Smith, B.B. Trans. Faraday Soc., 1969, 65, 1703-1708.

24 Latos-Grazynski, L.; Jezowska-Trzebiatowska B. J. Inorg. Nucl. Chem. 1981, 43, 1249-1253.

25 Smith, B.B.; Sawyer, D.T. Inorg. Chem., 1969, 8, 379-384.

26 Smith, B.B.; Sawyer, D.T. Inorg. Chem., 1968, 7, 1526-1532.

27 Freeman, M.A.; Van der Vaart, D.R.; Schultz, F.A.; Reilley, C.N. J. Coord. Chem. 1981, 11, 81-90.

28 Klotter, K., University of California, Berkeley, unpublished results.

29 Bailar, J.C., Jr. J. Inorg. Nucl. Chem. 1958, 8, 165-175.

30 Reeves, L.W.; Shaw, K.N. Can. J. Chem. 1970, 48, 3641-3653.

31 VanQuickenborne, L.G.; Pierloot, K. Inorg. Chem. 1981, 20, 3673-3677, and references therein.

32 For reviews see Fortman, J.J.; Sievers, R.E. Coord. Chem. Rev. 1971, 6, 331-375; Serpone, N.; Bickley D.G. Prog. Inorg. Chem. 1972, 17, 391-566.

33 Basolo, F.; Hayes, J.C.; Neumann, H.M. J. Amer. Chem. Soc. 1954, 76, 3807-3809.

34 Wilkins, R.G.; Williams, M.J.G. J. Chem. Soc. 1957, 1763-1769.

35 Mootz, D.; Wunderlich, H. Acta. Cryst. 1980, B36, 445-447.

REFERENCES (Continued)

36 Ho.; F.F.-L.; Reilley, C.N. Anal. Chem. 1970, 42, 600-605.

37 Evilia, R.F.; Young, D.G.; Reilley, C.N. Inorg. Chem. 1971, 10, 433-440.

38 Wentworth, R.A.D. Coord. Chem. Rev. 1972, 9 171-187.

39 Larsen, E.; LaMar, G.N.; Wagner, B.E.; Parks, J.E.; Holm,. R.H. Inorg. Chem. 1972, 11, 2653-2659.

40 Hoffman, R.H.; Howell, J.M.; Rossi, A.R. J. Amer. Chem. Soc. 1976, 98, 2484-2492.

41 Rabenstein, D.L.; Kula, R.J. J. Amer. Chem. Soc. 1969, 91, 2492-2503.

CHAPTER 5

^{1}H NMR STUDY OF LIGAND EXCHANGE WITH THE 1:2 ZINC(II):LIGAND COMPLEXES WITH MIDA AND EIDA

CONTENTS

INTRODUCTION

In the investigation given thus far, complexed iminodiacetate and N-substituted analogues are relatively non-labile or undergo intramolecular rearrangement without leaving the metal complex. Tridentate ida, mida or eida can also function as a substrate. Studies of ligand exchange[1,2,3,4] and ligand replacement[5,6,7,8,9,10] have been reported. In most cases, the difference in the dynamic behavior is small when ida is substituted for an N-substituted analogue (e.g., mida) and can be accounted for by electronic and steric effects.

Mirti and Gennaro[2,3] have shown that ligand exchange with $Zn(ida)_2^{-2}$ and $Zn(mida)_2^{-2}$ in solution with excess ligand occurs via different mechanisms. In the former, exchange occurs via a second-order process involving either unprotonated or mono-protonated iminodiacetate. In the latter, exchange occurs entirely by first-order dissociation of the complex. The difference in mechanisms has been related to the hindrance of ligand movement in the complex and the ability of the incoming molecule to approach the metal ion.[2,3] In the same study it was shown that the A and B methylene protons of the bis-ida complex are interconverting at a rate faster than expected from ligand exchange. An intramolecular rearrangement process is suspected.[3]

Interconversion of the A and B protons is not possible via any of the intramolecular rearrangement processes discussed thus far for the bis-ligand complexes. Interconversion involves breaking one of the four bonds to the ligand nitrogen. With complexes which contain a proton directly attached to a coordinated ligand nitrogen, the process probably involves loss of the amine proton,[11] in which case the process is not expected to occur in complexes where the amine proton has been substituted for an alkyl group. The absence of rearrangement

with N-alkyl substituted analogues would be supportive of the role of the proton-nitrogen bond in the mechanism.[11]

The earlier investigation of mida exchange with $Zn(mida)_2^{-2}$ using the proton NMR spectroscopy was performed at a single temperature (308 K).[2] In this study, ligand exchange is studied with $Zn(mida)_2^{-2}$ and with $Zn(eida)_2^{-2}$ in solution with varying metal-to-ligand ratios over the temperature range 273 K to 325 K. Results with the bis-mida and bis-eida complexes will indicate whether subtitution of an N-substituted methyl group for an ethyl group will affect the mechanism for exchange. A higher strength magnetic field (500 MHz) is used to obtain proton NMR spectra in which the relevant peaks are clearly separated. With the higher magnetic field, the complete four peak AB pattern of the bis-mida and bis-eida complexes can be seen. Consequently, it is possible to investigate the interconversion of protons in the A and B environments to determine whether an intramolecular process for interconversion is also operating with the mida and eida complexes.

EXPERIMENTAL

Iminodiacetic acid, N-methyliminodiacetic acid and N-ethyliminodiacetic acid were obtained by the methods described in Chapter 1. Zinc perchlorate hexahydrate, $[Zn(ClO_4)_2]\cdot 6H_2O$ (98.9%), was obtained from Aldrich and used without additional purification.

Solutions for NMR analysis were prepared entirely in 99.8% D_2O in order to minimize the water peak in the proton NMR spectrum. Some isotope dilution occurs due to the waters of crystallization in the salts and the absorption of H_2O during the preparation. The final solutions were typically 95 to 97% deuterium. Individual samples were prepared by mixing stock solutions of the reagents in the appropriate amounts. Each solution was brought to the desired pD by small addition of concentrated NaOD. Each NMR sample also contained ca.

0.008 M t-butanol. The proton peak of t-butanol is upfield and separated from other proton peaks. The natural linewidth of t-butanol is small (less than 0.15 Hz) and linebroadening due to field inhomogeneity was set equal to the observed linewidth of the internal t-butanol.

The pD measurements were taken with a standard pH electrode calibrated for H_2O solutions. The D^+ concentration was obtained with the following equation:[506]

$$pD = pH(\text{meter reading}) + 0.4 \cdot \left(\frac{[H_2O]}{55.5}\right)$$

Proton FT spectra were obtained with a Bruker AM-500 spectrometer. In a typical run, 8 scans were accumulated (16K data points each) over about 20 seconds with a pulse width of 15 x 10^{-6} s, a sweep width of 3500 Hz and a recovery time of 1.0 s. The temperature was controlled with the Bruker heating unit and monitored by substitution of an NMR tube containing ethylene glycol. The ethylene glycol sample was calibrated with a copper constantan thermocouple and is estimated to be accurate to within 0.2°.

The acid dissociation constant K_{1a} (= $[D^+][L^{-2}]/[DL^-]$) was determined for mida and eida in D_2O by observing the deuterium concentration in solutions containing equal amounts of the unprotonated and monoprotonated ligand in 99.8% D_2O. These values (log K_{1a}(mida) = -10.15; log K_{1a}(eida) = -10.55, 298 K) are ca. 0.5 pD units larger in magnitude than the corresponding equilibrium constants for H_2O solutions.[12,13]

RESULTS

Inversion of the Uncomplexed Ligand. Under certain conditions the lineshape of the methylene protons in uncomplexed mida is affected by both ligand exchange and inversion of the free ligand in solution.

For this reason, inversion of mida was investigated with solutions containing only the ligand. An earlier study reports the kinetics of inversion of ida and mida,[14] but the experimental conditions were considerably different than conditions used in this study.

The proton spectrum of a dilute mida solutions at pD 7.6 and 298 K contains a single broad peak for the methylene protons. Upon cooling the peak broadens further and eventually decoalesces into two peaks at about 275 K. The two peaks are assigned to protons in the nonequivalent methylene environments of the free ligand. Coalescence is due to inversion of the molecule about the pyrimidal nitrogen center which interchanges protons in the different sites.[15]

Rate information was obtained using several different less acidic solutions with varying ligand concentration and pD (See Appendix E-1). Under these conditions a single peak is seen for the methylene protons in the range 278 K to 314 K indicating that inversion is in the intermediate region (above coalescence) or fast exchange region on the NMR time scale.

The rate of inversion was obtained by simulating the methylene peaks for direct conversion of spins between the two possible states in the protonated form of the ligand:

$$HA \underset{k_{NB}}{\overset{k_{NA}}{\rightleftharpoons}} HB \qquad [5\text{-}1]$$

Under the conditions used in this study, it was not necessary to include exchange with protons in the deprotonated form of the ligand (A', B') since the deprotonated form is in very low abundance and exchange between HA and A' (and between HB and B') does not significantly alter the linewidth.

In equation [5-1], k_{NA} is the pseudo-first-order rate constant for the conversion of protons in the A state to the B state. For

simulating the spectra the chemical shift difference δ_{AB} (= 88 ± 1 Hz) and the coupling constant J_{AB} (= 16.1 ± 0.1 Hz) for the A and B protons were obtained from the spectrum of a 0.05 M solution of mida at pD 5.12 and 275 K where inversion is considerably slowed. These parameters were assumed to be constant with temperature and solution composition.

Values for the rate constant k_{NA} are given in Appendix E-1. It is seen that the rate of inversion increases with a decrease in ligand concentration and with a decrease in pD. Values of k_{NA}-versus-($[Dmida^-]/[D^+]$) are plotted in Figure 5-1. The data show a linear relationship with an intercept near zero at each temperature. The relationship can be written:

$$k_{NA} \propto \frac{[Dmida^-]}{[D^+]} \qquad [5\text{-}2]$$

A detailed analysis of nitrogen inversion has been given elsewhere.[16,17] The process can be described with the elemental steps given in Scheme 1. (The scheme is written with protons instead of deuterons to generallize the results.)

Scheme 1

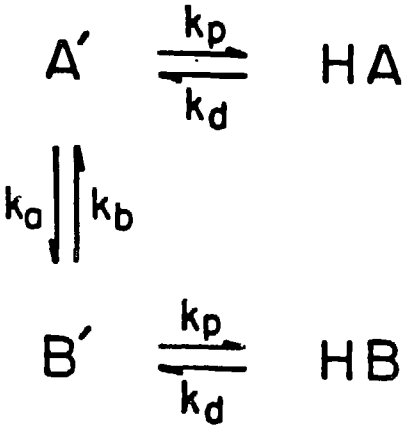

The monoprotonated form of the ligand is represented by HA (HB). The deprotonated form is represented by A' (B') Interconversion occurs between HA (HB) and A' (B') with the deprotonation rate constant k_d and protonation rate constant k_p as indicated. In addition, inversion occurs with rate constants k_a and k_b which are equal ($k_a = k_b = k_{inv}$) for inversion with mida.

Rate constant k_{NA} can be described in terms of the rate constants for the the elemental reactions in Scheme 1:[16]

$$k_{NA} = \frac{k_d k_{inv}}{2k_{inv} + k_p}$$

An identical expression can be written for k_{NB} since k_{NA} and k_{NB} are equal with the ligand in this study.

Two limiting conditions can be seen with this expression:[16]

Condition (A). If protonation is fast compared to the rate of inversion ($k_p >> k_{inv}$):

$$k_{NA} = k_{inv}\left(\frac{k_d}{k_p}\right)$$

$$= k_{inv}\left(\frac{K_{la}}{[H^+]}\right) \qquad [5\text{-}3]$$

An inverse linear relationship is expected between k_{NA} and $[H^+]$.

Condition (B). If inversion is fast compared to the rate of protonation ($k_{inv} >> k_p$):

$$k_{NA} = \frac{k_d}{2} \qquad [5\text{-}4]$$

Under condition (B) the dependence of the rate on pD and ligand concentration is associated with the deprotonation step. Two

mechanisms may be envisioned which differ in the nature of the base which attacks the proton of the HA (HB) species. Writing $Hmida^-$ for the protonated form of the ligand:

$$Hmida^- + OH^- \underset{k(-OH)}{\overset{k(OH)}{\rightleftharpoons}} mida^{-2} + H_2O \qquad [5\text{-}5]$$

$$Hmida^- + mida(*)^{-2} \underset{k(A)}{\overset{k(A)}{\rightleftharpoons}} mida^{-2} + Hmida(*)^- \qquad [5\text{-}6]$$

Rate constants k(OH), k(-OH) and k(A) are the second-order rate constants for the reactions as written. The asterisk (*) indicates a particular ligand undergoing reaction. In aqueous solution, a water molecule can also act as the attacking base, thereby forming a hydronium ion. This reaction is important only in acidic solutions and need not be considered here.

The pseudo-first-order rate constant k_d for the deprotonation of $Hmida^-$ and the rate constant k_p for the protonation of $mida^{-2}$ (Scheme 1) may be written:

$$k_d = k(OH)\,[OH^-] + k(A)\,[mida^{-2}]$$

$$k_p = k(-OH) + k(A)\,[Hmida^-]$$

These may be rewritten using expressions for $[OH^-]$ ($= K_w/[H^+]$) and $[mida^{-2}]$ ($= K_{1a}[Hmida^-]/[H^+]$). Substitution of k_d into equation [5-4] yields:

$$k_{NA} = \frac{k(OH)\,K_w}{2[H^+]} + \frac{k(A)\,K_{1a}[Hmida^-]}{2[H^+]}$$

Under condition (B), k_{NA} is expected to vary with a second-order dependence in amine concentration. A second-order dependence has been seen with some ternary amine, but usually under acidic condition.[13,16]

The results with mida (Figure 5-1) indicate that condition (B) is appropriate. Extrapolation of the data to low [$Dmida^-$] and high [D^+] indicates that k_{NA} becomes very small. Therefore, the following inequality can be written:

$$k(OH)\ K_W \ll k(A)\ K_{la}[Hmida^-] \qquad [5\text{-}7]$$

The data were fitted to a line with zero intercept. The value of k(A) at each temperature was obtained from the slope ($k(A) = 2(\text{slope})/K_{la}$). A plot of logarithm k(A)-versus-reciprocal temperature is given in Figure 5-2 where a linear relationship is seen. The activation parameters ($\Delta H^{\ddagger}$ = 10.8 kcal mol^{-1}, $\Delta S^{\ddagger}$ (298 K) = 6.7 eu) were obtained from the fitted line in the usual manner.

Under condition (B) only a lower limit can be determined for the inversion rate constant k_{inv} in Scheme 1. At room temperature k_p (= k(A)[$Hmida^-$]) is ca. 2 x 10^5 s^{-1} for a 0.1 M solution of $Hmida^-$. Assuming that k_{inv} is more than 2.5-fold faster than k_p, k_{inv} must be greater than 5 x 10^5 s^{-1} at 298 K. Reported values of k_{inv} for ternary amines with bulky substituents are ca. 10^5 - 10^7 s^{-1}.[18,19] Therefore, an inversion rate constant of 5 x 10^5 s^{-1} or greater for mida is not unreasonable.

The unexpected result from this analysis is that deprotonation of $Hmida^-$ is due primarily to attack by the free amine. If the left side of the inequality in equation [5-7] is less than the right side by a factor of at least 5, k(OH) must be less than about 2 x 10^9 s^{-1} (298 K) using the observed value of k(A) and $K_W(D_2O)$ = 0.15 x 10^{-14}.[12] This value is reasonable since the forward rate of reaction [5-5] with a hydroxide ion is expected to be diffusion controlled (k(OH) = 10^9 - 10^{10} s^{-1}, 298 K). However, the value of k(A) for the reaction with the deprotonated amine (2.0 x 10^6 s^{-1}) is less than values seen with other amines (k(A) = 10^7 s^{-1}).[13,19]

Ligand Exchange. The proton spectra of bis-ligand complexes $Zn(mida)_2^{-2}$ and $Zn(eida)_2^{-2}$ in solution with excess ligand at 282.2 K are shown in Figure 5-3(a) and Figure 5-3(b), respectively. The peak assignments and locations relative to internal t-butanol are given in Table 5-1. Under the slightly acidic conditions used with mida (pD 6.88), two broad peaks appear for the methylene protons in the unbound mida due to the slow rate of inversion (limited by the deprotonation step) as discussed above. With eida at pD = 8.22 (Figure 5-3), only a single sharp peak is seen for the methylene protons of the unbound ligand. A single peak is also seen under acidic conditions indicating that inversion is much more rapid with eida than with mida. The methylene peak with eida appears at the same location as the average of the A and B methylene proton peaks with mida (2.539 ppm).

The A-B pattern of the methylene protons in the 1:2 metal:ligand complex is clearly seen with both mida and eida (Figure 5-3). With eida, however, the pattern overlaps with the multiplet of the α-proton in the ethyl group of the free ligand.

1:2 Zn(II):mida. Proton spectra were obtained with a metal-ligand solution at several different temperatures. Representative spectra showing the free (downfield) and bound methylene protons are shown in Figure 5-4. The lineshape of both type of protons is very much dependent on temperature.

The spectra with mida and metal ion were analyzed by complete lineshape analysis using the model for exchange in Scheme 2:

Scheme 2:

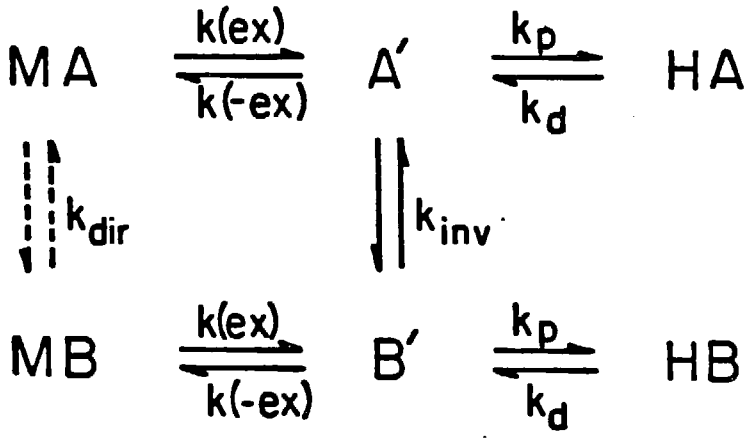

Three possible environments for each A and B methylene proton include the complexed state (MA, MB), the uncomplexed states with the free ligand void of its acidic protons (A', B') and the uncomplexed state with the monoprotonated ligand (HA, HB). Exchange occurs between MA (MB) and A' (B'), and between the A' (B') and HA (HB) . In addition, interconversion can occur between a proton in the A' and B' environments by inversion about the pyrimidal nitrogen in the deprotonated ligand.

Rate constants for exchange between A' (B') and HA (HB) and interconversion between the A' and B' can be related directly to the rate constants in Scheme 1. The pseudo-first-order rate constants for exchange between MA (MB) and A' (B') in Scheme 2 are given by rate constants k(ex) and k(-ex) as indicated. In consideration of the results with ida (See Introduction) it is appropriate to include a process for the direct interconversion between MA and MB (dotted arrows in Scheme 2) with rate constant k_{dir}. A non-zero value for

k_{dir} is evidence of an intramolecular inversion process with the metal-ligand species.

The spectra were simulated by the method of Binch[20] which provides for both chemical exchange and spin-spin coupling. The exchange matrix representing Scheme 2 is given in Appendix F. In the simulation, the natural transverse relaxation lifetimes T_2 of the methylene protons in the complexed and uncomplexed states were assumed equal to the longitudinal relaxation lifetimes T_1 for the methylene proton in $Zn(mida)_2^{-2}$ and $Hmida^-$, respectively. Measurements of T_1 were obtained by the inversion recovery method. Typical values are given in Table 5-2. In the observed proton spectra, the peak corresponding to A' (B') in Scheme 2 is coalesced with the peak for HA (HB) at all times, and the relative populations of the complexed and uncomplexed states were obtained from the intregration of the spectrum at each temperature. The chemical shift difference of a proton in the MA (MB) and HA (HB) states in the absence of exchange was set as needed to fit the spectrum. The location of the A' (B') peak was presumed to be 343 Hz upfield from the location of the HA (HB) peak.[21] Finally, the linebroadening due to magnetic field inhomogeneity was set equal to the width of the t-butanol peak in each spectrum. Typical values were between 0.8 and 1.5 Hz.

In simulating the spectra, the value of k_d and k_p were determined for each solution from the value of k(A) at each temperature and the dependence of the $Hmida^-$ concentration given above. The value of k_{inv} was assumed to be a factor of 500-time faster than k_p, thereby assuring that k_{inv} is not a factor in determining the shape of the line.

Evidence that the temperature and concentration dependence for deprotonation and inversion of the free ligand is still reasonable with metal-ligand solutions was seen in the free ligand peak in the spectra at the low end of the temperature range. Below about 280 K, ligand exchange with the complex is very slow and the line broadening of the free methylene proton is due almost entirely to the inversion

process (Scheme 1). It most cases, the linewidth of the simulated peak was within 10% of the observed linewidth using the rate constants determined earlier.

In simulating the spectra it was observed that the AB pattern of the bound methylene protons is highly dependent on the value of k(ex), while the lineshape of the free methylene proton is dependent primarily on the value of k(-ex) (as well as k_d). According to Scheme 2, rate constants k(ex) and k(-ex) are related by the expression:

$$k(ex) = k(-ex)\frac{[Dmida^-]\,K_{1a}}{2\,[Zn(mida)_2^{-2}][D^+]}$$

A fit of the free methylene proton peak determines k(-ex), and use of the above expression determines k(ex). Scheme 2 may be considered reasonable if the value of k(ex) determined in this manner produces a good fit of the A-B pattern for the bound methylene protons.

Simulated spectra are shown in Figure 5-4 using the value of k(ex) and k(-ex) determined as described above. An excellent fit is seen with both the free and bound methylene proton peaks.

The mechanism for exchange was previously determined to be dissociation of the bis-mida zinc complex:[2]

$$Zn(mida)_2^{-2} \underset{k_{-1}}{\overset{k_1}{\rightleftharpoons}} Zn(mida) + mida^{-2}$$

Similar A-B patterns were seen with solutions of varying free ligand concentration and pD between 7.0 and 9.0, thus confirming this mechanism of exchange. Rate constant k(ex) for conversion of a proton can be related to the rate constant for dissociation of the complex k_1:

$$k_1 = 2\,k(ex)$$

A plot of logarithm k_1-versus-reciprocal temperature (Figure 5-5) reveals a linear temperature dependence. The data were fitted to a line and the activation parameters (Table 5-3) were determined from the slope and the intercept in the usual manner. Also shown in Figure 5-5 is the rate of exchange with the same system at 308 K as determined by Mirti and Gennaro.[2]

1:2 Zn(II):eida. Simulation of both free and bound methylene line shapes with eida is complicated by the overlap of the resonance of the bound methylene proton with the multiplet of the α-proton in the free ligand (See Figure 5-3(b)) It is possible to include the α-proton multiplet in the analysis, but additional uncertainty is introduced in the rate constants and other parameters needed for describing the additional type of proton.

An alternative method was used for studying ligand exchange with the bis-eida complex. The rate of inversion of the uncomplexed eida ligand is fast and does not contribute to the linewidth of the free methylene proton. Therefore, the linewidth of the free methylene proton can be attributed entirely to the exchange broadening.

Possible reactions for describing ligand exchange are given below where L = $eida^{-2}$.

$$ZnL_2^{-2} \underset{k_{-1}}{\overset{k_1}{\rightleftharpoons}} ZnL + L^{-2} \qquad [\underline{I}]$$

$$ZnL_2^{-2} + H^+ \underset{k_{-2}}{\overset{k_2}{\rightleftharpoons}} ZnL + HL^- \qquad [\underline{II}]$$

$$ZnLL(*)^{-2} + L^{-2} \overset{k_3}{\rightleftharpoons} ZnL_2^{-2} + L(*)^{-2} \qquad [\underline{III}]$$

$$ZnLL(*)^{-2} + HL^- \overset{k_4}{\rightleftharpoons} ZnL_2^{-2} + HL(*)^- \qquad [\underline{IV}]$$

Reactions involving the 1:1 metal:ligand species can also be envisoned. They are expected to be unimportant based on results seen in the earlier study with the mida system.[2]

The rate of conversion between the protonated and unprotonated forms of the ligand is expected to be rapid compared to exchange:

$$HL^- \underset{\text{fast}}{\rightleftharpoons} H^+ + L^{-2}$$

Under these conditions, the pseudo-first-order rate constant for spins going from the uncomplexed state to the complexed state according to reactions I through IV can be expressed:

$$k_{HL} = \frac{k_1[ZnL_2^{-2}]}{([HL^-] + [L^{-2}])} + \frac{k_2[ZnL_2^{-2}][H^+]}{([HL^-] + [L^{-2}])}$$

$$+ \frac{k_3 K_{1a}[ZnL_2^{-2}][HL^-]}{([HL^-] + [L^{-2}])[H^+]} + \frac{k_4[ZnL_{-2}^{-2}]}{([HL^-] + [L^{-2}])}$$

where $K_{1a} = [L^{-2}][H^+]/[HL^-]$.

Experimental values of k_{HL} were obtained from the linewidth at half height of the free ligand less the line broadening due to field inhomogeneity. Values of k_{HL} are given in Appendix E-3 for solutions with near 1:3.0, 1:3.5, 1:4.0 and 1:5.0 Zn(II):eida ratios. Solutions with similar and varying D^+ concentrations are given to demonstrate the dependence of the rate on acidity.

A plot of k_{HL}-versus-$([Heida^-]+[eida^{-2}])^{-1}$ is given in Figure 5-6. The error associated with each measurement is due to a 5% uncertainty in the concentration of $Heida^-$ or an uncertainty of 1 Hz in the linewidth, which ever is greater. Figure 5-6 reveals a linear dependence on reciprocal $Heida^-$ concentration, consistent with reactions I and II. No dependence was seen on solution acidity indicating reactions II and III are unimportant for ligand exchange. The zero intercept at each temperature indicates reaction (IV) is also unimportant. Thus, reaction I is the only mechanism given above that adequately explains the results.

The rate constant k_1 for reaction I at each temperature was obtained from the slope of each line through the data. A plot of logarithm k_1-versus-reciprocal temperature with eida is shown in Figure 5-5. The data were fitted to a line which provided the enthalpy and entropy of activation given in Table 5-3 from the slope and intercept, respectively.

DISCUSSION

At room temperature ligand exchange with eida is slightly faster than exchange with mida. Very likely, both an enthalpy and entropy effect is involved with accommodating the larger N-ethyl group in eida compared with the N-methyl group in mida. The uncertainty in the data does not permit an estimation of the individual effects.

Ligand exchange occurs by the same mechanism with the bis-mida and bis-eida zinc complexes. A dissociative mechanism of exchange was previously established for the bis-mida complex.[2] A similar mechanism with the bis-eida complexes indicates that substitution of a methyl group for an ethyl group does not alter the mechanism. A dissociative mechanism probably exist with the bis-ida complex as well, but a second-order process involving unprotonated or monoprotonated ligand is much faster and prevents the observation of the slower dissociative mechanism with this complex.

The results show that a second-order or higher-order mechanism for exchange does not exist with the bis-mida and bis-eida complexes. This is probably due to a greater energy barrier required for the entry of an incoming ligand molecule in the coordination sphere of the bis-ligand metal complex. The large N-substituent group on the ligand can obstruct the approach of an incoming group. More likely, the bulkier N-substituted alkyl group tends to keep the donor atoms of the ligand in a position favorable for bonding by hindering the rotation of the iminodiacetate group away from the metal ion. Similar arguments have been used to explain kinetic results with other sterically crowded ligands.[3,14,10]

In addition to hindrance of ligand movement, increased basicity due to the electron-donating properties of the methyl group in mida and the ethyl group in eida may also be important in determining the exchange mechanism. A stronger metal-nitrogen bond with the more basic mida and eida ligands (See Table 1-2 of Chapter 1) means the ligand is less easily removed by an incoming group.

The use of a higher magnetic field (500 MHz) was necessary to resolve the complete AB pattern of the methylene proton in bound mida and eida. Under these conditions the AB pattern with mida could be analyzed for both ligand exchange and a possible intramolecular inversion process. Results with $Zn(mida)_2^{-2}$ indicate that the AB pattern can be explained entirely by ligand exchange ($k_{dir} = 0$), and that an intramolecular mechanism is not operating with this complex.

The absence of an intramolecular inversion process with the bis-mida metal complex is reasonable considering that either a carbon-nitrogen or a metal-nitrogen bond must be broken in order to achieve inversion (see Introduction). The observation of such a process with only the bis-ida complex gives further support to the role of the amine proton in this process.

The A-B pattern of the bound methylene protons must also be analyzed with the bis-eida complex in order to determine if an intramolecular process involving inversion is operating with this complex. While this was not done, results with the bis-mida complex suggest that such a process is not very likely with the bis-eida zinc complex.

TABLE 5-1

Peak Assignments in the ^1H NMR Spectrum Relative to Internal t-Butanol at 282.2 K*

(a) 1:3.6 Zn(II):mida solution		
free methylene ($-\underline{CH_2}-N$)	2.594,2.483	
bound methylene ($-\underline{CH_2}-N$) and 1.994	2.182,2.149,2.026	J_{AB} = 16.25 Hz, δ_{AB} = 76.1 Hz
free methyl ($N-\underline{CH_3}$)	1.705	
bound methyl ($N-\underline{CH_3}$)	1.161	
(b) 1:4.0 Zn(II):eida solution		
free methylene ($-\underline{CH_2}-N$)	2.539	
bound methylene ($-\underline{CH_2}-N$) and 2.040	2.136,2.103, 2.077	J_{AB} = 16.55 Hz, δ_{AB} = 25.0 Hz
free α ($-\underline{CH_2}-CH_3$)	2.090, 2.061‡	
bound α ($-\underline{CH_2}-CH_3$) and 1.486	1.529,1.515,1.500,	J = 7.00 Hz
free β ($N-CH_2-\underline{CH_3}$)	0.074,0.060,0.053	J = 7.29 Hz
bound β ($N-CH_2-\underline{CH_3}$)	-0.128,-0.142,-0.156	J = 7.15 Hz

* Spectra are shown in Figure 5-3.

‡ Two peaks in α-proton quartet are obscured by AB methylene pattern.

TABLE 5-2

Longitudinal Relaxation Times as Determined by Inversion Recovery

A. Methylene proton in mida complex with Zn(II):

Temperature	273 K	282 K	296 K
T_1, s	0.34	0.47	0.54

B. Methylene proton in uncomplexed mida:

Temperature	273 K	282 K	296 K
T_1, s	0.48	0.71	1.2

TABLE 5-3

Activation Parameters for Ligand Exchange

Complex	$\Delta H^{\ddagger}$ (kcal mol^{-1})	$\Delta S^{\ddagger}$ (eu, 298 K)	k_1 (s^{-1}, 298 K)
$Zn(mida)_2^{-2}$	12.2 ± 0.5	-9 ± 2	47 ± 1
$Zn(eida)_2^{-2}$	12.6 ± 0.7	-8 ± 2	53 ± 1

CAPTIONS TO FIGURES

Figure 5-1 Methylene proton interconversion rate k_{NA}-versus-($[Dmida^-]/[D^+]$) for solutions containing N-methyliminodiacetic acid and no metal ion.

Figure 5-2 Deprotonation rate constant k(A)-versus-reciprocal temperature for N-methyliminodiacetic acid.

Figure 5-3 Proton spectrua at 282.2 K with (a) a 1:3.6 Zn(II):mida solution at pD = 6.88 and (b) a 1:4.0 Zn(II):eida solution at pD = 8.22. Peak at 0 ppm is internal t-butanol.

Figure 5-4 Observed (a) and simulated (b) spectra of a 1:4 Zn(II):mida solution at different temperatures. Shown are the methylene proton peaks of the free ligand (downfield) and complexed ligand.

Figure 5-5 Ligand exchange rate constant k_1-versus-reciprocal temperature for $Zn(mida)_2^{-2}$ (○) and $Zn(eida)_2^{-2}$ (□). Also shown is the rate constant for mida exchange with $Zn(mida)_2^{-2}$ at 308 K according to Ref. 2 (●).

Figure 5-6 Exchange rate k_{HL}-versus-reciprocal $[Deida^-]$ for 1:3.0, 1:3.2, 1:3.6 and 1:4.0 Zn(II):eida solutions with varying temperature.

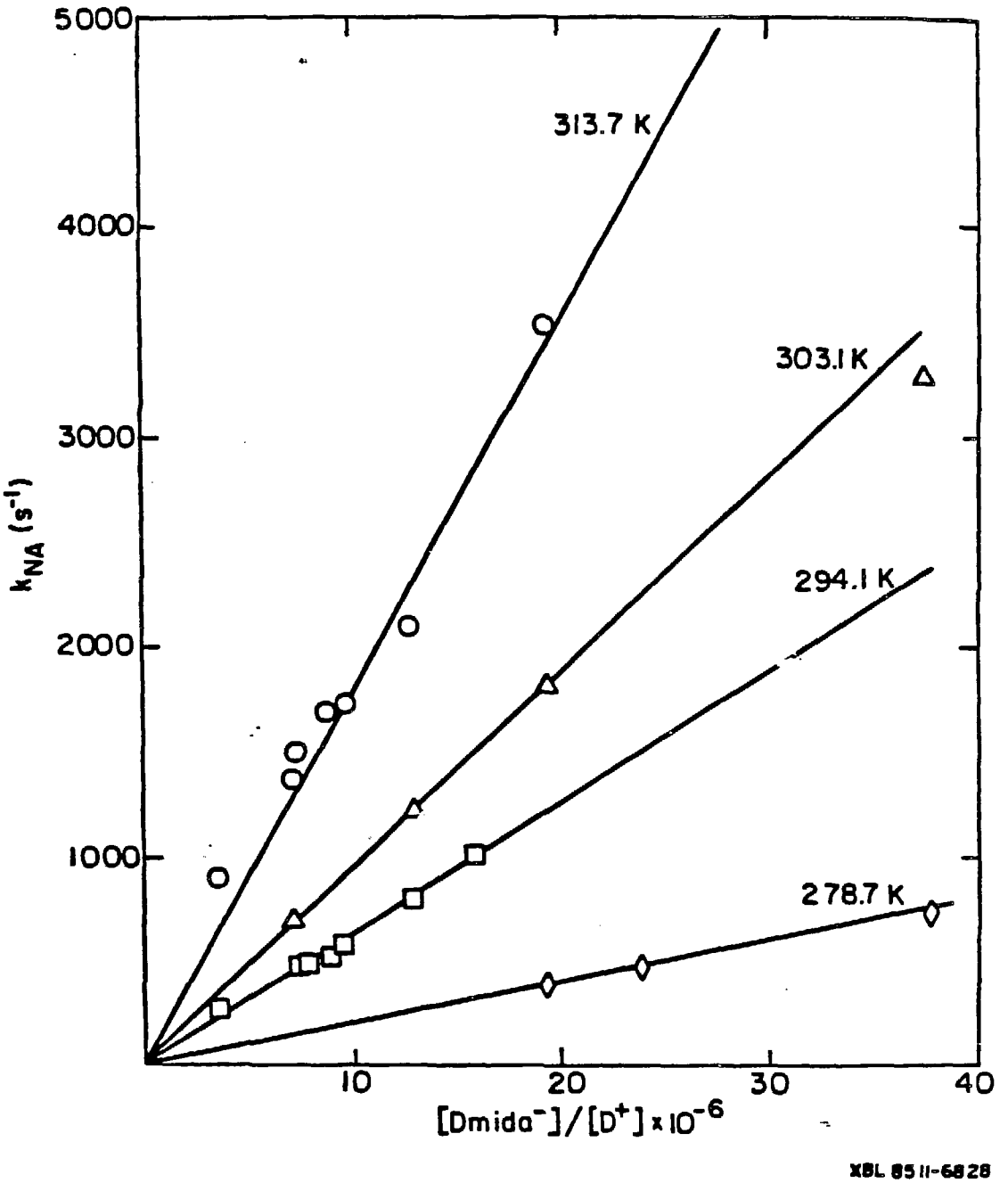
5000
4000
3000
2000
1000
k_{NA} (s^{-1})
313.7 K
303.1 K
294.1 K
278.7 K
10
20
30
40
[Dmida$^-$]/[D$^+$] x 10^{-6}
XBL 8511-6828

Figure 5-1

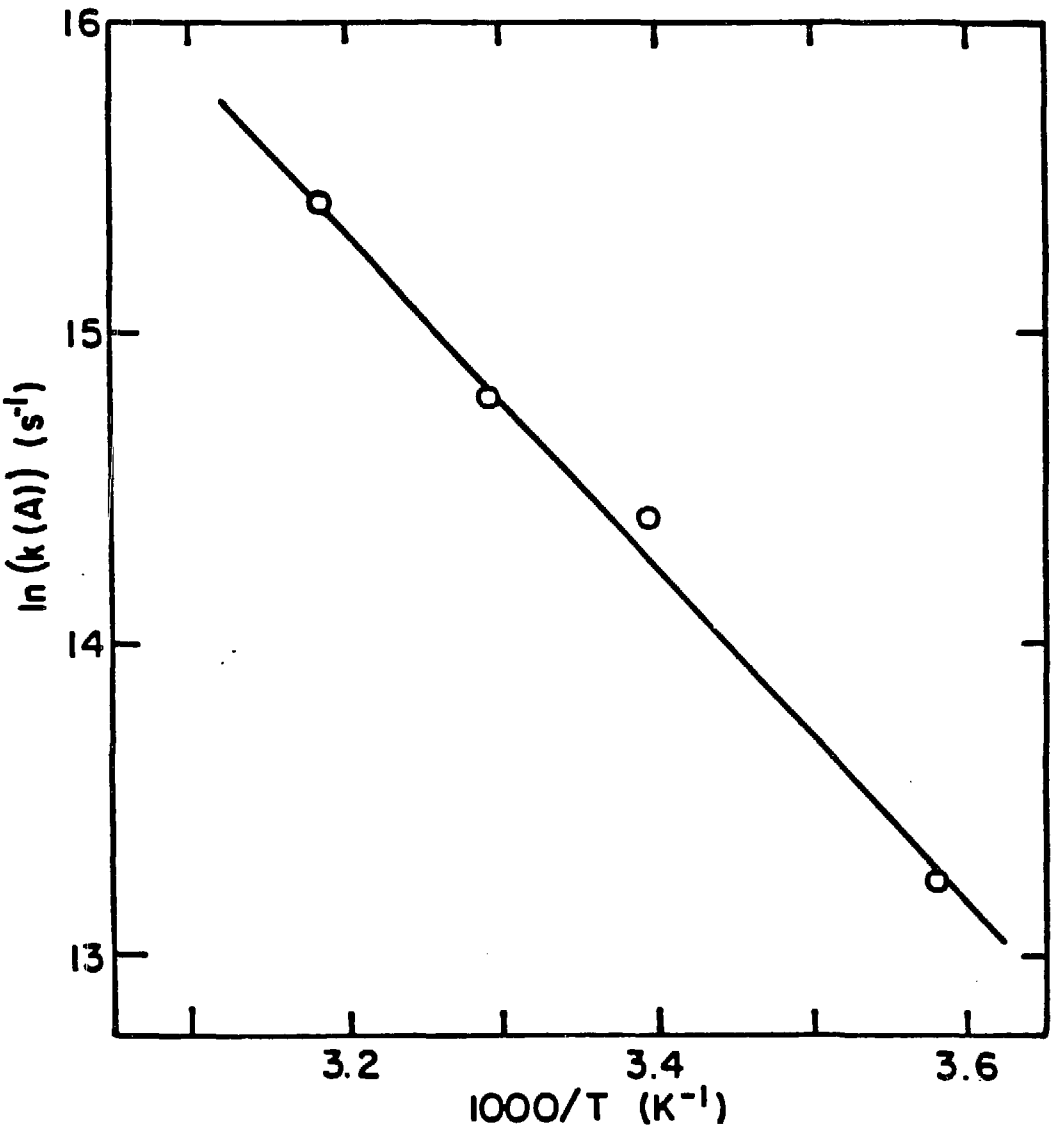

XBL 8511-6824

Figure 5-2

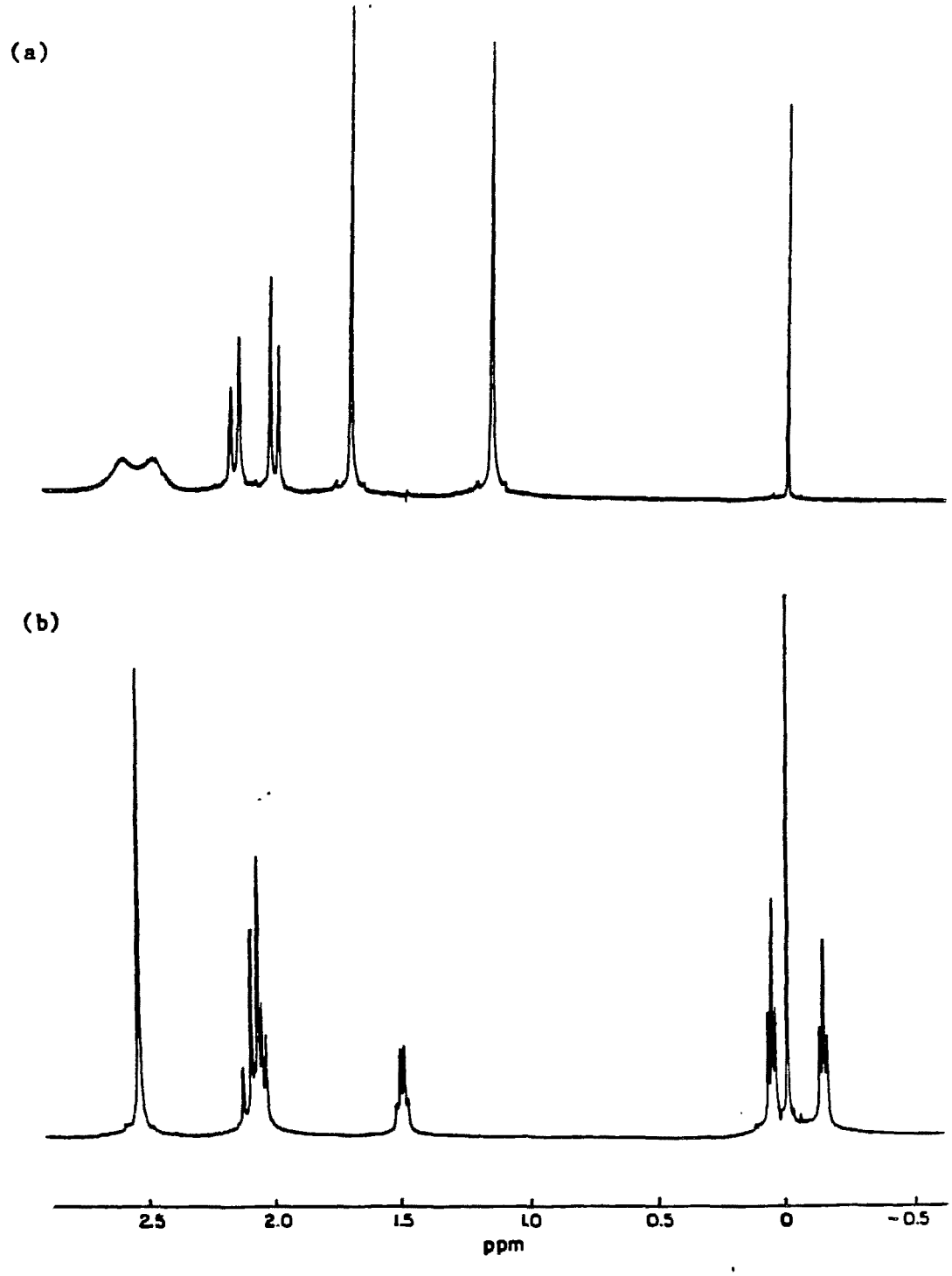

Figure 5-3

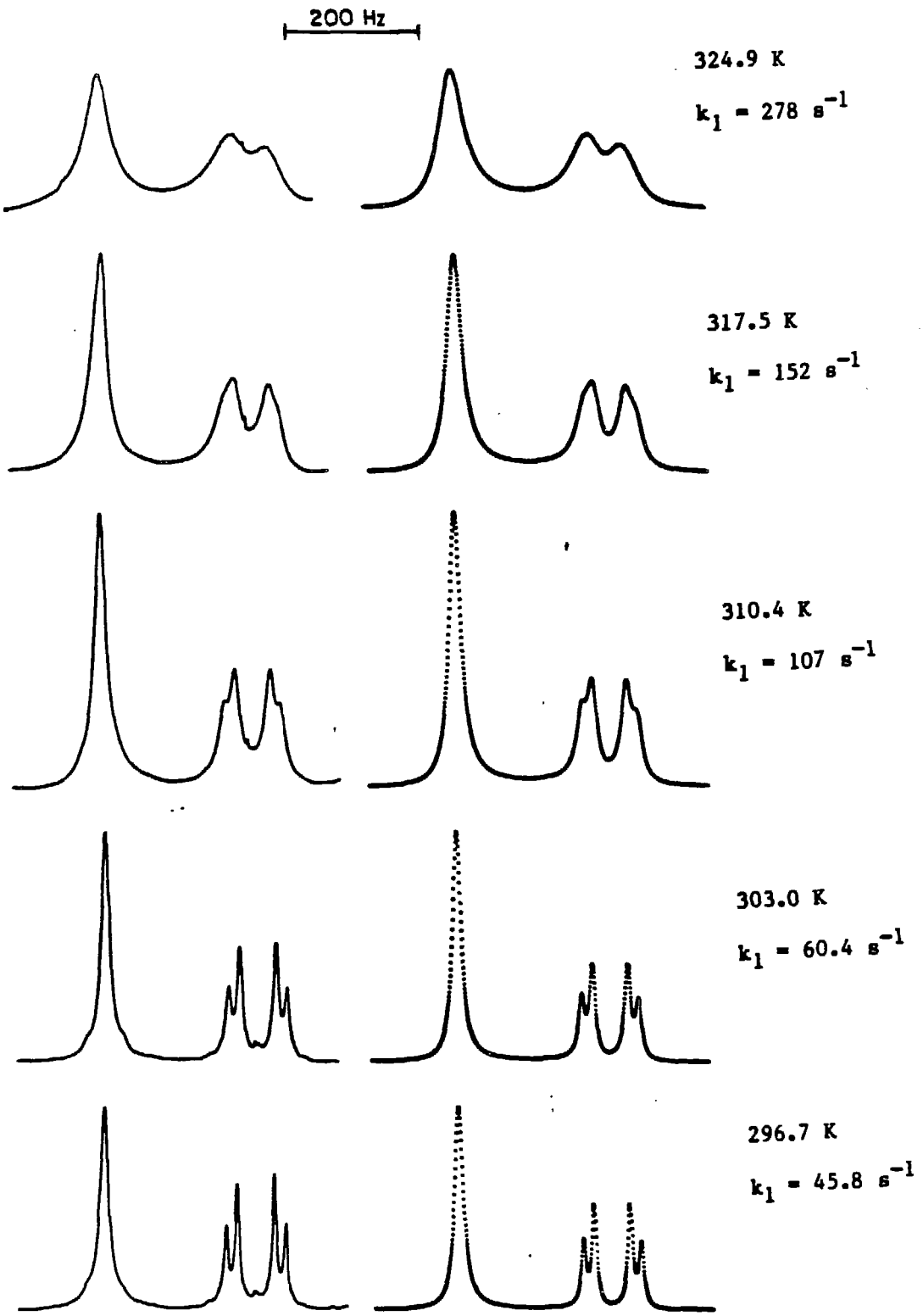
200 Hz
324.9 K
k_1 = 278 s^{-1}
317.5 K
k_1 = 152 s^{-1}
310.4 K
k_1 = 107 s^{-1}
303.0 K
k_1 = 60.4 s^{-1}
296.7 K
k_1 = 45.8 s^{-1}

Figure 5-4

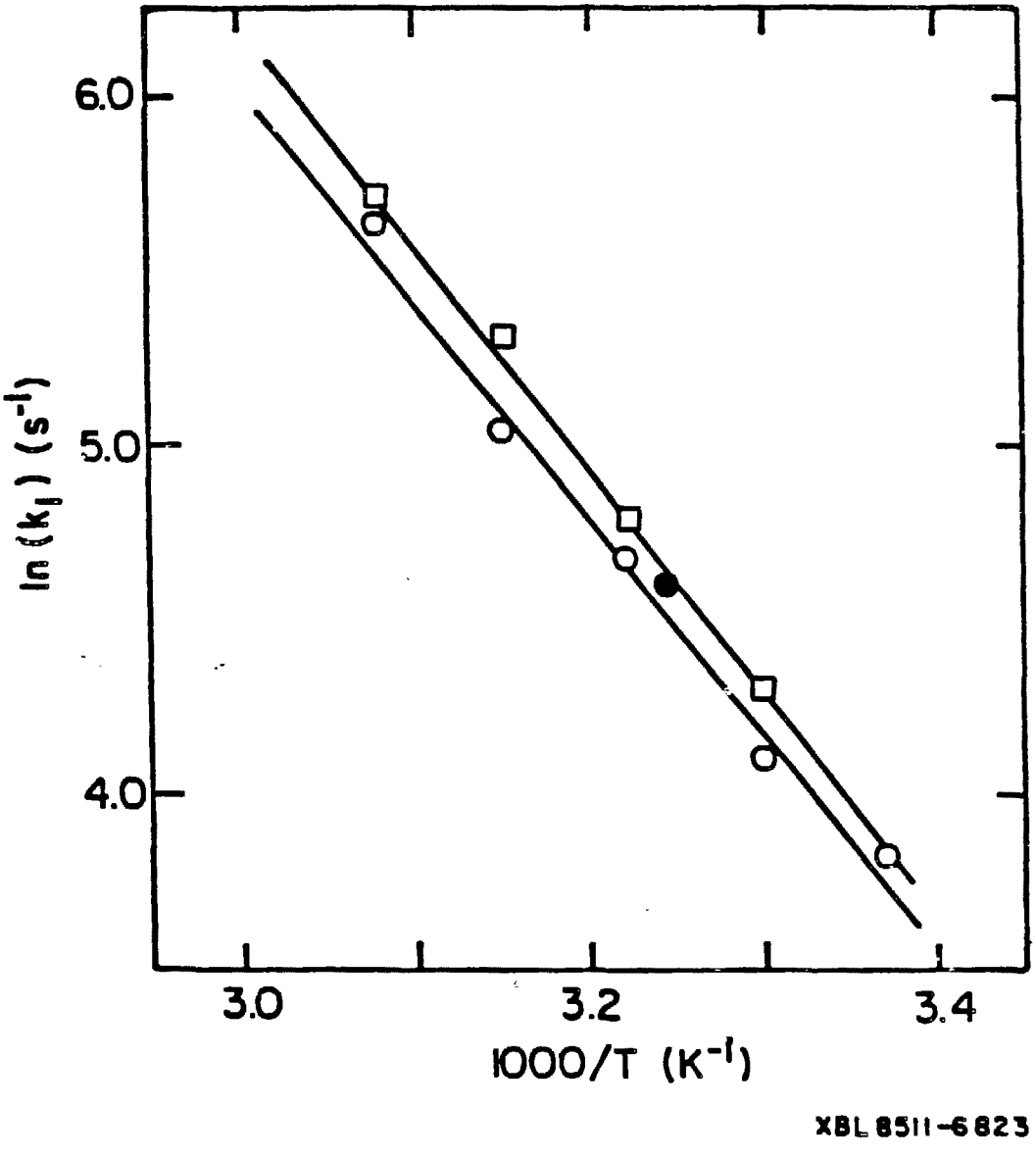

Figure 5-5

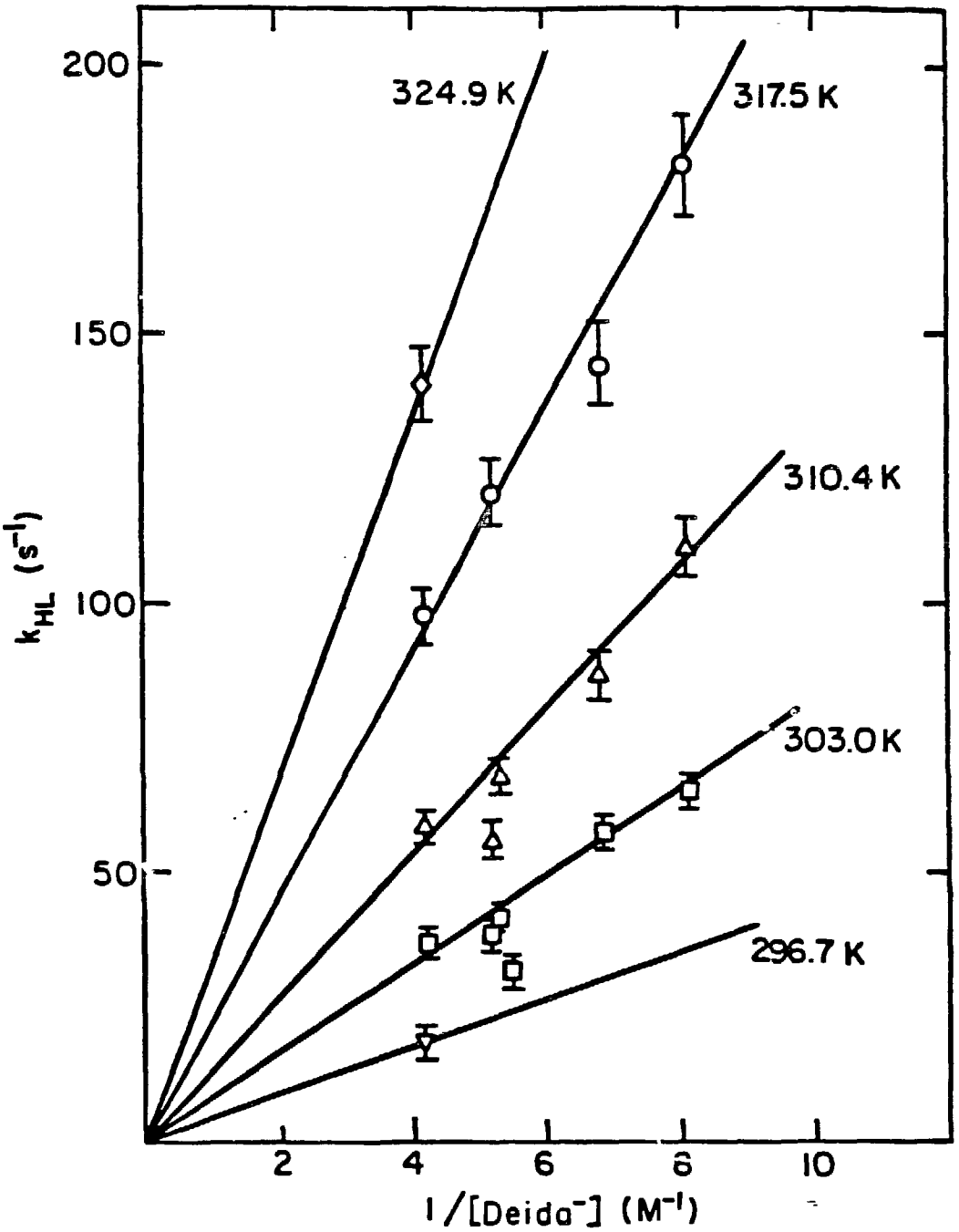
200
150
100
50
k_{HL} (s^{-1})
324.9 K
317.5 K
310.4 K
303.0 K
296.7 K
2
4
6
8
10
1/[Deida$^-$] (M^{-1})
XBL8511-6827

Figure 5-6

APPENDIX E-1: Linebroadening Data for Nitrogen Inversion in Uncomplexed mida

Temperature (K)	Ligand (M)	pD	$\Delta\nu 1/2^{*}$ (Hz)	k_{NA} (s^{-1})
278.7	0.100	8.29	35.1	395
	0.100	8.38	27.7	480
	0.100	8.58	17.3	730
294.1	0.100	7.86	27.4	485
	0.100	8.11	15.7	800
	0.100	8.20	12.3	1010
	0.050	7.84	57.4	275
	0.050	8.19	27.3	485
	0.050	8.24	23.3	560
	0.050	8.28	22.9	565
303.1	0.100	8.29	6.7	1835
	0.100	8.58	11.8	3280
	0.050	8.15	18.1	695
	0.050	8.42	10.1	1220
313.7	0.100	7.86	8.2	1495
	0.100	8.11	5.9	2100
	0.100	8.29	3.4	3555
	0.050	7.84	13.8	905
	0.050	8.15	9.0	1365
	0.050	8.24	7.2	1700
	0.050	8.28	7.1	1735
	0.050	8.42	5.7	2155

* Observed linewidth at half height of coalesced proton resonance of CH_2 less broadening due to magnetic field inhomogeneity.

APPENDIX E-2: Ligand Exchange Data with an Aqueous Solution containing 0.113 M $Zn(ClO_4)_2$ $6H_2O$, 0.463 M N-Methyliminodiacetic Acid and NaOD to pD 8.06.

Temperature (K)	$\Delta\nu 1/2^*$ (Hz)	$k_d^{\ddagger}$ (s^{-1})	k(ex) (s^{-1})
296.7	14.1	3.62×10^3	22.9
303.0	13.9	5.30×10^3	30.2
310.4	19.5	8.14×10^3	53.5
317.5	25.4	1.20×10^4	75.9
324.9	45.1	1.78×10^4	138.8

* Observed linewidth for methylene peak of uncomplexed ligand taken at half height less broadening due to magnetic field inhomogeneity.

‡ Calculated rate of deprotonation. See Text.

APPENDIX E-3: Line Broadening Data for Ligand Exchange with aqueous solutions containing $Zn(ClO_4)_2\ 6H_2O$, N-Ethyliminodiacetic Acid and NaOD.

Metal added (M)	Ligand added (M)	pD	Temperature (K)	$\Delta\nu 1/2^*$ (Hz)	k_{HL} (s^{-1})
0.110	0.344	8.33	303.0	20.6	64.6
			310.4	35.2	110.
			317.5	57.6	181.
0.110	0.367	8.25	303.0	18.3	57.5
			310.4	27.4	86.1
			317.5	45.8	143.
0.110	0.412	8.34	303.0	13.2	41.4
			310.4	17.8	56.0
			317.5	38.4	121.
0.110	0.412	9.02	303.0	10.1	31.7
			310.4	21.5	67.6
0.110	0.412	7.29	303.0	12.3	38.6
0.110	0.458	8.22	296.7	5.8	18.2
			303.0	11.8	36.9
			310.4	18.6	58.3
			317.5	31.1	97.6
			324.9	44.6	140.

* Observed linewidth for methylene peak of uncomplexed ligand taken at half height less broadening due to magnetic field inhomogeneity.

APPENDIX F: Exchange Matrix for Scheme 2 of Chapter 5

The first quadrant for the exchange matrix representing Scheme 2 according is given on the next page. The first and fourth quadrants are alike. All elements of the off-diagonal quadrants are zero. The rate constants are defined in the text.

	$[12]^1$ $([24]^1)$	$[13]^1$ $([34]^1)$	$[12]^2$ $([24]^2)$	$[13]^2$ $([34]^2)$	$[12]^3$ $([24]^3)$	$[13]^3$ $([34]^3)$
$[12]^1$ $([24]^1)$	$-k(ex)$ $-k_{dir}$	k_{dir}	$k(-ex)$	0	0	0
$[13]^1$ $([34]^1)$	k_{dir}	$-k(ex)$ $-k_{dir}$	0	$k(-ex)$	0	0
$[12]^2$ $([24]^2)$	$k(ex)$	0	$-k(-ex)$ $-k_p-k_{inv}$	k_{inv}	k_d	0
$[13]^2$ $([34]^2)$	0	$k(ex)$	k_{inv}	$-k(-ex)$ $-k_p-k_{inv}$	0	k_d
$[12]^3$ $([24]^3)$	0	0	k_p	0	$-k_d$	0
$[13]^3$ $([34]^3)$	0	0	0	k_p'	0	$-k_d'$

REFERENCES

1 Kula, R.J. Anal. Chem. 1967, 39, 1171-1175.

2 Mirti, P.; Gennaro, M.C. J. Inorg. Nucl. Chem. 1977, 39, 1259-1264.

3 Gennaro, M.C.; Mirti, P. J. Inorg. Nucl. Chem. 1981, 43, 1711-1717.

4 Southwood-Jones, R.V.; Merbach, A.E., Inorg. Chim. Acta 1978, 30, 135-143.

5 Hanna, S.B.; Hessley, R.K.; Nicholson, L.M. Inorg. Chim. Acta. 1977, 25, L7-L8.

6 Roche, T.S.; Wilkins, R.G. J. Amer. Chem. Soc. 1974, 96, 5082-5086.

7 Cassatt, J.C.; Wilkins, R.G. J. Amer. Chem. Soc. 1968, 90, 6045-6050.

8 Billo, E.J.; Smith, G.F.; Margerum, D.W. J. Amer. Chem. Soc. 1971, 93, 2635-2641.

9 Weyh, J.A.; Hamm, R.E. Inorg, Chem. 1969, 8, 2298-2302.

10 Coombs, L.C.; Margerum, D.W. Inorg. Chem. 1970, 9, 1711-1716.

11 Bernhard, C.A.; Bernauer, K. Helv. Chim. Acta 1977, 60, 2371-2378.

12 Glasoe, P.K.; Long, F.A. J. Phys. Chem. 1960, 64, 188.

13 Morgan, W.R.; Leyden, D.E. J. Amer. Chem. Soc. 1970, 92, 4527-4531.

14 Leyden, D.E.; Whidby, J.F. J. Phys. Chem. 1969, 73, 3076-3081

15 Rauk, A.; Allen, L.; Mislow, K. Angew. Chem. Inter. Engl. Ed. 1970, 9, 400-414.

16 Delpuech, J.-J.; Bianchin, B. J. Amer. Chem. Soc. 1979, 101, 383-389.

REFERENCES (Continued)

17 Delpuech, J.-J. Org. Mag. Res., 1970, 2, 91-107.

18 Saunders, M.; Yamada, F. J. Amer. Chem. Soc.,85, 1882.

19 Menger, F.M.; Thanos, T.E. J. Amer. Chem. Soc. 1976, 98, 3267-3271.

20 Binsch, G. J. Amer. Chem. Soc. 1969, 91, 1304-1309.

21 Kula, R.J. Anal. Chem. 1966, 38, 1382-1388.